INTRODUCTION

The Nuclear Physics Laboratory at the University of Washington in Seattle pursues a broad program of nuclear physics research. Research activities are conducted locally and at remote sites. The current program includes "in-house" research on nuclear collisions using the local tandem Van de Graaff and superconducting linac accelerators as well as local and remote non-accelerator research on fundamental symmetries and weak interactions and user-mode research on relativistic heavy ions at large accelerator facilities around the world.

Our results on hot Giant Dipole Resonance decay reverse longstanding conventional wisdom that the GDR width saturates at moderate excitation energy. We show, based on new preequilibrium and GDR decay measurements, together with a reanalysis of previous experiments, that the GDR width does not saturate, but appears to continue growing with excitation energy (temperature) in accord with theoretical expectations. These experiments are fundamental to understanding hot nuclear matter, in particular how normal modes of nuclear oscillation survive at high temperatures.

In the past year, we completed an extensive series of ^{4}He(a, g) reaction measurements of ^{8}Be analog-state g -decay, together with measurements of various g efficiency calibration reactions. Currently the data analysis is in progress to extract values for the isovector decay observables to be used in a precision A = 8 CVC/SCC test. When our results are combined with other experiments, we expect a sensitivity in the A = 8 system within a factor of 2 of that achieved in the A = 12 system by the Osaka group, who recently reported an exciting, small positive result.

The excitation energy dependence of the nuclear level density parameter has been studied by measuring evaporative proton and alpha spectra as a function of bombarding energy. The energy dependence observed is quite weak, but consistent with a recent theoretical prediction.

We have achieved a major milestone in our project to measure the S-factor for the ^{7}Be(p,g)^{8}B reaction. This S-factor is essential to our understanding of the solar production of energetic neutrinos. We have our experimental apparatus constructed and mostly debugged, and we have taken first data on the E_{cm} = 630 keV resonance and at 400 and 500 keV with a 13 mCi target. We have also measured the ^{7}Be(a,g) resonance reaction which we use as a target quality diagnostic.

The Russian-American Gallium Experiment (SAGE) has submitted an archive paper on the ^{51}Cr neutrino source experiment which is in press. The extraction data through December 1997 have been analyzed with the result that the solar neutrino flux times the Ga cross section is measured to be $67.2^{+7.2}_{-7.0}$, (statistical) $^{+3.5}_{-3.0}$ (systematic) SNU. These data are being prepared for publication.

The completion of construction of the Sudbury Neutrino Observatory was marked by an opening celebration April 29, 1998. Water fill began shortly before that, and is essentially complete as of this writing a year later. The water quality has met or exceeded expectations with respect to radioactivity, with the exception of Th in the heavy water, and it is likely that this too will fall within specifications once recirculation begins. Problems with high-voltage breakdown in connectors underwater have been substantially mitigated by re-gasifying the water with nitrogen. During the fill, many detector subsystems were brought to completion. The UW SNODAQ group has created a highly versatile realtime data-acquisition software system that has functioned superbly in the commissioning of the detector. The neutral-current detector (NCD) construction project centered at UW is nearing completion following a difficult, but successful, battle with residual ^{210}Po activity from radon daughters. All detectors, the NCD electronics, and the deployment system are expected to be finished this summer.

The emiT detector is in Seattle undergoing major upgrades to address problems encountered in the first run. It is expected that these upgrades will greatly enhance the high-voltage stability of the system, and enable the detector to meet its design goals. The second run of emiT is expected to commence in late 1999. Analysis of the data from the first run is essentially complete and is being prepared for publication.

We are preparing for the initial operation of RHIC later this year by preparing for HBT analysis of the data which will be produced by the STAR detector. This work includes an improved numerical procedure for dealing with HBT Coulomb corrections. We have continued our investigations of the phase space density of pions produced in ultrarelativistic heavy ion collisions and have found evidence of a universal scaling at CERN SPS energies.

In addition, during the past year the URHI group has made major improvements to NA49 global-variables EbyE analysis and STAR offline computing EbyE analysis software production. We have made several advances in fluctuation analysis theory (finite systems effects and the extension of linear response theory near a phase boundary and scale-dependent differential variance measures). We have made upgrades to STAR TPC tracking software and a generalized data browser and visualizer for URHI-related data (TPC tracking data, event generator output and general data bases).

Our equivalence-principle tests are becoming ever more powerful as we continue improving our torsion balances. This work has broad implications for cosmology and for Planck-scale physics-- for example Carroll has estimated that the slowly rolling scalar field scenario leads to "equivalence-principle" violations roughly 10^4 times larger than our 1994 limit. Our recent work on the strong equivalence principle has attained a differential acceleration sensitivity of 2×10^{-13} cm/s^2.

Our high-precision measurement of the positron-neutrino correlation in the superallowed decay of ^{32}Ar rules out scalar weak interactions at mass scales up to 4 times the W boson mass. A similar measurement in ^{33}Ar resolves a discrepancy regarding the Gamow-Teller contribution to the superallowed transition. The measurements also demonstrated the power of the technique for making precise measurements of the masses of nuclei far from stability.

As always, we encourage outside applications for the use of our facilities. As a convenient reference for potential users, the table on the following page lists the vital statistics of our accelerators. For further information, please write or telephone Professor Derek, W. Storm, Executive Director, Nuclear Physics Laboratory, University of Washington, Seattle, Washington 98195; (206) 543-4080, (e-mail: storm@npl.washington.edu) or can also refer to our web page: http://www.npl.washington.edu.

We close this introduction with a reminder that the articles in this report describe work in progress and are not to be regarded as publications or to be quoted without permission of the authors. In each article the names of the investigators have been listed alphabetically, with the primary author to whom inquiries should be addressed underlined.

We thank Richard J. Seymour and Karin M. Hendrickson for their help in producing this report.

Steve Elliott, Editor

Sre@u.washington.edu, (206) 543-9522

Barbara Fulton, Assistant Editor

TANDEM VAN DE GRAAFF ACCELERATOR

A High Voltage Engineering Corporation Model FN purchased in 1966 with NSF funds; operation funded primarily by the U.S. Department of Energy. See W.G. Weitkamp and F.H. Schmidt, "The University of Washington Three Stage Van de Graaff Accelerator," Nucl. Instrum. Meth. **122**, 65 (1974).

Some Available Energy Analyzed Beams

Ion	*Max. Current* *(particle m A)*	*Max. Energy* *(MeV)*	*Ion Source*
^{1}H or ^{2}H	50	18	DEIS or 860
^{3}He or ^{4}He	2	27	Double Charge-Exchange Source
^{3}He or ^{4}He	30	7.5	Tandem Terminal Source
^{6}Li or ^{7}Li	1	36	860
^{11}B	5	54	860
^{12}C or ^{13}C	10	63	860
* ^{14}N	1	63	DEIS or 860
^{16}O or ^{18}O	10	72	DEIS or 860
F	10	72	DEIS or 860
* Ca	0.5	99	860
Ni	0.2	99	860
I	0.01	108	860

* Negative ion is the hydride, dihydride, or trihydride.

Additional ion species available include the following: Mg, Al, Si, P, S, Cl, Fe, Cu, Ge, Se, Br and Ag. Less common isotopes are generated from enriched material.

BOOSTER ACCELERATOR

We give in the following table maximum beam energies and expected intensities for several representative ions. "Status of and Operating Experience with the University of Washington Superconducting Booster Linac," D.W. Storm *et al.*, Nucl. Instrum. Meth. A **287**, 247 (1990).

Available Energy Analyzed Beams

Ion	*Max. Current*	*Max. Practical*

	(pm A)	*Energy MeV*
p	>1	35
d	>1	37
He	0.5	65
Li	0.3	94
C	0.6	170
N	0.03	198
O	0.1	220
Si	0.1	300
^{35}Cl	0.02	358
^{40}Ca	0.001	310
Ni	0.001	395

TABLE OF CONTENTS

1.0 FUNDAMENTAL SYMMETRIES AND WEAK INTERACTIONS

1.1 Beta delayed alpha spectrum from ^{8}B decay and the neutrino spectrum in ^{8}B decay

E.G. Adelberger, H.E. Swanson and K.B. Swartz*

SNO will measure the energy spectrum of ^{8}B solar neutrinos reaching the earth. If neutrino oscillations occur, the spectrum will be distorted from its original shape and the deviation will contain information on the neutrino mixing parameters. Bahcall *et al.*[1] have pointed out that our ability to predict the undistorted shape of the ^{8}B neutrinos is limited by our knowledge of the final state continuum fed in ^{8}B decay. Two kinds of data are useful here, the beta and the beta-delayed alpha spectra in ^{8}B decay. Bahcall *et al.* showed that existing delayed-alpha data were inconsistent and chose to use a single measurement of the beta spectrum in obtaining a 'standard' ^{8}B spectrum. Because of the difficulty of making accurate beta spectrum shape measurements, we have chosen to make a careful remeasurement of the delayed alpha spectra in ^{8}Li and ^{8}B decays, paying special attention to the absolute calibration of the energy scale and to understanding the energy response of detectors. The ^{8}B data were taken during the period covered in the previous annual report.[2] Analysis of these data are still in progress. Careful attention is being paid to the absolute energy calibration which is based on the ^{148}Gd, ^{241}Au and ^{232}Th sources plus a relative calibration using a precision pulser. Source thicknesses were determined from data taken with the normal to the sources at various angles to the detector. Detector dead layer thicknesses were extracted from data when sources were moved in arcs centered on the Si detectors. Stopper foil thicknesses were determined by energy loss of ^{148}Gd α's in the foils. Results for the ^{8}B α-spectra will be presented as histograms as a function of E_α with corrections applied for all energy loss processes.

* Physics Department, Yale University, New Haven, CT.

[1] J.N. Bahcall *et al*., Phys Rev. C **54**, 411 (1996).

[2] Nuclear Physics Laboratory Annual Report, University of Washington (1998) p. 1.

1.2 Electron-neutrino correlations in ^{32}Ar and ^{33}Ar decays

E.G. Adelberger, M. Beck,[*] H. Bichsel, M.J.G. Borge,[†] A. García,[#] I. Martel-Bravo,[%] C. Ortiz,[#] H.E. Swanson, O. Tengblad[†] and the ISOLDE collaboration[%]

Our 1997 ISOLDE measurement of the electron-neutrino correlations in the superallowed decays of ^{32}Ar and ^{33}Ar was undertaken to search for scalar weak interactions which leave a "gold-plated" signature on the e-ν correlation coefficient a. If scalar couplings vanish, the ^{32}Ar decay will have a=+1, while scalar couplings, whatever their parity or time-reversal properties, lead to a <1. We measured a by analyzing the shapes of the delayed proton peaks following the superallowed decays. (Lepton recoil broadens the ^{32}Ar peak by ~30 keV, while the intrinsic width of the daughter state is only 20±10 eV.) We have continued to refine the analysis of our high-resolution proton spectra.[1] Our results are now in their final form and a paper on this work is being submitted.

During the last year the Monte-Carlo simulation of the experiment was improved to include the effects of a weak electron capture branch, the order-α radiative corrections[2] to the velocity distribution of the recoiling ^{32}Cl daughter nuclei, and the bending of the protons in the 3.5 T B-field. We fitted our data by folding the results of the Monte-Carlo simulation (which accounted for the mean energy losses of the individual protons from each decay event) with an analytic lineshape consisting of two low-energy exponential tails folded with a Gaussian. The ^{32}Ar and ^{33}Ar data were fitted by varying the weak interaction parameters $\tilde{C}_s$ and $\tilde{C}'_S$ (defined in Ref. 1) as well as the 6 free parameters of the lineshape (position, magnitude, plus 4 parameters describing the shape). The resulting lineshape was then compared to a "first principles" calculation that included the following effects:

1) the gaussian electronic resolution as measured by a pulser (3.0 keV and 3.3 keV, respectively),

2) a gaussian contribution from electron-hole statistics (Fano factor = 0.1),

3) energy-loss straggling (from both electronic and nuclear collisions) in the 22.7 μg/cm^2 catcher foil,

4) energy-loss straggling in the 22.6 μg /cm^2 dead layers of the PIN detectors (taking into account the fact that a significant fraction of the energy lost to delta electrons was deposited in the sensitive volume of the detectors),

5) energy lost to phonons rather than ionization of the Si detector, and

6) escape of the Si X-rays (the single escape probability is about 19%).

The good agreement of the extracted and calculated lineshapes gave us additional confidence in the analysis.

Our 1σ experimental ^{32}Ar constraint (which for the case of vanishing Fierz interference is a=0.9989±0.0052(stat.) ±0.0036(syst.) corresponds to a lower limit on the mass of a scalar particle with gauge coupling strength of $M_S \geq 4.1M_W$. Our constraints on $\tilde{C}_s$ and $\tilde{C}'_S$ are shown in Fig. 1.2-1, along with those from previous studies of Fierz interference[3] and the R-coefficient in ^{19}Ne beta decay.[4]

The electron-neutrino correlation in the superallowed decay of ^{33}Ar probes the Fermi-GT ratio of this $1/2^+ \rightarrow 1/2^+$ transition as well as weak-interaction parameters. We assume the Standard Model weak interaction and use a to measure B(F)/B(GT). Our preliminary ^{33}Ar result, a=0.944±0.002±0.003, disagrees with a previous determination,[5] a=1.02±0.02, but is in reasonable accord with a shell-model prediction,[6] a=0.93.

---

[*] Katholieke Universiteit, Leuven, Belgium.
[†] Institute de Estructura de al Materia, SCIC, Madrid, Spain.
[#] Department of Physics, University of Notre Dame, Notre Dame, IN.
[%] PPE Division, CERN, Geneva, Switzerland.
[1] Nuclear Physics Laboratory Annual Report, University of Washington (1998) p. 2.
[2] F. Glück, Nucl. Phys. A **628**, 493 (1998).
[3] W.E. Ormand, B.A. Brown and B.R. Holstein, Phys. Rev. C **40**, 2914 (1989).
[4] M.B. Schneider *et al.*, Phys. Rev. Lett. **51**, 1239 (1983).
[5] D. Schardt and K. Riisager, Z. Physik A **345**, 265 (1993).
[6] B.A. Brown and B.H. Wildenthal, At. Data Nucl. Data Tables **33**, 347 (1985).

Our results also give good values for the widths of the analog states in ^{32}Ar and ^{33}Ar. We obtain $\Gamma(^{32}Ar)=(20\pm10)$ eV and $\Gamma(^{33}Ar)= (180\pm15)$ eV. This latter result disagrees with the value $\Gamma = 115\pm15$ eV from the $^{32}S(\bar{p},p)$ reaction.[7] We plan to resolve this discrepancy by repeating the $^{32}S(\bar{p},p)$ measurement at the University of Wisconsin.

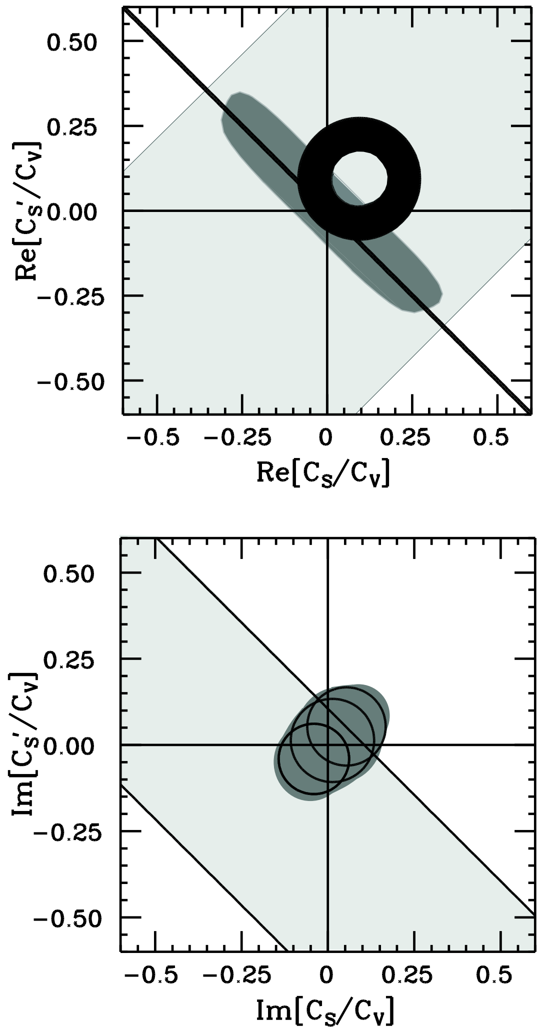

Fig. 1.2-1. 95% confidence limits on $\tilde{C}_S$ and $\tilde{C}'_S$. Upper panel: time-reversal-even couplings. The annulus is from our work; the narrow diagonal band is the Fierz-interference result from Ref. 4. The broad diagonal band shows result from *A*, *B*, *a* and $t_{1/2}$ in *n* decay;[8] the sausage-shaped area includes, in addition, constraints from positron helicities in ^{14}O and ^{10}C (Ref. 9),[9] Fierz interference in ^{22}Na (Ref. 10)[10] and *a* in ^{6}He decays. Lower panel: time-reversal-odd couplings. The circles are from our work and correspond to $\tilde{C}_S$ and $\tilde{C}'_S$ phases $\pm90^o$, $+45^o$ and -45^o. The shaded oval is the constraint with no assumptions as to this phase. The diagonal band is from the R-coefficent in ^{19}Ne decay (Ref. 4).

[7] P.M. Endt, Nucl Phys. A **521**, 1 (1990).
[8] Particle Data Group, Eur. Phys. J. C **3**, 622 (1998).
[9] A.S. Carnoy *et al*., Phys. Rev. C **43**, 2825 (1991).
[10] H. Wenninger, J. Stiewe and H. Leutz, Nucl. Phys. A **109**, 561 (1968).

1.3 Determination of the response function and efficiency for the 3 large NaI spectrometers

J.F. Amsbaugh, M.P. Kelly, J.P.S. van Schagen, K.A. Snover and D.W. Storm

In our measurement of the radiative isovector M1 and E2 decay widths (see Section 1.4) a set-up consisting of 3 large NaI spectrometer[1] is used. Since the γ-rays of interest in the ^{4}He(α,γ)^{8}Be radiative capture reaction have an energy of ≈13 MeV, it is important to know the efficiency $\eta\Delta\Omega / 4\pi$ and response for each NaI spectrometer for γ-ray energies in this range.

Last year we reported on an elegant way to measure these quantities simultaneously using the $^{10}B(^3He, p\gamma)^{12}C$ reaction[2] at E(^{3}He) = 4.1 MeV. The set-up has been improved by using a $\Delta E - E$ Si-telescope at 0°, consisting of a 200 μm thick transmission Si-detector and a 3000 μ thick Si(Li)-detector. This allows a better separation of the contribution of the (^{3}He,p) channel in the singles spectrum from the contributions due to (^{3}He,d) and (^{3}He,α). Furthermore, the 13 mg/cm^2 Ni stopper foil was moved closer to the target. Both improvements lead to a much better separation of the proton group populating the 15.11 MeV level in ^{12}C in the proton singles spectrum from the proton group from the ^{12}C(^{3}He,p)^{14}N$_{g.s.}$ reaction. The measured absolute efficiencies $\eta\Delta\Omega / 4\pi$ with a cut on the γ-ray energy of 12 MeV, are 1.49×10^{-3} (UW), 1.58×10^{-3} (Illinois) and 2.04×10^{-3} (OSU) with an error of ±2.4%. In addition, during the He+He runs the relative efficiencies at 15.1 MeV between the different detectors were also measured using the ^{12}C(p,γ)^{13}N reaction at E_p = 14.26 MeV.

In the Fig. 1.3-1, a typical γ-ray spectrum gated on protons populating the 15.11 MeV level in ^{12}C is shown. The curve is the result of a response function fit to the data. The response function used in the fit is given by Sandorfi and Collins[3] and consists of a gaussian part plus an exponential tail on the low energy side.

Using the same set-up, the efficiency and response function have been measured at E_γ = 8.31 MeV using the ^{13}C(^{3}He,pγ)^{15}N reaction. The response for γ rays of 13.3 MeV has been measured by studying the ^{15}N(p,γ)^{16}O reaction at E_p = 1.26 MeV. The analysis of these reactions is underway, with the goal of determining the dependence of the detector response on gamma energies.

Illinois Line, fitted

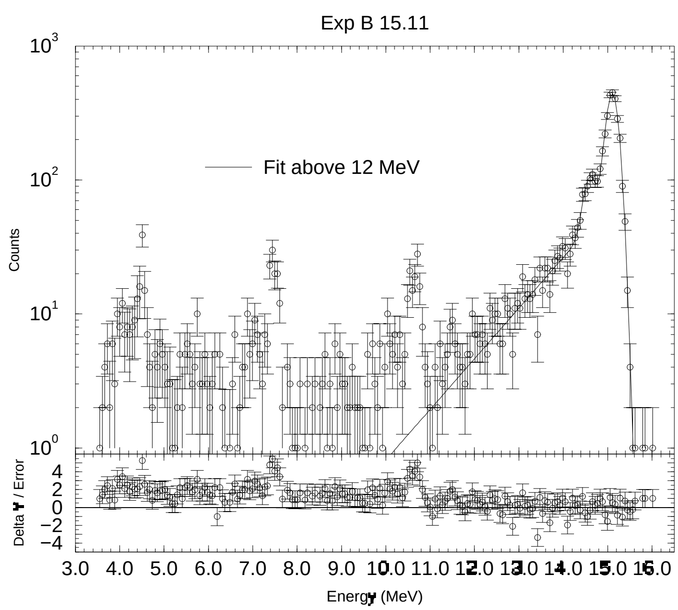

Fig. 1.3-1. Gamma-ray spectrum for Illinois detector gated on protons populating the 15.11 MeV level in ^{12}C. The curve is the result of a fit to the response in the region above E_γ = 12 MeV.

[1] Nuclear Physics Laboratory Annual Report, University of Washington (1997) pp. 57-58.
[2] Nuclear Physics Laboratory Annual Report, University of Washington (1998) p. 6.
[3] A.M. Sandorfi and M.T. Collins, NIM **222**, 479 (1984).

1.4 Precision measurements of the angular distribution and excitation function of the $^{4}He(\alpha,\gamma)^{8}B$ reaction

J.F. Amsbaugh, M.P. Kelly, J.P.S. van Schagen, K.A. Snover and D.W. Storm

A high-precision measurement of the $^{4}He(\alpha,\gamma)^{8}Be$ radiative capture reaction has been performed with the purpose of determining the isovector M1 and E2 decay widths for a precision test of CVC and second class currents in the mass-8 system.[1] Data have been collected with our 3 large NaI spectrometer set-up[2] during two data taking periods. In the measurement a short gas-cell (3.75" diameter) was filled with He gas at 750 Torr. At each beam energy, the background was measured by replacing the He-gas with H_2-gas at 675 Torr. This ensures the same energy loss of the beam over the gas-cell as when it is filled with He-gas and therefore a similar background due to the Kapton windows. The beam energy was monitored in between runs using two Si-detectors at ±25° and a thin C scattering foil in a separate scattering chamber upstream.

In Fig. 1.4-1, the data collected in the first run are shown. The data points were obtained by integrating the background subtracted spectra over a sliding window with limits which shift proportional to the beam energy. As reference values, limits of 12 MeV and 15.5 MeV at E(^{3}He) = 34.1 MeV were employed. The curves through the data are the result of a simultaneous fit of the angular distribution and the excitation function using a formalism given by Barker[3] and specifically Eq. (1) in De Braeckeleer[4] for the analytic form. The result for the isoscalar to isovector M1 ratio is $\varepsilon = 0.00 \pm 0.02$. For the isovector E2 to isovector M1 ratio δ_1 we obtain $\delta_1 = 0.03 \pm 0.03$ while the isoscalar E2 to isovector M1 ratio $\delta_0 = 0.15 \pm 0.04$, in good agreement with our results from the Mark I experiment (see Ref. 3). Fig. 1.4-2 shows the data collected during the second data taking run, for which the statistics are twice that of the first run. Analysis of the second run as well as a determination of the absolute isovector M1 decay width are in progress.

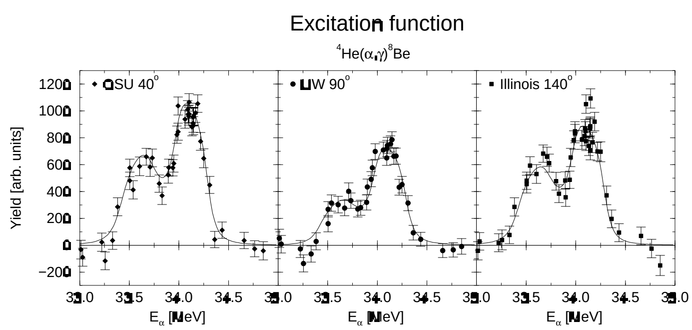

Fig. 1.4-1. Excitation curves for the $^{4}He(\alpha,\gamma)^{8}Be$ reaction measured with the OSU, UW and Illinois detectors. The curves through the date are discussed in the text.

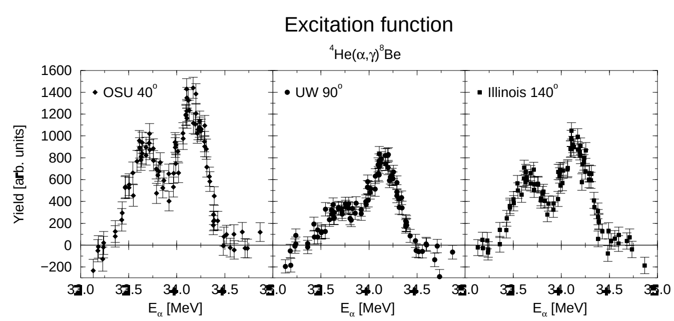

Fig. 1.4-2. Excitation curves for the $^{4}He(\alpha,\gamma)^{8}Be$ reaction measured with the OSU, UW and Illinois detectors in the second data taking run. The magnitude of the yields differ due to the detector efficiencies and the reaction angular distribution.

[1] Nuclear Physics Laboratory Annual Report, University of Washington (1998) p. 7.
[2] Nuclear Physics Laboratory Annual Report, University of Washington (1997) pp. 57-58.
[3] L.D. De Braeckeleer *et al*., Phys. Rev. C **51**, 2778 (1995).
[4] L.D. De Braeckeleer *et al*., Phys. Rev. C **52**, 3509 (1995).

1.5 Gamma ray spectrum from the $^4He(\alpha,\gamma)^8Be$ reaction

J.F. Amsbaugh, J.P.S. van Schagen, K.A. Snover and D.W. Storm

In order to determine the isovector M1 width in the transition from the analog of the ground states of ^{8}Li and ^{8}B to the 3 MeV state in ^{8}Be, it is necessary to remove the effects of transitions to the tails of the resonances. This can be done using the R-matrix formalism in conjunction with a measurement of the gamma ray spectrum at a single angle and beam energy, provided the spectrum can be determined at low gamma ray energy where contributions from the tail become significant. In a previous measurement[1] the quantity R_γ, the ratio of the isovector transition matrix elements to the tail and to the state at 3 MeV was defined. Results of that measurement were $R_\gamma = 1.6 \pm 1.8$ These results disagreed with shell-model predictions,[1] which suggested values between -3 and -6. The poor accuracy resulted from the poor quality of the gamma ray data for energies below about 11 MeV and from limited information on the response function.

In order to obtain better spectra, we built the large gas cell described previously,[2] and we have fit the data obtained with it using the R-matrix formalism, in conjunction with the improved line shapes described in Section 1.3. The beam energy was integrated across the large gas cell, with photon production weighted by the geometrical acceptance calculated for the shielding geometry. Data above 9.75 MeV photon energy are fit. The fit results and the data are shown in Fig. 1.5-1. The χ^2 value is 100.4 for 100 degrees of freedom. The preliminary value of R_γ that we now obtain is -12 ± 1.4.

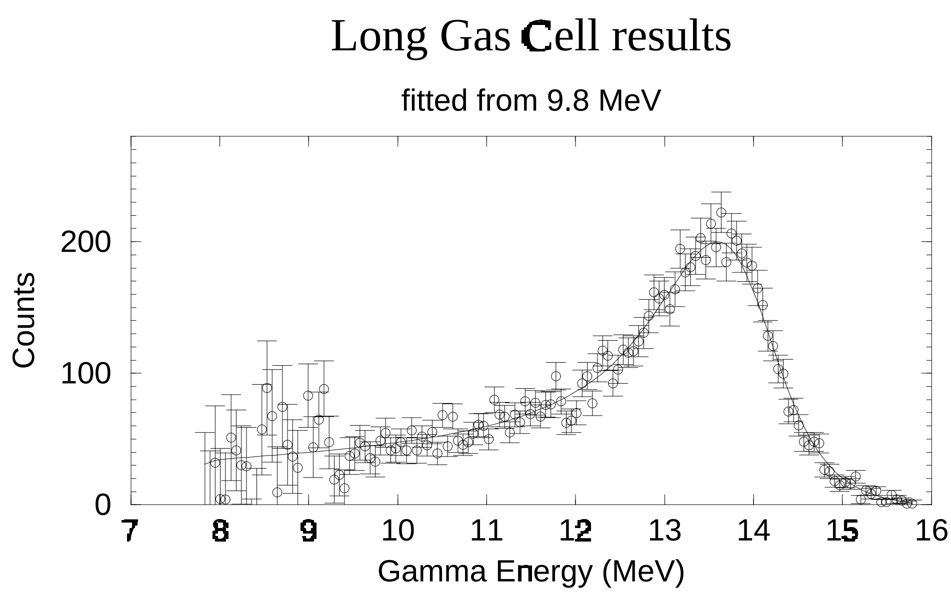

Fig. 1.5-1. Photon spectrum obtained with the large gas cell, with an incident beam energy of 34.1 MeV. The fit, described in the text, is to the data above 9.75 MeV. The normalization, location of the 3 MeV state, and the ratio R_γ, described in the text, are varied.

[1] L. D. DeBraeckeleer *et al.*, Phys Rev C **51** 2778 (1995).
[2] Nuclear Physics Laboratory Annual Report, University of Washington (1997) p. 7.

1.6 Time reversal in neutron beta decay – the emiT experiment

M.C. Browne, H.P. Mumm, A.W. Myers, R.G.H. Robertson, T.D. Steiger, T.D. Van Wechel, D.I. Will and J.F. Wilkerson

The emiT experiment is a search for time-reversal (T) invariance violation in the beta decay of free neutrons. The observation of CP (charge conjugation - parity) violation in the neutral kaon system, coupled with the theoretical expectation that the combined CPT symmetry must hold, indicates that T-violation must occur at some level in weak decays. However, today some 35 years since its discovery, the origin of CP violation is still not well understood. Although CP violation can be accommodated within the standard model of nuclear and particle physics, it may also be an indication of physics beyond the current standard model.

The T-violating observables in beta decay are predicted to be extremely small in the standard model and hence beyond the reach of any current measurements.[1] But potentially-measurable T-violating effects are predicted to occur in some non-standard models, such as left-right symmetric models, exotic fermion models, and lepto-quark models.[2,3] Hence a precision search for T-violation in neutron beta decay allows one to test for physics beyond the current standard model.

emiT probes the T-odd triple correlation (between the neutron spin and the momenta of the neutrino and electron decay products) in the neutron beta-decay distribution. The coefficient of this correlation, *D*, is measured by detecting decay electrons in coincidence with recoil protons while controlling the neutron polarization.

The emiT experiment utilizes a beam of cold (<10 meV), polarized neutrons from the Cold Neutron Research Facility at the National Institute of Standards and Technology (NIST) in Gaithersburg, MD. The collaboration includes scientists from Los Alamos National Laboratory, NIST, the University of California at Berkeley/Lawrence Berkeley National Laboratory, the University of Michigan, the University of Notre Dame, and the University of Washington's Nuclear Physics Laboratory.

The emiT experiment was installed on the NG-6 beamline at NIST from November of 1996 until September of 1997. A total of roughly 14 million coincidence events were recorded and the maximum sustained coincidence rate observed was ~7 Hz. Analysis of these data is nearly complete and we expect to achieve a sensitivity to *D* at least comparable to the current combined world average. The sensitivity of the initial run will almost certainly be limited by systematic errors which arose from disabled channels in the proton detector segments. The root cause of this problem was excessive energy loss in the proton detectors and associated dead time, noise, and electronic failures due to high voltage sparks. Work is underway on an upgrade to the apparatus (see the next section), which should solve the problems experienced in the first run. A new measurement is planned at NIST in 2000.

---

[1] M. Kobayashi and T. Maskawa, Prog. Theor. **49**, 652 (1973).
[2] P. Herczeg, in *Progress in Nuclear Physics*, W.-Y.P. Hwang, ed., Elsevier Sciences Publishing Co. Inc. (1991) p. 171.
[3] E.G. Wasserman, *Time Reversal Invariance in Polarized Neutron Decay*, Ph.D. thesis, Harvard University, (1994).

1.7 Improvements to the emiT detector

M.C. Browne, H.P. Mumm, A.W. Myers, R.G.H. Robertson, T.D. Steiger, T.D. Van Wechel, D.I. Will and J.F. Wilkerson

Technological advances in neutron polarization and an optimized detector geometry should allow emiT to attain a sensitivity to D of 3×10^{-4}, given the current neutron capture flux available at the NG-6 beamline at NIST (1.4×10^{9} n/cm^{2}s). This level of sensitivity represents a factor of five improvements over previous neutron T tests, and may permit restrictions to be placed on several extensions to the Standard Model that allow values of D near 10^{-3}.

The emiT detector consists of four plastic scintillator paddles for electron detection and four arrays of large-area PIN diodes to detect protons. The eight detector segments are arranged in an alternating octagonal array about the neutron beam. The angle between any given proton detector and it's opposing electron detectors is 135°. This takes advantage of the fact that the electron--proton angular distribution is strongly peaked around 160° due to the disparate masses of the decay products. When compared to the 90° geometry used in previous experiments, an octagonal geometry results in an increased signal rate equivalent to roughly a factor of three increase in neutron beam flux.[1]

The protons produced in the decay of free neutrons have a relatively low energy. (The Q-value for n-decay is 782 keV, producing protons with energies <751 keV.) While this allows for a delayed coincidence trigger between the proton and electron (eliminating much of the background due to cosmic rays) it makes detection difficult. The PIN diode array and associated electronics are therefore held at -30 to -36 kV to accelerate the protons to a detectable energy.

Throughout the first run the PIN diodes exhibited a higher than expected energy loss, effectively pushing the proton signal into the background. Using an energy window which included a reasonable fraction of the decay protons resulted in a dramatically increased coincidence rate. To counter this problem the detector was run at around 36 kV, higher than the nominal design value. Operating at this higher voltage led to more frequent instances of high voltage related breakdown and the associated damage to sensitive DAQ electronics. As a consequence, emiT's forty-eight populated proton detector channels were often not operating simultaneously. As the detector was not fully symmetric, systematic effects were less effectively canceled.

In order to assure that the second run is not affected by these problems, a number of detector upgrades are currently in progress at NPL. Upgrades include isolation of the VME shaper ADC cards through the use of analog fiber-optic links, improvements to the DAQ electronics, and considerable changes in the data acquisition software. In addition, replacement of the PIN diode detectors with either PIPS or Surface Barrier detectors is under consideration, and attempts are being made to isolate the locations of high voltage breakdown. It is possible that minor design changes will alleviate this problem.

The fiber-optic links are modular in design, allowing for easy replacement of failed parts. The links will isolate much of the DAQ electronics. Damage due to breakdowns is therefore expected to be much less. Sharper thresholds in the proton DAQ shaper ADC boards will reduce background rates, allowing operation at lower voltages. Replacement detectors will have thinner dead layers, also allowing operation at lower voltages. In addition, changes in the DAQ software will allow closer monitoring of the state of the detector. With these changes it is likely that the second run will meet the design goal of 3×10^{-4}.

[1] E.G. Wasserman, *Time Reversal Invariance in Polarized Neutron Decay*, Ph.D. thesis, Harvard University (1994).

1.8 PNC spin-rotation of cold neutrons in a liquid helium target

E.G. Adelberger, S. Baessler, J.H. Gundlach, B.R. Heckel, D.M. Markoff,* U. Schmidt and H.E. Swanson

The major accomplishments of the experiment to measure the parity violating rotation of the polarization vector of a cold neutron beam as it traverses a target of liquid helium are listed below. The goal of the research is to measure the PNC neutron-alpha coupling constant, from which the weak pion-nucleon coupling constant can be extracted.

This experiment receives support from the National Science Foundation, as well as from the Department of Energy through the Nuclear Physics Laboratory. The NSF grant was renewed for three years in June, 1998. The renewal was to support the second round of experimental measurements at the NIST reactor. The first measurements were completed in 1997 and proved to be of sufficient quality to warrant further effort.

The Spin Rotation collaboration has been enlarged significantly. For the second phase of the experiment, investigators from TUNL and Indiana University have joined the group. New collaborators include M. Snow and G. Hansen from Indiana University, D. Haase and C. Gould from TUNL, P. Huffman from NIST, and U. Schmidt and S. Baessler from the University of Washington. They join the original collaboration of B. Heckel, E. Adelberger, D. Markoff, F. Weitfeldt, S. Penn, J. Gundlach, S. Dewey, and H.E. Swanson. The collaboration has held two meetings during the past year to design the new experiment.

The major breakthrough on the experimental side has been the decision to rebuild the cryostat to make the helium targets superfluid. The superfluid density is 20% larger than that of normal liquid helium, making the PNC signal 20% larger, and more importantly, superfluid helium does not support temperature gradients or the formation of bubbles that could lead to systematic errors.

During the past year, problematic components of the original cryostat (mostly arising from unreliable commercial glue joints) have been replaced by reliable indium seals. The major task that remains before new data can be taken is to rebuild the helium targets to support the use of superfluid helium. The design of this new target chamber has been agreed upon and drawings are being prepared for our shops.

* TUNL, North Carolina State University, Durham, NC.

1.9 Construction and tests of a new rotating equivalence principle test apparatus

E.G. Adelberger, M. Benz, J.H. Gundlach, B.R. Heckel, B.P. Henry, C.D. Hoyle, S. Merkowitz and H.E. Swanson

We are building a new rotating torsion balance to search for violations of the equivalence principle due to new fundamental forces with Yukawa ranges >1 m. As described in previous reports, the balance will consist of a composition-dipole pendulum containing titanium, beryllium, or aluminum testbodies. The pendulum is suspended inside a vacuum chamber which hangs from a gimbal attached to a constantly rotating turntable.

We are currently operating a test torsion balance that is primarily intended for measuring and nulling the ambient low-order gravity gradients and for debugging the turntable. The balance is surround by a constant-temperature shield inside a hermetically sealed enclosure. The temperature of this enclosure will be actively controlled.

The Q_{21}, Q_{22}, Q_{31} gravity gradients, have been measured by mounting special testbodies on the pendulum. We have installed ~800 kg of machined Pb masses which compensate the Q_{21} gravity gradient to about 101%. A more precise cancellation will be made once the final local mass distribution is established. The Q_{21} compensation then allowed us to measure the Q_{31} gradient and design appropriate compensators. A set of Q_{22} compensators has been installed.

The design for the final pendulum has been finished and is being manufactured by a commercial company.[1] The pendulum body will be made from beryllium and carry 8 barrel-shaped testbodies bolted into conical seats. When outfitted as a composition dipole, the pendulum's first non-vanishing m=1 multipole moment nominally occurs at l=7. The m=0 moments, which could turn into a m=1 moment due to an unwanted tilt of the pendulum, vanish up to l=5. The pendulum will have four flat mirrors mounted to its side, one of which will be used for two reflections of the autocollimator light beam using a stationary edge reflector. Our final pendulum design was based on aluminum prototypes manufactured in our shops that were used to test the reproducibility of testbody positioning in the conical seats. The beryllium, aluminum and titanium testbodies have been designed and various prototypes have been built. Special gradiometer bodies for this pendulum have also been designed.

We have tested several heat-treating schemes using radiative heating with adjacent hot filaments in an attempt to quickly reduce the fiber drift relaxation rate and the associated torsional noise. Even though several hundred °C were reached in the fiber, a bake of the entire system for one day at ~80° C produced the smallest fiber drift rates.

[1] Spreedring Inc., Cullman, Alabama.

1.10 Construction of an apparatus to measure the gravitational constant

E.G. Adelberger, J.H. Gundlach, B.R. Heckel and H.E. Swanson

We have built the main components of a rotating torsion balance apparatus dedicated to measure the gravitational constant. The apparatus consists of a flat vertical pendulum suspended from a thin torsion fiber inside a vacuum can located between a set of attractor masses. The vacuum can is mounted on a turntable and initially rotates at a constant speed. A feedback is then turned on that accelerates the turntable to minimize the torsion fiber twist. Therefore the gravitational angular acceleration is directly transferred to the turntable and we have demonstrated[1] that this acceleration can be read out with an commercial angle encoder. Since the fiber twist is minimal in our method uncertainties due to in- and anelasticity[2,3,4] do not enter directly. The flat vertical pendulum is used to reduce uncertainties due to the mass distribution of the pendulum: the pendulum's mass quadrupole moment, q_{22}, divided by the moment of inertia to which the dominant torque is proportional will become a constant. A certain aspect ratio of a rectangular pendulum and an attractor mass distribution as shown in the figure below and described in more detail in Ref. 1 will eliminate any significant coupling due to other multipole moments. The attractor masses are mounted on a second coaxial turntable. They can be rotated at a different speed and direction and will effectively discriminate against gravitational angular accelerations due to objects in the vicinity.

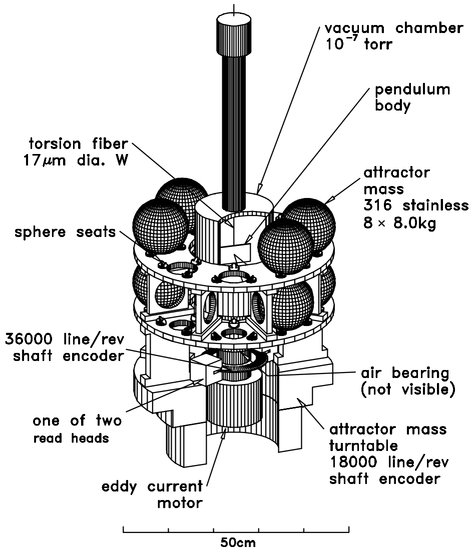

We have built all the major components of the apparatus. The pendulum is made from a 1.5 mm thick, 76 mm wide gold coated glass plate hung from a 17 μm diameter W-fiber. A parallel laser beam from an autocollimator is reflected by a series of mirrors twice from the front and twice from the back side of the plate. The system amplifies the twist angle optically by eight while it is insensitive to rotations about any other direction. The vacuum chamber is pumped by an 8l/s ion pump to the 10^{-7} torr range and sits on an airbearing turntable. A 36,000 line/rev optical shaft encoder that is read with two readheads was mounted directly to the airbearing. The system is driven by an eddy current motor consisting of a stator from a 400 hz motor and a copper drag cup. The motor is driven with three phases powered with three op-amps. A digital signal processor (DSP) will compute the feedback function directly from the autocollimator signal.

Fig. 1.10-1. Schematic of the apparatus.

The attractor turntable is finished. It is loaded with eight 125 mm diameter 316-stainless steel spheres weighing ~8 kg each and placed at a radius of 165 mm. Each sphere sits on three stainless steel seats that are mounted in a cast aluminum plate which in turn is supported from a 5cm thick aluminum disk bolted to the turntable. The turntable itself is made from a high precision steel double angular contact trust bearing on which a 18,000 line/rev angle encoder is mounted. A small DC motor is driving the system with a friction drive. The DSP will be used to hold the rotation rate constant.

The DSP was interfaced with 8 DAC's and 16 ADC's to read both angle encoders and several other sensors. It will upload the data directly to its PC host computer.

After placing the apparatus in its final location in the center of the cyclotron cave, we expect to begin debugging and data taking in the next year.

The ultimate precision on G we hope to achieve with this instrument is in the 10^{-5} range.

---

[1] J.H. Gundlach *et al*., Phys Rev. D **54**, R1256 (1996).
[2] K. Kuroda, Phys. Rev. Lett. **75**, 2796 (1995).
[3] C.H. Bagley and G.G. Luther, Phys. Rev. Lett. **78**, 3047 (1997).
[4] S. Matsumura *et al*., Phys. Lett A **244**, 4 (1998).

1.11 New result of the Rot-Wash torsion balance

E.G. Adelberger, J.H. Gundlach, B.R. Heckel, C.D. Hoyle, G.L. Smith and H.E. Swanson

Since our last report,[1] we have reduced the statistical uncertainty of our equivalence principle data and improved our understanding of gravitational systematic effects.

Because of the close proximity of the attractor to the pendulum, gravitational effects have always been the major systematic concern with this apparatus. We measure the imperfections of the pendulum by rotating sections of the attractor on lazy susans; we measure imperfections of the attractor by using special gradiometer test bodies. With this information, we may correct our signal for the three lowest order torques in the gravity gradient expansion. To test our ability to make such corrections, we produced a pendulum with large values of the two lowest order gravitational moments and placed it in a source with similarly large gradients. We then proceeded with our normal data-taking protocol. We expected the gravitational corrections to account for the observed torques in this case, since any other perturbations will be tiny compared to the exaggerated gravitational signal. Indeed, after applying our standard analysis, we found the corrected signal to be within 1.1 standard deviations of zero (Fig. 1.11-1). The uncertainty in these corrections is ~0.7% of the observed signal.

Our preliminary equivalence principle results yield a differential acceleration, a_{Cu}-a_{Pb}, of $(-0.7\pm2.9) \times 10^{-13}$ cm/s^2 toward ^{238}U. For comparison, it would take 11 days at this acceleration for an object's speed to match that of the continental drift in the east pacific (8.8 cm/yr). We expect to publish a complete description of this experiment with new results in the coming months.

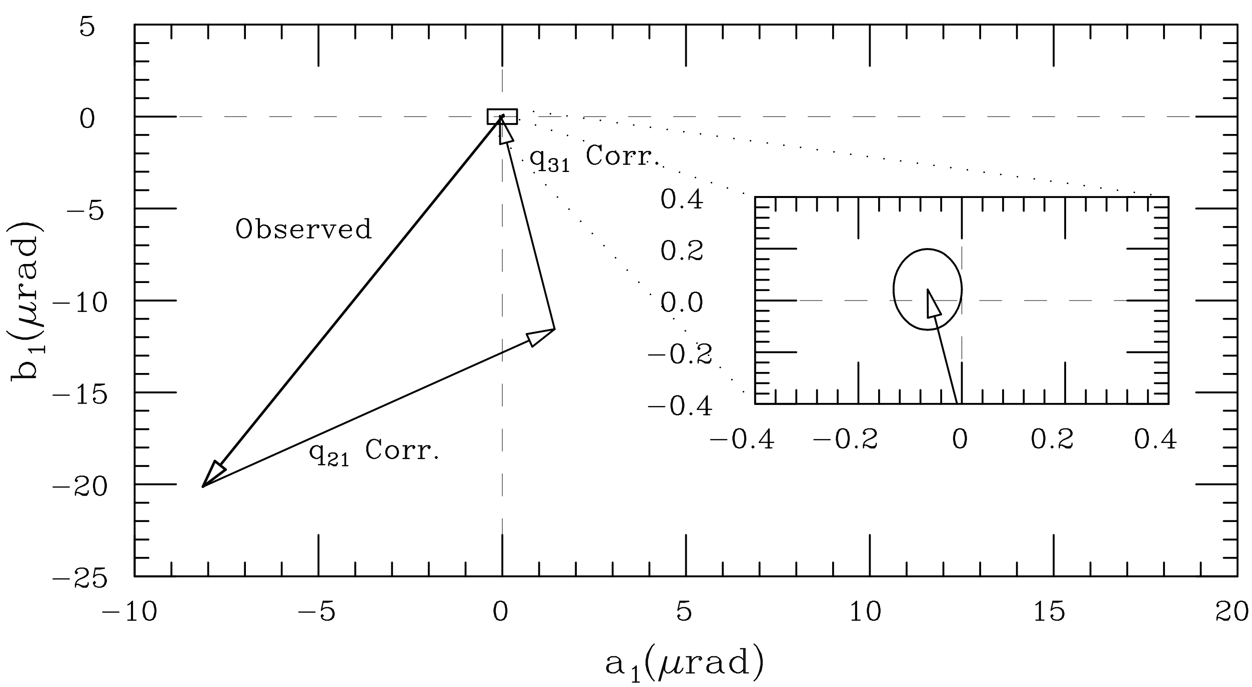

Fig.1.11-1. The vectors describing the observed torque on the pendulum and the calculated gravitational corrections under the exaggerated circumstances are shown. The shaded region is the 1-σ uncertainty in the difference.

[1] Nuclear Physics Laboratory Annual Report, University of Washington (1998) p. 15.

1.12 An unambiguous test of the Equivalence Principle for gravitational self-energy

E.G. Adelberger, S. Baeβler, J.H. Gundlach, B.R. Heckel, S.M. Merkowitz, U. Schmidt and H.E. Swanson

Einstein's Equivalence Principle (EP) requires the exact identity of gravitational and inertial masses. The Strong Equivalence Principle (SEP) specializes this to the component of mass due to gravitational self-energy. The SEP is an important test of theories of gravity because it probes a nonlinear aspect of the interaction, and is violated by metric theories that contain more than one field. Nordtvedt[1] noted that the SEP could be tested by using Laser Lunar ranging (LLR) to compare the accelerations of the earth and moon towards the sun. (Tests of the SEP require astronomical bodies -- gravitational self-energy reduces the earth's and moon's mass by only 4.6 and 0.2 parts in 10^{-10} respectively.) One analysis[2] of the LLR data yield $\Delta a_{LLR} / a_s = (3.2\pm4.6)\times10^{-13}$ and another analysis[3] independent of the first yields $\Delta a_{LLR} / a_s = (-3.6\pm4.0)\times10^{-13}$. (We define $\Delta a / a_s = (a_e - a_m) / [(a_e + a_m)/2]$, a_e is the acceleration of the earth towards the sun, and a_m is the acceleration of the moon towards the sun.)

However, the LLR result is ambiguous because the earth and moon "test bodies" differ in two important ways: the earth is more massive than the moon (which probes the EP for gravitational self-energy) and the earth has an Fe-Ni core while the moon does not (which probes the usual composition-dependence test of the EP). We remove the ambiguity of this important test by using a torsion balance to compare the accelerations of "moon" and "earth core" test bodies towards the sun, thereby probing the composition dependent effect alone. In the last year we upgraded the Eöt-Wash II torsion balance with a new turntable controller which enabled us to increase our signal frequency, and we decreased the fiber noise by running at a lower temperature. Our current result for a composition-dependent component of the earth-moon differential acceleration is $\Delta a_{CD} / a_s = [-2\pm3(\text{stat.})\pm2(\text{syst.})]\times10^{-13}$.

Table 1.12-1. Preliminary error budget.

Source of error:	$\delta(\Delta a_{CD} / a_s)$
Diurnal tilt variations	2.1×10^{-13}
Gravity gradients	0.9×10^{-13}
Temperature effects	0.6×10^{-13}
Magnetic effects	0.05×10^{-13}
Statistical error	3.0×10^{-13}

The LLR results from Refs. 2 and 3 and our data imply $\Delta a_{SEP} / a_s = \Delta a_{LLR} / a_s - \Delta a_{CD} / a_s = (5\pm6)\times10^{-13}$ and $(-2\pm5)\times10^{-13}$, respectively, providing a test of the SEP at the 1.4×10^{-3} level.

The uncertainty of LLR analysis is expected to drop by a factor of 2-3 in the near future.[4] Further upgrades of our apparatus are underway to decrease the statistical error and the tilt sensitivity. These upgrades should yield a sufficiently good result that our data will not limit the precision of the SEP test. Preliminary results are reported in proceedings.[5,6] One of us (S.B.) thanks the Alexander v. Humboldt-Stiftung for their financial support.

[1] K. Nordvedt, Phys. Rev. D **37**, 1070 (1988).
[2] J.G. Williams *et al.*, Phys. Rev. D **53**, 6730 (1996).
[3] J. Müller *et al.*, *Proceedings of the 8th Marcel Grossman Meeting*, Jerusalem,Israel, 1997.
[4] K. Nordvedt, private communication.
[5] E.G. Adelberger, *Proceedings of the WEIN Conference*, Sante Fe, NM 1998.
[6] B. Heckel *et al.*, *Proceedings of the 32nd COSPAR Scientific Assembly*, Nagoya, 1998.

2.0 NEUTRINO PHYSICS

2.1 The Sudbury Neutrino Observatory

Q.R. Ahmad, J.F. Amsbaugh, M.C. Browne, T.V. Bullard, T.H. Burritt, P.J. Doe, C.A. Duba, S.R. Elliott, J.E. Franklin, A.A. Hamian, G.C. Harper, K.M. Heeger, M.A. Howe, R. Meijer Drees,[*] A.W. Myers, A.W.P. Poon,[†] R.G.H. Robertson, H. Seifert,[#] M.W.E. Smith, T.D. Steiger, T.D. Van Wechel and J.F. Wilkerson

The Sudbury Neutrino Observatory (SNO), is a joint Canadian/US/UK effort to measure the spectral distribution and flavor composition of the flux of the higher-energy, ^{8}B neutrinos from the Sun by using a 1000 metric ton detector of heavy water. The SNO detector relies on three different neutrino interaction processes.

$^{2}\mathrm{H} + \nu_{\mathrm{e}} \rightarrow \mathrm{p} + \mathrm{p} + \mathrm{e}^{-}$	Charged Current (CC);
$^{2}\mathrm{H} + \nu_{\mathrm{x}} \rightarrow \mathrm{p} + \mathrm{n} + \nu_{\mathrm{x}}$	Neutral Current (NC);
$\mathrm{e}^{-} + \nu_{\mathrm{x}} \rightarrow \mathrm{e}^{-} + \nu_{\mathrm{x}}$	Elastic Scattering (ES).

Because of this unique sensitivity to the known flavors of neutrinos, SNO should be able to yield a definitive answer to the question of whether neutrino flavor oscillations are occurring in the Sun. As a second generation solar neutrino detector, SNO will also have a significant increase in statistical sensitivity compared to present detectors assuming an energy threshold of 5 MeV, the SNO detector, is expected to observe 12.7 CC events/day (Standard Solar Model/2), 5.5 NC events/day (SSM), and 1.2 ES events/day (SSM/2).

This past year SNO and the University of Washington SNO group have achieved a number of major milestones. Construction of the detector was completed and the filling and commissioning phase of the experiment was started. By the end of 1998, the detector had been filled past the halfway point with heavy water. The acrylic vessel has proven to be sound and has behaved as expected during the fill process.

In April 1998, the underground commissioning of the electronics and data acquisition systems was initiated. The SNO data acquisition (DAQ) system and monitoring tools developed by the UW group are currently in routine use supporting readout of the full set of PMT electronics. The object oriented data acquisition system has proven to be quite robust during recent data collection runs. These tools are essentially ready for the start of production solar neutrino runs.

A large amount of commissioning data and source calibration data has now been acquired with the DAQ system. We have been involved in various aspects of the analyses of these data.

Our major effort to develop a discrete neutral current sensitive detector (NCD) array has also progressed. We have now entered full production and are busy constructing the ^{3}He-filled Ni proportional counters. By the end of 1998 we had delivered 15% of the neutral current array to site along with a preliminary NCD data acquisition system. This system is installed and operating underground and we are currently acquiring cool-down data from these counters.

The completion of the heavy water fill to the full 1000 ton capacity of SNO was finished April 26, 1999; acquisition of solar neutrino data should commence shortly thereafter.

---

[*] 8140 Lakefield Drive, Burnaby, British Columbia, Canada.
[†] Lawrence Berkeley Laboratory, Berkeley, CA.
[#] Sudbury Neutrino Observatory, Sudbury, Ontario, Canada.

2.2 SNO commissioning activities

Q.R. Ahmad, M.C. Browne, C.A. Duba, A.A. Hamian, M.A. Howe, K.M. Heeger, A.W. Myers, R. Meijer Drees,* P.M. Thornewell† and J.F. Wilkerson

During 1998 all major construction activities on the SNO detector reached completion, and commissioning activities took precedence. During the year, personnel from all SNO institutions participated in the commissioning tasks at the SNO site in Sudbury, Ontario. The commissioning of the detector involved, among other things, the successful integration and interfacing of the following detector components:

- Photo multiplier tubes (PMTs);
- Electronics;
- Data Acquisition;
- Calibration;
- Analysis.

The SNO group at the University of Washington along with other members of the collaboration was directly involved in the systematic task of integrating these components into the detector and subsequently verifying that the overall system was functioning within allowed parameters. As a result of the concerted efforts of the collaboration, we currently have in place all the primary and critical components of the detector and the commissioning phase of the experiment is nearing completion.

An integral part of the detector commissioning is the demonstration of a robust and dependable Electronics and Data Acquisition System (EDAS). The on-site deployment and successful integration of an optimally functional EDAS required the critical characterization and shakedown of all hardware and software components of this system. Members of the UW DAQ group, working in close concert with the Electronics group, spent a considerable amount of time on-site to facilitate and oversee the commissioning of the EDAS. The UW SNO group has also been involved in building comprehensive data analysis and data monitoring tools which have been utilized to study the data acquired during the commissioning phase.

SNO started taking air-fill (no water) data with partial electronics installed underground during the winter of 1998. In March the collaboration reached a major milestone by recording the first physics event at SNO, which at the time had around 1500 active photo multiplier tubes. The event comprised a muon traversing the edge of the acrylic vessel, producing light and illuminating the active PMTs. By that time we had managed to implement the DAQ system to the extent that we were able to routinely take data with a minimal amount of expert intervention. Part of the DAQ commissioning process has been both to optimize the software performance and to tune the software to allow easy and clear operator interactions with the complex detector electronics. The resulting intuitive and user friendly DAQ design has proven quite successful and enabled us to quickly train SNO personnel to become detector operators.

* 8140 Lakefield Drive, Burnaby, British Columbia, Canada.
† F5 Networks Inc., Seattle, WA.

2.3 The SNO data acquisition system

Q.R. Ahmad, C.A. Duba, A.A. Hamian, P. Harvey,* K.M. Heeger, M.A. Howe, R. Meijer Drees,† A.W. Myers, J. Roberts,# P.M. Thornewell,% T.D. Van Wechel and J.F. Wilkerson

The SNO data acquisition system (DAQ) is designed to provide continuous readout of the 9547 photomultiplier tubes (PMTs) that comprise the detector. The system has been described in some detail in the 1997 Annual Report,[1] only an overview is provided here. The DAQ is divided into four main processes: system initialization and control; hardware readout; event building and data stream recording; and monitoring. The first of these is accomplished by the SNO Hardware Acquisition Realtime Control program (SHaRC), a C++ object oriented code running on a 250 MHz PPC computer. Hardware readout is provided through a VME based Motorola MVME167 68040 single board computer running an optimized C hardware readout program. Event building and subsequent recording of the data stream are handled by processes running on a SUN Ultra Sparc 1 workstation. Online data monitoring is supported through a client/server approach; the data are shipped from the DAQ SUN to a server process ("Dispatcher") that allows multiple monitoring clients to subscribe and view the data stream in near time.

The past year has marked some very important milestones for the SNO DAQ group. In April 1998, the complete system was used to acquire data with approximately half of the PMTs fully instrumented. In August 1998, with all of the PMTs operational, SNO DAQ was used to acquire the first commissioning data sets. In Fall 1998, sustained data throughput rates up to 400 kB/s were demonstrated, with burst rates up to 600 kB/s. The ability to handle these rates represents a significant upgrade to the event building software, which was implemented in the past year.

The SHaRC program has undergone an intensive period of upgrades, optimization, and testing in order to provide the many, sometimes complicated, levels of initialization and control for the detector, while retaining its straightforward operator interface. For the first time in 1998, non-expert detector operators were trained to use SHaRC to perform standard tasks, and the operator feedback was useful for keeping the user interface easy to use. In addition to providing control of essentially every aspect of the SNO hardware, SHaRC also provides the ability to insert and manipulate various calibration sources in the detector. This feature was tested with several different sources, and found to perform reliably. In late 1998, the ability to continuously run the DAQ with no stops or pauses between runs was added; this continuous running mode is a very important feature of the system, particularly in the event of a supernova. As part of this mode, the DAQ software supports restarting the various processes with no loss of detector data.

In 1998, the DAQ group provided full support of the DAQ system including the continuous presence in Sudbury of one or more group members. The on-site personnel were actively involved in solving day-to-day DAQ questions, and also in the ongoing code verification and implementation process. The overall response to the SNO DAQ by the detector operators, and by the collaboration as a whole, has been very positive.

Although the goal of providing a fully operational system by the time the detector is ready to begin taking solar neutrino data has been met, there are always enhancements to be added. The DAQ group continues to add to and modify various aspects of the system, incorporating feedback from the electronics group and operators.

---

* Queen's University, Kinston, Ontario, Canada.
† 8140 Lakefield Drive, Burnaby, British Columbia, Canada.
# Sudbury Neutrino Observatory, Sudbury, Ontario, Canada.
% F5 Networks Inc., Seattle, WA.
[1] Nuclear Physics Laboratory Annual Report, University of Washington (1997) pp. 20-23.

2.4 Overview and status of the SNO DAQ SHaRC control software

Q.R. Ahmad, Y.D. Chan,[*] P. Harvey,[†] M.A. Howe, F. McGirt,[#] R. Meijer Drees,[%] J. Roberts,[+]
P.M. Thornewell and J.F. Wilkerson

The SNO Hardware Acquisition Real time Control (SHaRC) code provides the control interface for the Sudbury Neutrino Observatory DAQ system. It is compiled with the MetroWerks Code Warrior compiler and runs on Macintosh PowerPC computers. SHaRC exploits the object-oriented nature of C^{++} to fully encapsulate a complete easy–to–use graphical user interface to the SNO data acquisition hardware.

The interface provides for initialization of the entire hardware system and can probe the system to configure automatically the dialogs and the databases with the location and identifications of the hardware that is actually present and working. As the figure shows, there is a hierarchy of dialogs that allows one to display information at any level of the detector hardware. The system-level dialog depicts the actual layout of the electronic crates on the deck. Clicking on a crate brings up a dialog showing crate-level information. Clicking on a front-end card in a crate will bring up information about that card and so on down to a level that displays information about a particular photomultiplier tube.

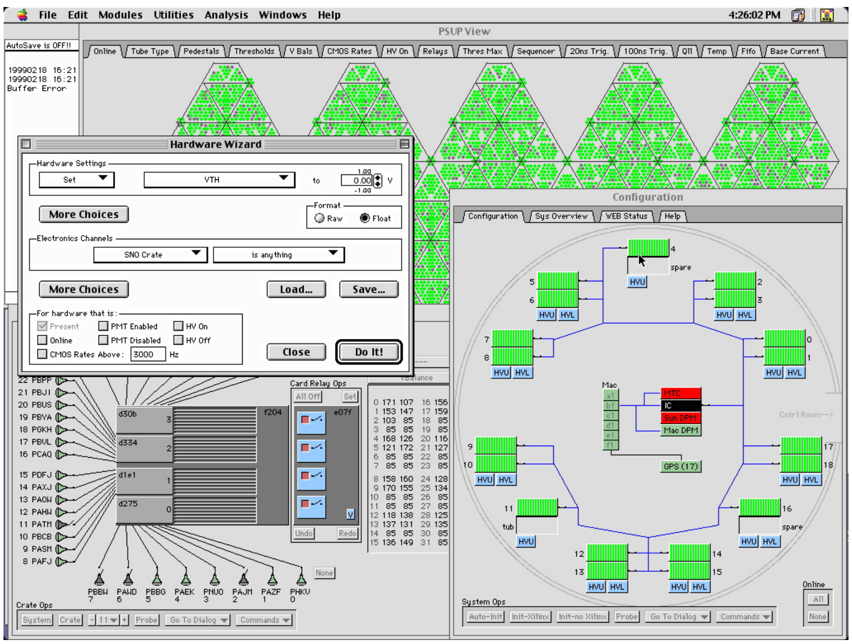

Fig. 2.4-1. A screen dump showing SHaRC in action.

A high-voltage control and safety system is built into SHaRC. HV supplies can be ramped at custom rates. Noise rates can be monitored to have the HV supplies automatically shut down in the event of certain types of breakdown. Also, the operator can panic ramp the high voltage back to zero at any time for a particular supply, or for the entire detector. The state of the high voltage system is clearly shown on all of the hardware-display dialogs.

There is an alarm system to alert the operators to unusual events. For example, if a hardware problem causes the data buffers to begin filling on a particular card an alarm is posted. There is even an option to take such cards offline automatically and to start a new run in those cases.

In addition, there are dialogs to start/stop runs, display run and data-flow information, and automatically schedule certain calibration and monitoring tasks. A “Hardware Wizard” allows one to program a highly selectable set of hardware parameters.

In addition to the SNO hardware objects, database objects provide for storage of electronics constants and a run history. At the start of every run, the databases that have changed are copied into a run-history folder. There is an interface to allow the configuration of the detector to be restored to the state it was in during any previous run. Hardware constants can be loaded manually, via automatic calibration routines, or from databases kept by other groups, such as the electronics group.

SHaRC is now in routine and continuous use in the SNO experiment.

[*] Lawrence Berkeley National Laboratory, Berkeley, CA.
[†] Queen’s University, Kingston, Ontario, Canada.
[#] Los Alamos National Laboratory, Los Alamos, NM.
[%] 8140 Lakefield Drive, Burnaby, BC, Canada.
[+] Sudbury Neutrino Observatory, Sudbury, Ontario, Canada.

2.5 SNO data stream monitoring

Q.R. Ahmad, C.A. Duba, A.A. Hamian, P. Harvey,* M.A. Howe, R. Meijer Drees,† J. Roberts,#
P.M. Thornewell% and J.F. Wilkerson

Monitoring of the SNO data stream is accomplished via several independent programs which provide complementary information. Near time monitoring uses the client/server approach described in Section 2.3, while offline analysis often uses one or more of these programs, reading data from SNO-defined, ZEBRA-formatted[1] "ZDAB" output data files.

Developed by C.A. Duba, SNOStream is a SNO customized front end to the "Histo" software package.[2] SNOStream supports a broad array of data-stream monitoring tools, including front-end-card and timing-card acquisition rates, trigger information, event information, and data-stream integrity checks. SNOStream receives the data stream from the dispatcher and passes selected portions to Histo for online graphical display. SNOStream can bin and histogram multiple events, and can also plot the data as functions of time, and of electronics crate and slot. Recent capabilities allow SNOStream also to view data from standard SNO ZDAB data files. SNOStream is proving to be a versatile monitoring tool and is currently being used to develop supernova-burst monitoring capabilities.

XSNOED is an X-windows event viewer, written by P. Harvey, that runs on site SUN workstations for near-time monitoring, but can also be run on other UNIX platforms, including DEC alphas and LINUX, for offline analysis. Events can be viewed in a spherical or flat map of the PMT support structure (PSUP) and/or in a map of the electronics crates. Either the charge data or time distribution data can be selected for viewing, with a color map representing the scale. In addition to the event maps, data for each event can be viewed as a histogram. When running in continuous mode, XSNOED displays events which satisfy a user-specified trigger, at a rate which is also user-selected. If an event of particular interest is observed, it is trivial to halt the continuous updating and "backup" to the desired event.

A more recent addition to the monitoring tools is a stand-alone PSUP Snapshot Viewer developed by J. Roberts, which is based on the PSUP and Crate View objects developed for the SHaRC program (see Section 2.4). In SHaRC, these views provide a wide variety of information, such as the discriminator threshold settings, the temperature of the electronics cards, and which PMTs are offline or online. Using the Snapshot Viewer, the saved data and parameters from previous runs can quickly be recalled and reviewed.

A set of SNO analysis tools has been developed at Queen's University for use with ROOT, a comprehensive object oriented framework for data analysis applications developed at CERN.[3] This package has recently been installed on computers at NPL, and it is envisioned that ROOT will be used as a major tool for offline data analysis of SNO data at UW. In addition to offline applications, the SNO/ROOT analysis package has recently been expanded to include some online event monitoring. This extended capability is currently being tested, and will be used during future data taking activities.

---

* Queen's University, Kingston, Ontario, Canada.
† 8140 Lakefield Drive, Burnaby, British Columbia, Canada.
# Sudbury Neutrino Observatory, Sudbury, Ontario, Canada.
% F5 Networks Inc., Seattle, WA.
1 A Fortran-based memory management system.
2 www-pat.fnal.gov/nirvana/histo.html.
3 http://root.cern.ch.

2.6 The Neutral Current Detector Project at SNO

J.F. Amsbaugh, M.C. Browne, T.V. Bullard, T.H. Burritt, P.J. Doe, C.A. Duba, S.R. Elliott, J.E. Franklin, G.C. Harper, K. M. Heeger, A.W. Myers, R.G.H. Robertson, M.W.E. Smith, T.D. Steiger, T.D. Van Wechel and J.F. Wilkerson

SNO will detect Cerenkov light emitted from electrons or positrons produced by charged-current neutrino interactions. This reaction will provide a measure of the flux of electron neutrinos from the sun. Neutrinos of any active flavor can produce free neutrons in the heavy water by neutral-current interactions. Thus the measurement of the neutron production is a measurement of the total flux of neutrinos from the sun. Since solar burning produces only electron neutrinos, a comparison of the total neutrino flux to the electron neutrino flux could provide strong evidence for neutrino oscillations and therefore neutrino mass. The neutral current detectors (NCD's) are an array of 300 ^{3}He filled proportional counters designed to detect such neutrons. These NCDs are made by chemical vapor deposition (CVD) on a mandrel to form Ni tubing and endcap components. The CVD process results in very low U and Th contamination (1-2 ppt Th). A quartz tube forms the high voltage and signal feedthrough to a Cu anode wire.

Most of the tubes were stored in an underground location at Index, WA to reduce cosmogenic activation. Unfortunately the air contained a very high level of Rn (900 pCi/l). As a result, counters constructed from these tubes had very high ^{210}Po-alpha decay rates (~8000 alphas/m^2/day). The noble metal Po adheres very strongly to Ni and plates out on Ni in acidic solutions. Hence electropolishing is the only technique known to us to remove the Po. Electropolishing, which keeps the radioactivity in solution, had reduced the tubes to this level from an initial rate of 10^5 alphas/m^2/day. But as a comparison, counters built early on before storage underground had an alpha rate of <100 alphas/m^2/day. Systematic studies of this problem were difficult because testing a new electropolishing procedure required counter assembly. To address this issue, we built an anode wire support structure that could be installed into a tube without laser welding the endcap-feedthrough assembly in place. As a result of these studies, the electropolishing procedures were improved and typical initial alpha rates are again near 100 alphas/m^2/day.

The various parts needed to assemble endcaps are being fabricated and most are completed. As they are produced, they are being shipped to IJ Research in Santa Ana, California and being assembled. There was also a delay in the delivery of endcaps due to difficulties with the company's RF sputterer. This problem has been addressed. We should start receiving endcaps again imminently.

The NCD's must have very little radioactivity as they will reside in the sensitive inner region of the SNO detector. All parts which comprise the NCD's are being radioassayed to verify their cleanliness. We have assayed samples of almost all materials to be used in the array and all small fabricated parts. This radioassay program is nearing completion. The results indicate that the added photodisintegration background in SNO due to the NCD's will be less than that due to the impurity of the heavy water.

Tests of the remotely operated vehicle to be used in the installation of the counters into SNO have been successful. The initial assembly of the deployment hardware is beginning as most of the engineering is nearing completion. The design, prototyping and test of the anchor assemblies for the counter strings are complete and fabrication of the parts is beginning.

We have delivered 15% of the array underground at SNO. These counters are being studied to understand their contamination level. We will compare this measured number to our radioassay predictions.

Although we have had delays due to the Po contamination and endcap production, we have successfully built and operated 103 detectors of which 80 are part of the array. These have included spare counters for the array, counters to verify the radiopurity, and counters for underwater pressure testing. Our present production schedule will have all detectors underground in Sudbury by late 1999, ready for deployment after a period of cooldown during which cosmogenic ^{56}Co decays away.

2.7 Electronics for the NCD array

M.C. Browne, K.M. Heeger, A.W. Myers, R.G.H. Robertson, T.D. Van Wechel and J.F. Wilkerson

The SNO neutral-current detector (NCD) array will be used to detect neutrons liberated by the neutrino disintegration of deuterium. There are 96 `strings' of ^{3}He-filled detectors to be placed in the heavy water, each connected to a separate external 91-Ω current preamplifier via a cable.

Above an input signal of 200 nA, the event rate is dominated by neutrons and alpha particles. Neutrons from muon interactions and NC events are expected to be detected at a rate of 50 per day, and alphas 1000 - 10000 per day. The longest duration of the signal (apart from the ion tail) is about 3 μs, corresponding to the drift time across a detector. With integration to match this time, smaller signals due to betas and gammas can be detected.

The signal current contains a great deal of information that can be used to distinguish between neutrons and other types of event, and to locate events along the length of the detector. High-speed digitization is necessary to recover the position information in particular. To reduce costs one may take advantage of the low rates and multiplex (MUX) the data. But to recover very small signals from the noise, and to deal with high burst rates such as might occur during a supernova, 96 channels of spectroscopy-quality shapers and ADCs are also provided.

Signals from preamplifiers enter 2 parallel buffers, one driving 20-m long cables to the shaper-ADCs that reside in VME, and the other driving eight 12-to-1 multiplexers (MUX) via discriminators and 320-ns delay lines. The shaper-ADCs are the same basic units used in the emiT experiment (*q.v.*), but with time constants chosen to match the proportional counters. Pre-production shaper-ADCs are under construction.

The MUX units are AD8180 high-speed video switches. To reduce level shifts, a dummy unit is always connected to the common output except when a signal is present.

The MUX output goes to an AD8307 logarithmic amplifier. Logarithmic amplifiers make it possible to digitize signals having a wide dynamic range with a fixed precision of about 1% of voltage (for an 8-bit digitizer). The offset for a log amp functions as a gain control and is set by a DAC level supplied from a controller. The offset is also necessary to prevent rectification of the quiescent input noise, as the log amp is indifferent to the sign of the input voltage. The output is a current that is buffered by two op-amps before being sent to a digitizer.

The 2 digitizers are Tektronix 754A digitizing 4-channel oscilloscopes with 50k of memory. Each scope services 48 inputs (4 MUX boxes) autonomously. The scopes are set up by GPIB or front-panel input.

The GPIB bus links the 2 scopes and the calibration pulser to VME. At the time of the initial trigger, and again at the time of the end of readout, the MUX hit pattern (48 bits) can be recorded by strobing latches. By reading out the latches at some point during scope readout and then just after scope readout, it can be determined if additional inputs were received while the scope was dead. As the scopes are dead during readout time (up to 1s), no digitization of events arriving then will be obtained, but the shaper-ADC system will give the total energy of each event.

A 2-channel prototype MUX system has been tested, and MUX boards have been designed.

2.8 In situ determination of backgrounds from neutral current detectors in the Sudbury Neutrino Observatory

M.C. Browne, T.V. Bullard, P.J. Doe, C.A. Duba, S.R. Elliott, K.M. Heeger, A.W.P. Poon* and R.G.H. Robertson

The use of ultra-low background ^{3}He proportional counters in the SNO detector will provide a means of measuring the neutral-current interaction rate of solar neutrinos. Since the binding energy of the deuteron is only 2.2 MeV gamma rays from natural decay chains in the proportional counters photodisintegrate the deuteron and thus simulate the neutral-current signal. This poses stringent radiopurity requirements for the counters. An *in situ* measurement of the background from seven neutral-current detectors will determine the activity of ^{232}Th in the neutral current detectors and thus determine an upper limit on the photodisintegration background generated by the radioactivity in the NCD array.

The Neutral Current Detector (NCD) array consists of 775 m of ^{3}He proportional counters arranged in 96 strings with 300 counters. The counter bodies are made of about 450 kg of ultra-pure CVD nickel which contains natural U and Th. The photodisintegration gammas are produced in the decays of the $^{232}\mathrm{Th}(^{208}\mathrm{Tl} \rightarrow ^{208}\mathrm{Pb},\ E_{\gamma} = 2.615\ \mathrm{MeV})$ and $^{238}\mathrm{U}(^{214}\mathrm{Bi} \rightarrow ^{214}\mathrm{Po},\ E_{\gamma} = 2.445\ \mathrm{MeV})$ chains and in the decay of the relatively long-lived cosmogenically produced ^{56}Co.

A Construction Hardware In Situ Monitoring Experiment (CHIME) has been designed to measure the NCD originated background in the presence of the D_2O contribution prior to the deployment of the entire NCD array. It is an *in situ* measurement of the construction materials used in the NCD array. Seven individual counters arranged in a close-packed configuration with a total mass of about 5000 g and a length of 45" will be deployed as a background test source in the SNO detector. The construction materials and procedures for the CHIME counters are essentially identical to those in the real NCD array with the difference being that the CHIME counters are not active.

In order to allow the ^{56}Co to decay, the CHIME must be stored underground for at least 3 months. It was placed on the 6,800' level on December 20, 1998, and will not be ready for deployment until after April 1999.

A radon emanation test will be conducted on the CHIME while it is underground to assure its cleanliness before deployment. The detection limit for ^{228}Th is about 5 disintegrations per day and for ^{226}Ra about 2.5 disintegrations per day. These are the amounts that would be in secular steady state with 0.6 microgram ^{232}Th and 2 micrograms ^{238}U respectively. The radon emanation test hardware is currently being tested at LANL and will be shipped to Sudbury by April. It is anticipated that one month will be required to establish the equipment underground and conduct the emanation tests.

The deployment of CHIME is expected to be no different than that of a standard calibration source and will have minimum impact on the SNO operating schedule. The CHIME is negative buoyant and can be deployed along the central axis of SNO using the existing calibration source deployment hardware and manipulator system. Monte Carlo studies have shown that the presence of CHIME will have no measurable impact on the physics goal of SNO.

The complete geometry of CHIME, the SNO detector response, and all important decay schemes can be simulated using the SNO Monte Carlo code. Preliminary studies of the reconstruction distribution and the energy spectra have shown that an analysis approach based on fiducial cuts and the shape of the ^{56}Co energy distribution will allow us to discriminate the ^{56}Co contribution to the photodisintegration background with high enough accuracy. In addition, further techniques will be investigated to distinguish between reconstructed events in the fiducial volume due to ^{208}Tl decays in the CHIME and the D_2O.

It is expected that the Construction Hardware In Situ Monitoring Experiment will allow us to determine the photodisintegration background from the NCD array at the level of 10% of solar module after two weeks of *in situ* counting.

---

* Lawrence Berkeley Laboratory, Berkeley, CA.

2.9 Using a remotely operated vehicle to deploy neutral current detectors in the Sudbury Neutrino Observatory

J.F. Amsbaugh, T.H. Burritt, P.J. Doe, G.C. Harper and M.W.E. Smith

The deployment of the NCDs into SNO must be done with a minimum of down time for the observatory, yet must be carried out with care, so not to contaminate the heavy water or damage the acrylic vessel it is contained in. The primary tool for this task is a remotely operated vehicle (ROV) designed by Deep Ocean Engineering. In addition, there are some essential items of deployment hardware that are being designed and fabricated in house at NPL.

The procedures for deployment must be carefully thought out and rigorously tested. This process has begun, with the ROV being tested in a 20 ft deep pool at Los Alamos National Laboratory, a collaborator in this project. Members of NPL have traveled to Los Alamos for these tests and have become proficient at operating the ROV. A series of dummy detectors were captured by the ROV, taken to the bottom of the pool and deployed into anchors on an acrylic panel. The environment in the pool was set up to simulate that of SNO, with similar lighting and background appearance. The tests were successful, demonstrating that the ROV provides a sound technique for NCD deployment.

The water depth at SNO complicates the deployment program, with the ROV operating at 60 ft below the deck. In addition, the NCD cables, which run inside the upper hemisphere of the acrylic vessel, must hook into a cable attachment ring at the bottom of a 24 ft acrylic chimney. To overcome these difficulties, along with the constraints of overhead clearance, the following hardware has been designed and is being fabricated at NPL.

- Global View Camera mechanism, to assist in viewing both the ROV and the NCD cables.
- Haul Down, for moving detectors to the bottom of the vessel for capture by the ROV.
- Manipulating Pole, for rearranging NCD cables in the chimney of the acrylic vessel.
- Welding Station, for laser welding the individual NCDs together as they are deployed.
- Deployment Platform, to integrate the hardware and cover the open vessel.

Construction of these items is now 80% complete and it is expected that all hardware will be completed by the end of March. Testing of individual items will continue at the University of Washington through March, using a tank in the Engineering Department. During April, at the Los Alamos pool, we will be testing the hardware and ROV as an integrated system. Several members of NPL will be visiting Los Alamos during this period to design and participate in these tests.

A program is being developed to train deployment personnel. Approximately 12 people will need to become proficient in laser welding, ROV operation and general deployment duties. It is expected that more than half of these people will come from NPL and will be trained sometime during the next six months.

2.10 Initial results from the cool-down phase of the Neutral Current Detector (NCD) Program for the Sudbury Neutrino Observatory

M.C. Browne, S.R. Elliott, R.G.H. Robertson, T.D. Steiger and J.F. Wilkerson

The NCD group has developed material preparation and construction techniques in order to produce counters with intrinsically low levels of ^{238}U and ^{232}Th. These isotopes give rise to background neutrons through photodisintegration of deuterium. An additional problematic isotope is ^{56}Co, which is a spallation product of cosmic rays with nickel. In order to allow this cosmogenic activation to decay away prior to NCD deployment in SNO, a storage period known as the "cool-down phase" has been implemented.

The goals of the cool-down phase are to quantify potential backgrounds to the NCDs while safely delivering and characterizing the NCDs at the underground SNO facility. These backgrounds can be grouped into two categories: backgrounds due to the environment (thermal and fast neutrons, fission gammas), and intrinsic backgrounds to the counters (alpha particles from U, Th and Po).

There are currently about 115 m of counter underground in the cool-down phase (~15% of the NCD array). Subsets of these counters have been running nearly continuously for six months. The data taken during the past year have provided an initial estimate of the potential NCD backgrounds.

The primary measurement during the cool-down phase in 1998 was an attempt to assess the bulk U and Th contamination in the NCD construction materials. In a plot of projected track length (charge-pulse risetime) against total energy, events from bulk alpha emitters occupy regions different from surface activity. Initial results indicate bulk alpha activity from low-energy and high-energy regions of this plot between 2.28 ± 0.78 and 1.20 ± 1.1 alphas/m^2/day. Monte Carlo studies predict 2.0 alphas/m^2/day for U and 0.5 for Th contamination at the 10 ppt level. Fast neutron interactions in the counters also contribute some events, thus indicating that these values are an upper limit on the U and Th contamination.

The production of NCDs in 1998 was significantly affected by contamination of ^{210}Po on the nickel tubes. Additional construction techniques were implemented to remove the majority of this contaminant. Reduction of Po by >1000 was demonstrated at the University of Washington but was limited by hadronic interactions in the counters from cosmic rays. The cool-down phase was thus used to test the surface preparation techniques. The average number of counts recorded on the NCDs in the cool-down phase in the ^{210}Po peak window was 8.28 ± 1.17 alphas/m^2/day, corresponding to a reduction of about 10^3. Additional long-term tests demonstrated that the activity was decaying with the anticipated 138-day half-life – confirming the success of the surface preparation techniques.

In 1999, long-term alpha analysis is planned to obtain better statistics on the bulk U and Th contamination levels. Additional counters are scheduled for shipment to SNO late Spring 1999.

2.11 Sensitivity of NCDS to Supernovae during cool-down

M.C. Browne, C.A. Duba, S.R. Elliott and R.G.H. Robertson

During the aforementioned cool-down phase of the NCDs, all 96 strings of proportional counters will monitor neutrons inside SNO's control room for no less than six months. These neutrons will mostly be created in (α,n) reactions within the norite walls of the Creighton mine. However, elevated neutrino fluxes, such as would be present during a supernova core-collapse, will create elevated neutron liberation rates within the norite. The higher neutron liberation rate will create a larger neutron flux within the control room, which may be detected by any operating NCD strings.

Although the probability of a detectable supernova event during the relatively short-duration cool-down phase is low, this test should provide valuable data as to the feasibility of using proportional counters for supernova detection. These data could be used to assess proposals such as OMNIS[1] and LAND.[2] We will test supernova event backgrounds, counter geometric efficiencies, neutrino target materials, data acquisition systems, and supernova alert protocol. The results of these tests could then be used to optimize supernova detection strategies for permanent supernova detectors.

Norite rock is an igneous silicate, made of mostly silicate, a rather poor material in terms of neutrino-neutron cross section. However, the norite contains non-negligible amounts of aluminum, calcium, iron, sodium, and magnesium. Convoluting the energy-dependant neutrino-neutron cross sections of the major constituents of norite with the expected neutrino energy spectra in core-collapse events yields a net neutron production rate of roughly 8×10^{-6} n/g for a distance of 1 kpc.

The total mass of norite, to which the cool-down array will be effectively sensitive, is:

$$M_s = \frac{r(L\times\varepsilon_L)}{(l\times\varepsilon)R_{\alpha n}} \quad \frac{7000d^{-1}(775m\times.40)}{(16.5m\times.60)2.8g^{-1}yr^{-1}}$$

Where r is the rate of neutron detection with the current cool-down array, l is the length of the current array, ε is the geometric efficiency of the NCD setup, L is the length of the complete array, and $R_{\alpha n}$ is the measured rate of (α,n) creation within the norite.[3]

M_s works out to be 3×10^7 g, which implies that only ~4 neutrons will be detected for a galactic-center supernova at 8 kpc. Unfortunately, this is not much higher than the background rate due to norite (α,n). The predicted signal-to-background depends on the supernova model that is used; a one-second burst-model supernova would provide a ratio 7:3, while the data from supernova 1987a seems to favor a ten-second burst, and thus a ratio of 34:30.[3] In either case, the chance of triggering on most galactic supernova events is negligible without additional signal-to-background improvements.

One possible improvement would involve the insertion of a moderator, such as paraffin or water, into the NCD array, and would amplify both signal and background, effectively increasing the statistical significance of an event. A second improvement could be made by repositioning the counters in the NCD array, thereby increasing the geometric efficiency by minimizing detector "shadowing" within the control room. Finally, a substantial amount of ^{208}Pb would dramatically increase the sensitivity of the NCDs to supernovae, since Pb has a neutrino-neutron cross-section by mass almost 20 times higher than norite. When this is coupled with Pb's long neutron absorption length and very low neutron background, even 10 tons of strategically placed Pb with moderator should more than double the expected neutron flux from supernovae without substantially altering the background.

[1] OMNIS-an improved low-cost detector to measure mass and mixing of mu/tau neutrinos from a galactic supernova, P.F. Smith-, Astroparticle-Physics.vol.8, no.1-2; Dec. 1997; pp. 27-42.
[2] LAND lead astronomical neutrino detector: LAND, C.K. Hargrove, I. Batkin, M.K. Sundaresan and J. Dubeau, Astroparticle-Physics.vol.5, no.2; Aug. 1996; pp. 183-96.
[3] Annex 9 Report, SNO proposal, 1987, E.D. Earle *et al.*

2.12 SAGE: The Russian American Gallium Experiment

S.R. Elliott and J.F. Wilkerson

The Russian-American Gallium Experiment (SAGE) is a radiochemical solar neutrino flux measurement based on the inverse beta decay reaction, $^{71}Ga(\nu,e^-)^{71}Ge$. The threshold for this reaction is 233 keV, which permits sensitivity to the p-p neutrinos that dominate the solar neutrino flux. The target for the reaction is 55 tonnes of liquid gallium metal stored deep underground at the Baksan Neutrino Observatory in the Caucasus Mountains in Russia. About once a month, the neutrino induced Ge is extracted from the Ga. ^{71}Ge is unstable with respect to electron capture ($\tau_{1/2}$ = 11.43 days) and, therefore, the amount of extracted Ge can be determined from its activity as measured in small proportional counters. The experiment has measured the solar neutrino flux extractions between January 1990 and December 1997 with the result $67.2^{+7.2}_{-7.0}$ (statistical) $^{+3.5}_{-3.0}$ (systematic) SNU, which was reported at the Neutrino 98 Conference in Japan in June 1998. This is well below the standard solar model expectation of 129 SNU. Additional extractions are being analyzed. The Figure below shows a plot of the extraction data.

The collaboration has used a 517-kCi ^{51}Cr neutrino source to test the experimental operation. The energy of these neutrinos is similar to the solar ^{7}Be neutrinos and thus makes an ideal check on the experimental procedure. We have published this result in 1996. The result, expressed in terms of a ratio of the measured production rate to the expected production rate,[1] is 0.95 ± 0.12. This indicates that the discrepancy between the solar model predictions and the SAGE flux measurement cannot be an experimental artifact. The work has also been described in a long archive paper that is currently in press.[2]

In collaboration with the Institute for Nuclear Research, we submitted a grant request to CRDF.[3] This two year grant request was funded in 1997 and is now complete. The monies were used to support Russian scientists employed to continue solar neutrino observations.

SAGE is a mature experiment whose operation has become routine. The University of Washington plays a role in the analysis of the data. We are assisting in the design and construction of new proportional counters for the experiment. With the publication of the Cr data, the focus is now on the writing of archive papers summarizing the experimental procedure and its solar neutrino results.

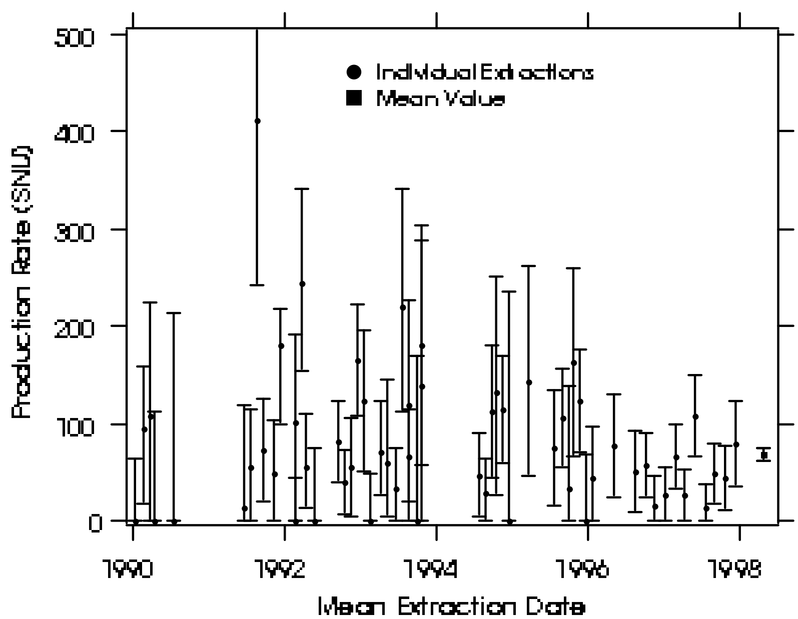

Fig. 2.12-1. The individual measurements of the solar neutrino production rate.

---

[1] J.N. Abdurashitov *et al*., Phys. Rev. Lett. **77**, 4708 (1996).
[2] J.N. Abdurashitov *et al*., Phys. Rev. C, in press.
[3] Civilian Research and Development Foundation for the Independent States of the Former Soviet Union, Award # RP2-159, Proposal # 3126.

3.0 NUCLEUS-NUCLEUS REACTIONS

3.1 The GDR width in highly excited nuclei

M.P. Kelly, M. Kicinska-Habior,[*] J.P. Lestone,[†] J.F. Liang,[#] K.A. Snover, A.A. Sonzogni,[%]
Z. Trnadel[*] and J.P.S. van Schagen

We have completed new measurements of ^{18}O + ^{100}Mo reactions from E(^{18}O) = 122 to 214 MeV in order to understand better the width evolution of the hot GDR versus excitation energy in near-Sn compound nuclei. Our approach combines results from separate measurements of light-charged particles, γ rays and evaporation residues. First, we have measured light charged particle emission and deduced the effect of preequilibrium energy and mass loss prior to compound nucleus decay. Large preequilibrium losses of approximately 20% of the full fusion excitation energy and several mass units are observed for bombarding energies as low as 11 MeV/nucleon. Second, using a new array of three large NaI spectrometers along with a γ-ray multiplicity array, we have measured the γ-ray emission cross sections and angular distributions for five bombarding energies. These data permit a direct separation of the statistical GDR component from the underlying bremsstrahlung. Last, the measured evaporation residue excitation function were used to extract the GDR strengths with good accuracy.

Our analysis of GDR spectra includes a simultaneous fit of statistical emission plus bremsstrahlung to both the measured γ-ray strength function and the $a_1(E_\gamma)$ coefficient determined from the angular distributions. A careful account of the important dynamical effects of preequilibrium energy loss and bremsstrahlung emission is necessary for a reliable determination of the GDR parameters. Further insight into the excitation energy dependence of the GDR is gained by examining the dependence of the fitted parameters on the average thermal energy following giant-dipole emission, or equivalently the temperatures, rather than on the initial compound nucleus excitation energy. Results for the energy dependences of the GDR strength, width and centroid energy are determined and the measured widths are compared with the results of thermal fluctuation calculations of the width of the GDR. An additional contribution to the width of the GDR equal to twice the compound nucleus evaporation width may also become important at the higher energies. The result of this study is a new and qualitatively different understanding of the temperature evolution of the GDR in hot nuclei; namely, the width of GDR does not saturate but continues to increase up to at least T~2.4 MeV, which represents the highest temperatures for data measured here. Previously measured widths, reanalyzed for this study, give additional support for an increasing width up to T~3.2 MeV. Width results are summarized in the figure below.[1]

[*] Warsaw University, Warsaw, Poland.
[†] Los Alamos National Laboratory, Los Alamos, NM.
[#] Oak Ridge National Laboratory, Oak Ridge, TN.
[%] Argonne National Laboratory, Argonne, IL
[1] M.P. Kelly, K.A. Snover, J.P.S. van Schagen, M. Kicinska-Habior and Z. Trznadel, Phys. Rev. Lett., in press.

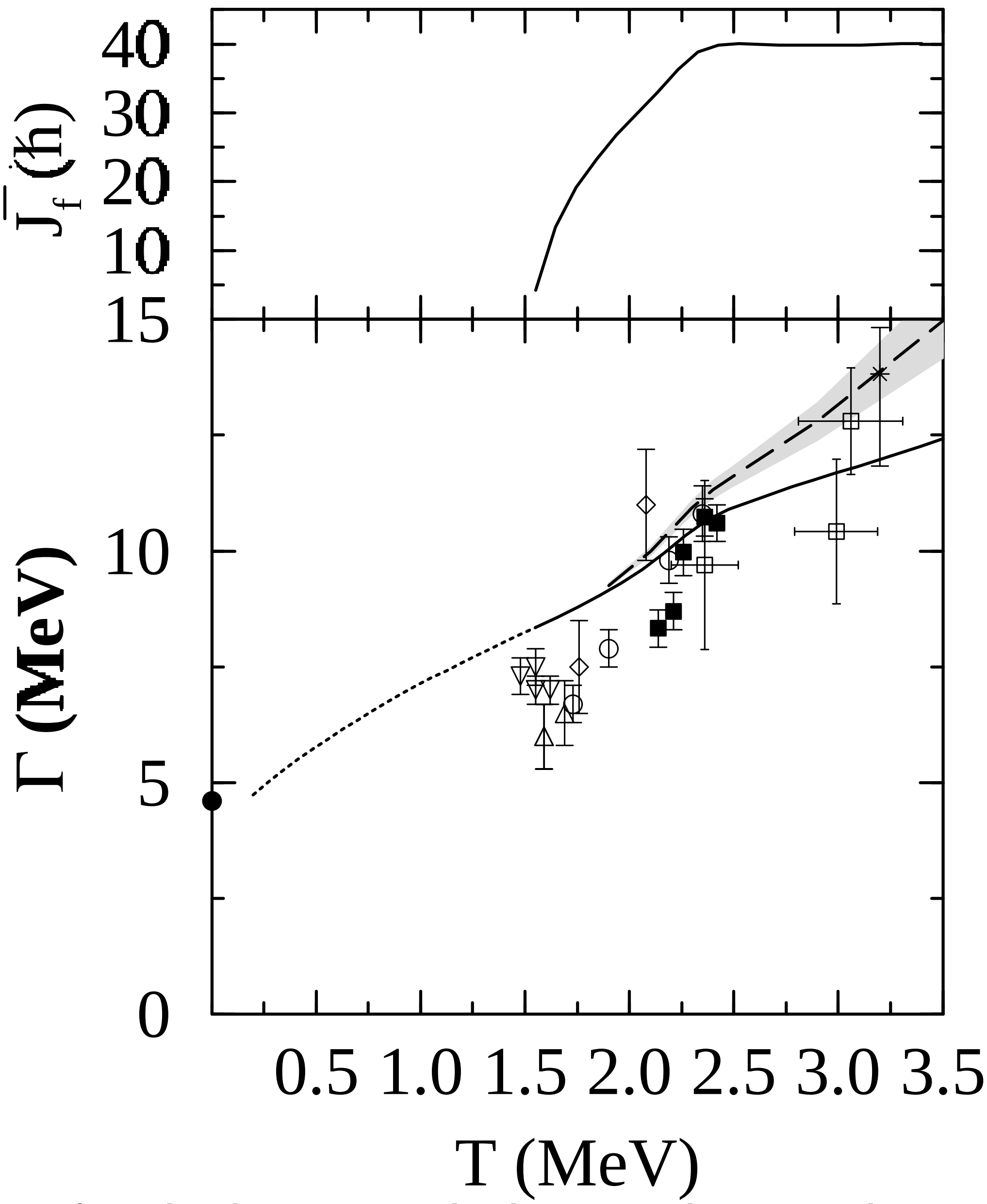

Fig. 3.1-1. Decay of Sn and nearby mass compound nuclei. Top panel: average angular momentum for GDR decay in ^{18}O + ^{100}Mo. Bottom panel: points - measured GDR widths. Filled squares are the result of the present study. Solid line - thermal fluctuation calculation of Kusnezov and Alhassid (private communcation). Dashed line – includes the additional additive contribution $2\Gamma_{evap}$.

3.2 High-energy γ-ray emission in ^{12}C + $^{58,64}Ni$ reactions at 6--11 MeV/u

M.P. Kelly, M. Kicinska-Habior,* J.P.S. van Schagen, K.A. Snover and Z. Trznadel*

Recently, the ^{12}C + $^{24,26}Mg$ and the ^{18}O + ^{100}Mo mass-asymmetric heavy-ion reactions at 6-11 MeV/u have been used to disentangle statistical high-energy γ-ray emission and bremsstrahlung emission by measuring both γ-ray spectra and angular distributions.[1,2] In this manner, reliable Giant Dipole Resonance (GDR) parameters and bremsstrahlung parameters have been extracted. In order to obtain similar information concerning the bremsstrahlung process and the GDR built in compound nuclei formed in medium-mass heavy-ion collisions the ^{12}C + $^{58,64}Ni$ reactions were studied at the University of Washington Nuclear Physics Laboratory using the FN Tandem Van de Graaff together with the Superconducting Linear Accelerator. High-energy γ-ray spectra at angles 40°, 55°, 90°, 125° and 140° were measured with a new triple NaI-spectrometer set-up[3] at beam energies of 5.5, 8 and 11 MeV/u. The angular coefficients A_0, a_1 and a_2 in the nucleus-nucleus CM frame have been extracted from Legendre Polynomial fits to the singles data and to the fold $\geq$2 data for both reactions. The results for ^{12}C + ^{64}Ni are shown in Fig. 3.2-1. A large bremsstrahlung component which increases with projectile energy is clearly visible at γ-ray energies above 20 MeV in A_0 as well as in a_1. The anisotropy observed in the a_2 coefficient suggests a small deformation of the nuclei formed. A similar behavior was found for the ^{12}C + ^{58}Ni reaction. Simultaneous fits of theoretical calculations to both A_0 and a_1 coefficients are in progress.

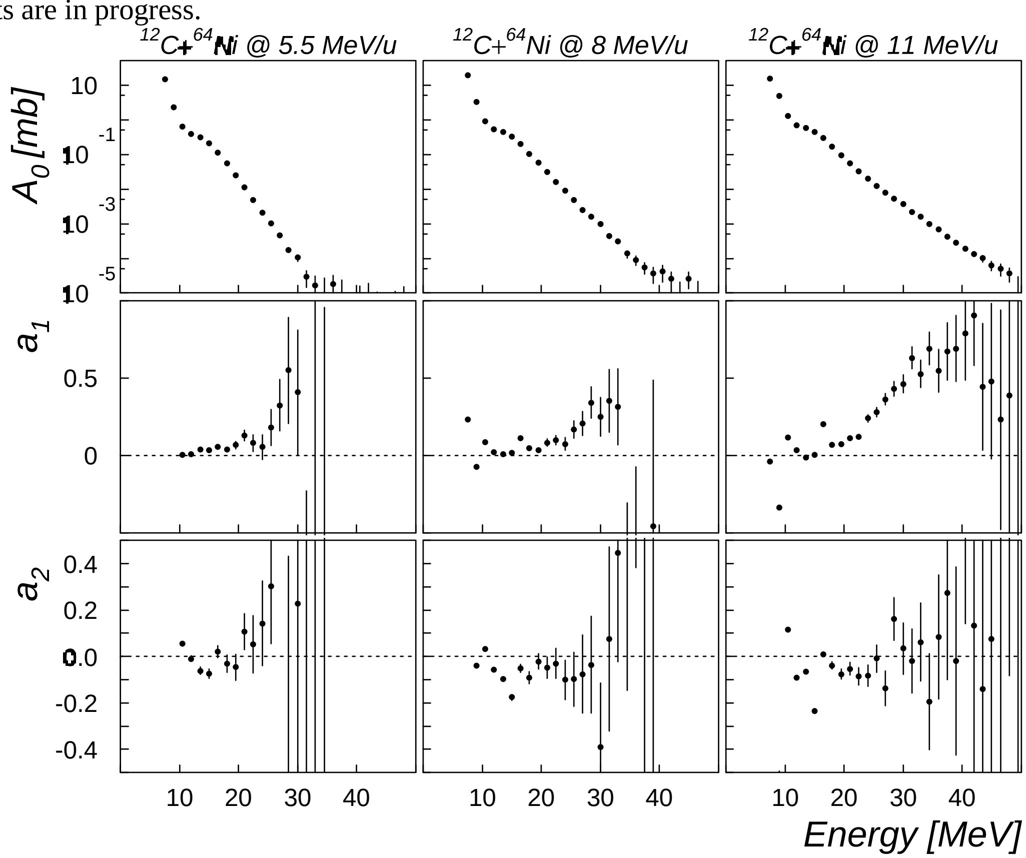

Fig. 3.2-1. Measured high-energy γ-ray spectra A_0 (top row), and angular distribution a_1 (middle row) and a_2 (bottom row) coefficients for ^{12}C + ^{64}Ni at 5.5, 8 and 11 MeV/u.

* Institute of Experimental Physics, Warsaw, Poland.

[1] M.P. Kelly, K.A. Snover, J.P.S. van Schagen, M. Kicinska-Habior and Z. Trznadel, *Proceedings of the Topical Conference on Giant Resonances*, May, 1998, Varenna, Italy, Nucl. Phys. A, in press.

[2] M. Kicinska-Habior, Z. Trznadel, M.P. Kelly, K.A. Snover and J.P.S. van Schagen, *Proceedings of the Topical Conference on Giant Resonances*, May, 1998, Varenna, Italy, Nucl. Phys. A, in press.

[3] Nuclear Physics Laboratory Annual Report, University of Washington, (1997) p. 57.

3.3 Scaling properties of the GDR width in hot rotating nuclei

Y. Alhassid,* D. Kusnezov * and K.A. Snover

We have examined[1] the experimental and theoretical systematics of the giant dipole resonance width in hot rotating nuclei as a function of temperature T, spin J and mass A from A = 45 to 208. The calculations are based on the theory of adiabatic thermal shape fluctuations in the liquid drop model, which is known to be generally very successful in describing experimentally measured GDR widths. Calculations for a number of different nuclei were examined and an empirical scaling was deduced, resulting in a simple phenomenological function $\Gamma(A,T,J)$ which approximates the global behavior of the calculated GDR width. The deduced function is

$$\Gamma(T,J,A) = \Gamma(T,J=0,A)\left[L\left(\frac{J}{A^{5/6}}\right)\right]^{4/[(T/T_0)+3]}$$

where $\Gamma(T,J=0,A) = \Gamma_0(A) + c(A)\ \ln(1+T/T_0)$ and $c(A) = 6.45 - A/100$.

$\Gamma_0(A)$ is usually extracted from the measured ground-state GDR width in neighboring spherical nuclei, and typically lies in the range 3.8 - 5 MeV. T_0 = 1 MeV is a reference temperature. $L(\xi)$ represents the scaling function for the width at constant T, as a function of $\xi = J/A^{5/6}$, where $L(\xi) \cong 1 + 1.8\{1+\exp[(1.3-\xi)/0.2]\}^{-1}$. The angular momentum scaling as $J/A^{5/6}$ may be understood as due to the dominance of the rotation energy $J^2/2I$ at high spin, where the moment of inertia $I \propto A^{5/6}$. A comparison with available data shows agreement within ±20% for most measurements.

In a separate project, the dependence of the GDR width at low spin and low to moderate temperature was reexamined in two cases of recent experimental and theoretical interest, the decays of $^{120}Sn^*$ and $^{208}Pb^*$ populated by inelastic alpha scattering. Our calculated widths are significantly larger than previous ones,[2] and disagree with published data.[3] A revised computation of the proper temperature scale brings the data into fair agreement with theory in the case of ^{208}Pb but not ^{120}Sn.

---

* Yale University, New Haven, CT.

[1] D. Kusnezov, Y Alhassid and K.A. Snover, Phys. Rev. Lett. **81**, 542 (1998).

[2] W.E. Ormand, P.F. Bortignon, and R.A. Broglia, Phys. Rev. Lett. **77**, 607 (1996); W.E. Ormand *et al.*, Nucl. Phys. A **614**, 217 (1997).

[3] E. Ramakrishnan *et al.*, Phys. Rev. Lett. **76**, 2025 (1996); Phys. Lett. B **383**, 252 (1996).

3.4 ^{17}O inelastic scattering study of the GDR width in decays of excited ^{120}Sn nuclei

J.R. Beene,[*] Y. Blumenfeld,[†] M. Halbert,[*] F. Liang,[*] E. Mohrmann, T. Nakamura, [†] K.A. Snover, M. Thoennessen,[†] E. Tryggestad[†] and R. Varner*

In November 1998 we had a 1-week run at the National Superconducting Cyclotron Laboratory in which we attempted to measure the GDR decay of excited ^{120}Sn nuclei populated by the inelastic scattering of ^{17}O nuclei at a bombarding energy of 80 MeV/nucleon. The measurement was patterned after an earlier MSU experiment which looked at ^{120}Sn decays populated by inelastic alpha particle scattering.[1] In contrast to the usual fusion-evaporation studies, inelastic scattering/decay experiments populate much lower spins and thus probe GDR properties in a different region of spin and temperature parameter space. The motivation for an ^{17}O experiment is 2-fold: 1) GDR widths deduced in the ^{120}Sn($\alpha,\alpha'\gamma$) experiment are not in good agreement with theory, and they are also systematically higher than fusion-evaporation results at low excitation energies where the spins and temperatures are similar in the 2 types of reactions;[2] 2) a recent experiment suggests significant preequilibrium emission may occur in the ($\alpha,\alpha'\gamma$) experiment prior to the formation of an equilibrated excited nucleus.[3] In contrast to alpha particle inelastic scattering, ^{17}O inelastic scattering is known to have much smaller nucleon knockout cross sections and thus there is the hope that preequilibrium processes might be weaker in the ^{17}O case. A good ^{17}O inelastic scattering experiment might also offer the opportunity to explore better the low-spin low-temperature region of GDR decay of Sn compound nuclei where measured GDR widths from fusion-evaporation reactions lie below theory.[4]

We used the S800 superconducting spectrometer to detect the inelastically scattered ^{17}O particles, near O°, approximately 150 detectors of the ORNL-TAMU-MSU BaF_2 array to detect the gamma rays, and an array of CsI detectors to measure preequilibrium charged particle emission. One difficulty we experienced was a substantial gamma background in the BaF2 detectors and ^{17}O background in the S800 focal plane detectors due to stopped and scattered beam, respectively. Because the software for optimized angle and position cuts in the focal plane detection was not available on line, the efficacy of such cuts will be determined in the off-line analysis currently in progress.

[*] Oak Ridge National Laboratory, Oak Ridge, TN.
[†] Michigan State University, East Lansing, MI.
[1] E. Ramakrishnan *et al*., Phys. Rev. Lett. **76**, 2025 (1996).
[2] D. Kusnezov, Y. Alhassid and K.A. Snover, Phys. Rev. Lett. **81**, 542 (1998).
[3] D. Fabris *et al*., J. Phys. G **23**, 1377 (1997), Phys. Rev. C **58**, R624 (1998).
[4] M.P. Kelly *et al*., Phys. Rev. Lett., in press.

3.5 Investigation of the temperature dependence of the level density parameter: results from the $^{19}F + {}^{181}Ta \rightarrow {}^{200}Pb$ system

A.L. Caraley, B.P. Henry, J.P. Lestone* and R. Vandenbosch

During the last few years, we have been studying both the fusion-evaporation and fusion-fission channels of the $^{19}F + {}^{181}Ta \rightarrow {}^{200}Pb$ reaction with the goal of determining the Fermi-gas level density parameter and its *possible* dependence on the temperature of the emitting system. Fabris *et al.*[1] have reported, based on α-particle results from the same $^{19}F + {}^{181}Ta$ system, that the level density parameter decreases dramatically from A/8.3 MeV^{-1} at a thermal excitation energy of U=20 MeV to A/12 MeV^{-1} at U=100 MeV. Last year we presented preliminary results from an experiment that measured light-charged particles (LCP) in coincidence with evaporation residues (ER) at E_{lab}=121, 154 and 195 MeV.[2] This year we have performed several additional experiments. Another LCP-ER coincidence data set was collected at E_{lab}=179 MeV. In addition, to guide the simulations necessary to determine particle multiplicities, thorough measurements of the relative ER singles efficiency as a function of the deflector voltage were performed at all four beam energies. Also, another LCP-ER coincidence experiment at E_{lab}=154 MeV was conducted. For this experiment, the light-charged particles were detected at $\theta_{lab} = +160^\circ$ and at $\theta_{lab} = -160^\circ$ in order to determine any influence of the ER coincidence requirement on the LCP spectral shapes. The resulting spectral shapes at the two angles were determined to be essentially identical. These findings, as well as the results of extensive statistical-model-based simulations, have confirmed that the spectra collected previously at $\theta_{lab} = +160^\circ$ are unaffected by kinematic bias.

The coincident light-charged particles have been analyzed to determine both apparent temperatures and multiplicities. The multiplicity results for α-particles at $\theta_{lab} = +160^\circ$ and at $\theta_{lab} = -160^\circ$, shown in Fig. 3.5-1a are consistent with those of Hinde *et al.*[3] and Fabris *et al*. The error bars on the present results reflect the systematic uncertainties associated with the simulations. The solid and dashed lines indicate multiplicities calculated using Monte Carlo CASCADE[4,5] with a_n equal to A/11 MeV^{-1} and A/13 MeV^{-1}, respectively. Apparent temperatures were extracted from the center-of-mass energy spectra by fitting a generalized Maxwellian distribution to the high-energy slopes of the spectra. The α-particle results are shown as the solid points in Fig. 3.5 1b. Results of identical analyses of spectra calculated using Monte Carlo CASCADE, with a_n equal to A/11 MeV^{-1}, A/12 MeV^{-1} and A/13 MeV^{-1}, are indicated by the solid, dashed and dotted lines, respectively. Although not shown here, calculations with JOANNE[6] yield nearly identical results for both the multiplicities and the spectral shapes. As illustrated in Figs. 3.5-1a and 3.5-1b, our experimental results are consistent with standard statistical model predictions using a constant level density parameter of ~A/13 MeV^{-1}.

However, as suggested by several theoretical discussions,[7,8,9] it is possible that an equally good description of the particle spectra can be made using a level density parameter that varies smoothly with excitation energy. In Fig. 3.5-2 a comparison is made between the experimental α-particle apparent temperatures and several calculations using excitation energy dependent level density parameters. The solid line is a calculation using the strong energy dependence as determined by Fabris *et al*. The three dot-dashed curves are the results of calculations with the parameterization of Fineman *et al.*,[10] a_n = A/(8.2 MeV + $\kappa\cdot$U/A) with κ=4.3, 3.0 and 2.0, based on the work of Shlomo and Natowitz.[8] The result of a calculation based on the recent work of De *et al.*,[9] where a_n = A/(9.5 MeV + 1.3·T) for A=208, is illustrated by the dashed curve. It is evident that our data do not support a strong energy dependence of the level density parameter. Instead, the data indicate that calculations with a value of κ between 3.0 and 4.3 could possibly reproduce the experimental

* Los Alamos National Laboratory, Los Alamos, NM.
1 D. Fabris *et al*., Phys. Rev. C **50**, R1261 (1994).
2 Nuclear Physics Laboratory Annual Report, University of Washington (1998) p. 30.
3 D.J. Hinde *et al*., Nucl. Phys. A **385**, 109 (1982).
4 F. Pühlhofer, Nucl. Phys. A **280**, 267 (1977).
5 M.G. Herman, U. of Rochester Nuclear Structure Laboratory Report UR-NSRL-318 (1987), unpublished.
6 J.P. Lestone, Nucl. Phys. A **559**, 277 (1993).
7 J.P. Lestone, Phys. Rev. C **52**, 1118 (1995).
8 S. Shlomo and J.B. Natowitz, Phys. Rev. C **44**, 2878 (1991).
9 J.N. De *et al*., Phys. Rev. C **57**, 1398 (1998).
10 B.J. Fineman *et al*., Phys. Rev. C **50**, 1991 (1994).

results. This value of κ would be comparable to those determined by Fineman *et al*. for the ^{193}Tl and ^{213}Fr systems. Furthermore, although the offset needs to be reduced, the prediction by De *et al*. follows the same trend as the experimental data. In either case, it appears that a quite modest excitation energy dependence is adequate to describe our results.

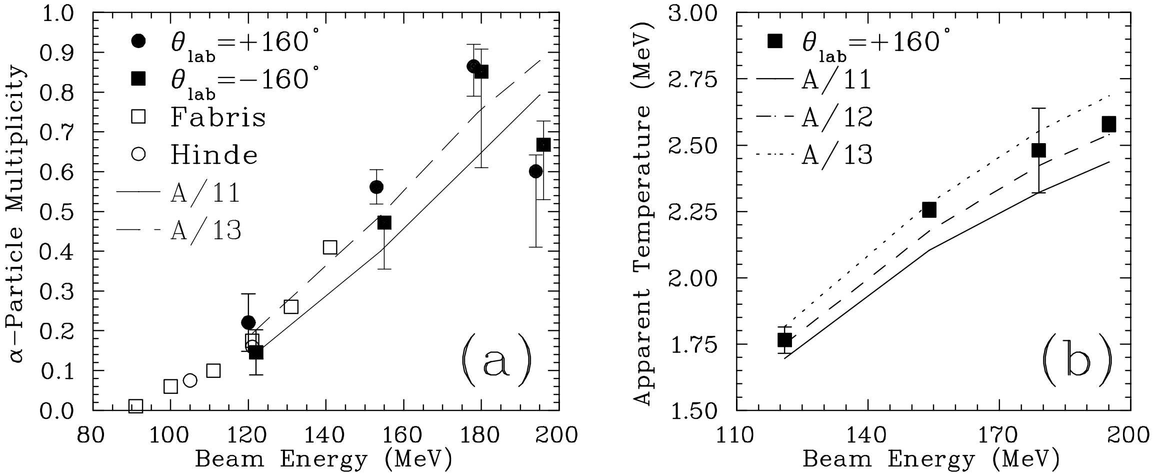

Fig. 3.5-1. α-Particle Multiplicities (a) and Apparent Temperatures (b). The solid points are results from the present experiment. The lines are the results of statistical model calculations described in the text.

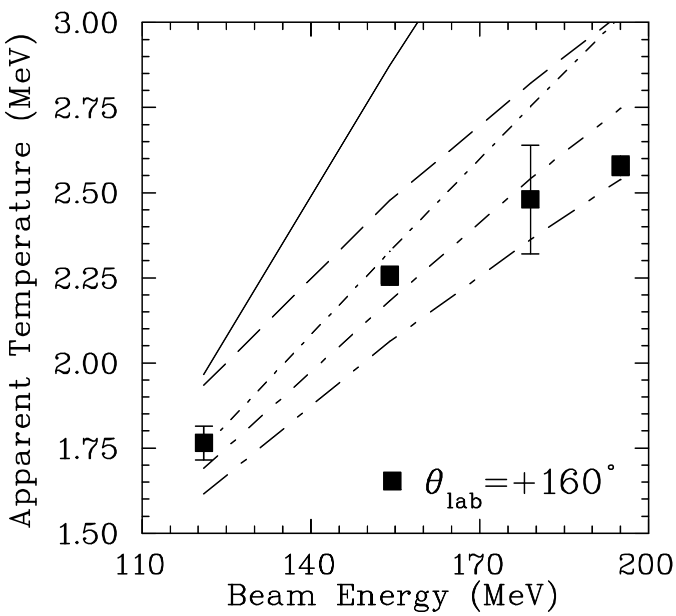

Fig. 3.5-2. Comparisons of calculations with temperature-dependent level densities. The solid points are the experimental α-particle apparent temperatures. The solid and dashed lines illustrate results of calculations with the excitation energy prescriptions of Fabris *et al*. and De *et al*., respectively. The three dot-dashed curves illustrate results of calculations with the parameterization of Fineman *et al*. and κ equal to 4.3, 3.0 and 2.0 (top to bottom).

4.0 NUCLEAR AND PARTICLE ASTROPHYSICS

4.1 The $^7Be(p,\gamma)^8B$ cross section at astrophysically interesting energies

E.G. Adelberger, J.-M. Casandjian, A. Junghans, E. Mohrmann, K.A. Snover, T.D. Steiger, H.E. Swanson and the TRIUMF Collaborators[*]

The apparatus and target development for our $^7Be(p,\gamma)$ experiment has been mostly completed and debugged.[1] In December 1998 we saw our first alpha particles from the decay of ^8B produced by $^7Be(p,\gamma)$. At that time we also completed the design and installation of our proton shields to reduce scattered proton background in the alpha particle detectors. This background was produced by beam hitting the aperture plate on the opposite end of the rotating arm from the target, during the beam flux monitoring (target counting) phase of the arm rotation.

At this point, several different preliminary measurements have been carried out:

1) Yields from $^7Be(p,\gamma)$ have been measured at 5 proton energies spanning the $E_p(cm) = 630$ keV resonance as well as points at 400 and 500 keV, all with statistical uncertainties ~10% or smaller. The relative yields are in good agreement with Filippone[2] except that the resonance appears somewhat broader.

2) A thick target yield curve for the $E_\alpha = 953$ keV resonance in $^7Li(\alpha,\gamma)$ has been measured.

3) Several $^7Be(\alpha,\gamma)$ yield curves have been measured over the narrow resonance at $E_\alpha = 1376$ keV. Sharp resonance curves have been observed with a rise of 2 keV or so, indicating good accelerator beam energy resolution.

Measurements 2) and 3) were carried out using the large UW NaI spectrometer, which was moved for this purpose to the ^7Be target chamber in Cave 1. Measurements 1) and 3) were carried out with a 13 mCi ^7Be target doped with ^9Be. The ^9Be doping was to permit a $^9Be(p,\gamma)$ resonance diagnostic measurement in the eventuality that the $^7Be(\alpha,\gamma)$ measurement proved too difficult, or that an alpha beam of the required intensity was not available. However, the $^7Be(\alpha,\gamma)$ resonance measurement succeeded very well. The observed FWHM is about a factor of 2 larger than the width expected based on only Li+Be in the target, and is thus very encouraging in terms of target purity, although there is a long high energy tail on the resonance. A similar measurement with an undoped ^7Be target showed a resonance profile a factor of 2 narrower. We also plan to measure the $^7Be(p,\gamma)$ resonance yield with good statistics on top of the 630 keV resonance for various sweeping amplitudes and hence various beam flux nonuniformities. This will determine the target uniformity and hence the required beam flux uniformity.

Several improvements are being worked on, including electronic noise reduction in the NaI and Silicon detector signals due to pickup/ground loops as well as noise from the arm rotation motor/computer. Our plans for the near future are for further $^7Be(p,\gamma)$ measurements with more active targets.

---

[*] N Bateman, L Buchmann, A Zyuzin, J Vincent *et al*., TRIUMF, Vancouver, Canada.

[1] Nuclear Physics Laboratory Annual Report, University of Washington (1998) p. 10.

[2] B.W. Filippone *et al*, Phys Rev C **28**, 2222 (1983).

4.2 Installation of chamber and beamline for the $^{7}Be(p,\gamma)^{8}B$ experiment

J.F. Amsbaugh, J.-M. Casandjian,[*] C.E. Linder and T.L. McGonagle

This experiment rotates an arm-mounted target to positions for beam irradiation and for detector counting of the target. Other positions place apertures on the opposite end of the arm into the beam. The radioactive ^{7}Be targets used in the cross-section measurements will produce 10 to 40 mCi of γ-rays with an energy of 478 keV. Radiation safety dictated many design choices for the experiment chamber.

The chamber uses welded aluminum construction and is electrically isolated from the beamline, supports and vacuum equipment. A ferro-fluidic rotary feedthru is provided for the target arm. Ultra high vacuum is provided by a CryoTORR8[1] cryopump. Three 80 liter sorption pumps provide the chamber roughing vacuum. These sorption pumps will be used for cryopump roughing once high activity targets have been used in the chamber. The cryopump overpressure valve is replaced with a sealed check valve whose exhaust is plumbed to a HEPA type N filter that exhausts into the room. The three sorption pump outlets vent through another HEPA filter. The chamber is vented to overpressure, measured by a thin film pressure sensor, with dry nitrogen. The overpressure is relieved though a valve and a 6 by 6 inch HEPA filter exhausting to the room. While the chamber is open, negative pressure is maintained by a blower through the filter. All three filters are surveyed for ^{7}Be contamination. The upstream beamline has been upgraded with a second cryopump whose overpressure is plumbed to the same HEPA filter, but very little contamination is expected here. Vacuum pressure measurement is done with hot cathode ion, pirani, and thermocouple gauges in both areas. Typical operating vacua are $1.0\text{-}3.0 \times 10^{-7}$ Torr.

The major source of ^{7}Be contamination is sputtering by the beam. A liquid nitrogen cooled aperture and annular trap as close as possible to the target intercepts this sputtered material. A second liquid nitrogen trap is in the beamline just upstream of the chamber gate valve. Silicon diodes on the traps and sorption pumps provide liquid present, trap cold, and trap warm indicators. Two channels were modified to provide cryopump temperatures. Contamination from target evaporation due to beam heating is eliminated by water cooling the target and interrupting the beam for insufficient water flow.

A 75 pound tungsten alloy cup can be raised to surround the target with about 6 cm of shielding, allowing personnel to work near the chamber. A pneumatic cylinder moves the shield and a mechanical latch keeps the shield up in case of loss of air or electrical power. Both are required to unlatch and lower the shield.

A 80486 Personal Computer-based programmable controller[2] provides flexible system control and graphic programming interface. It also runs a pushbutton and status light panel for normal user operation. This controller is dynamically programmed with the safety interlocks, vacuum interlocks, sorption pump pumping sequences, vacuum system controls, etc.

[*] GANIL, BP 5027, 14076 Caen, Cedex 5, France.
[1] CTI Cryogenics, Waltham, MA.
[2] Nuclear Physics Laboratory Annual Report, University of Washington (1993) p. 89.

4.3 WALTA: The Washington Large-area Time-coincidence Array

J.G. Cramer, P.J. Doe, S.R. Elliott, D.J. Prindle, J.F. Wilkerson and the WALTA collaboration[*]

We are forming a collaboration for the development of a distributed detector network. This system will support measurements of air showers from ultra-high energy cosmic rays and can also support a broad class of other physical measurements, for example a network of seismographs for geophysics studies. We call the overall network NNODE (Northwest Network for Operation of Distributed Experiments), and we call the cosmic ray measurement component WALTA (WAshington Large-area Time-coincidence Array). The project is to be a direct physical science outreach program between faculty and students of the University of Washington and the science teachers and students of Washington-area middle schools and high schools (grades 7-12). The WALTA[1] part of the project is modeled on the ALTA initiative pioneered by the University of Alberta and currently being implemented in the Alberta Provincial School System. The local collaboration includes members of the Nuclear Physics Laboratory, physics department personnel in the cosmic ray and physics education groups, and a department of education faculty member from Seattle University.

Each WALTA/NNODE measurement module is envisioned to consist of a computer with an Internet connection, a GPS timing system, and measuring equipment. The measuring devices will be of several types. The WALTA modules will consist of scintillation paddles to be placed at the school to detect distributed particle showers produced at the top of the atmosphere by ultra-high energy ($\sim 10^{20}$ eV) cosmic rays. The UW Geophysics Department group plans to install seismographs to the NNODE network that will become part of the Pacific Northwest Seismograph Network. Three other groups have expressed some interesting possibilities of adding additional measurement units to the NNODE network

WALTA/NNODE aims to provide students the opportunity to become active participants in forefront scientific projects. A cornerstone of the program will be to install a WALTA/NNODE measurement module at each participating school. This will allow direct hands-on participation by the teachers and students in active experiments as collaborators with UW faculty and students. Each module will be supplied with special display and analysis software so that students and teachers can monitor both the local and the collective measurements made by WALTA/NNODE as well as use the data for class projects. In addition we will develop an educational program to help link aspects of the individual experiments with elements of the middle and high school science curriculum. We envision direct faculty visitation and involvement with the teachers and students as well as UW based workshops aimed at the teachers and students. It may even be possible to enlist the help of the students in the construction of the WALTA measurement modules. We plan for both UW graduate students and undergraduate students to actively participate in the project.

The WALTA/NNODE modules involve state of the art hardware and software technology. Learning details about the technology utilized in the WALTA/NNODE modules (Field Programmable Gate Array electronic chips, custom CMOS electronic circuits, GPS receivers for determining absolute timing to 20 nanoseconds, real-time object oriented programming, distributed programming) may also be worth incorporating into the outreach program.

The project offers a unique win-win aspect that does not depend on participant altruism for success. The participating scientist will be able to address one of the major unsolved problems in contemporary astrophysics with a unique measurement tool. The students and teachers will be able to learn about scientific techniques, mathematical tools, and the latest measurement technology. The teachers will be part of a rich environment of scientific research from which they can draw materials that give immediacy and emphasis to their teaching.

---

[*] The non-NPL members of the WALTA collaboration include: Paula Heron and Peter Schaffer from the Physics Education Group; Jeffry Wilkes and Eric Zager from the Cosmic Ray Group; and Mark Roddy from the department of education at Seattle University.

[1] The WALTA web page can be found at http://www.phys.washington.edu/~walta.

5.0 ULTRA-RELATIVISTIC HEAVY IONS

5.1 Event-by-event analysis overview

L.D. Carr, D.J. Prindle, J.G. Reid, T.A. Trainor and D.D. Weerasundara

The URHI program has as its goal the discovery and study of the quark-gluon plasma. We study full QCD in the neighborhood of the phase boundary between hadronic and partonic matter. Well-established study techniques already applied to this problem depend on inclusive analysis of multiparticle distributions. Event-by-event (EbyE) physics is a more recent effort to study event-wise dynamical fluctuations and correlations as a means to probe the detailed shape of the phase boundary. Some of these techniques have well-established analogues in the study of normal-matter phase transitions in bulk matter. But there are important differences having to do with finite systems, incomplete equilibration and relativistic kinematics. The development of EbyE techniques in heavy ion collisions has been pioneered by the UW group within the NA49 collaboration at SPS/CERN, and is now continuing with the STAR collaboration at RHIC/BNL.

NA49 The NA49 EbyE program at the CERN SPS has had two major aspects: 1) application of scaled topological measures (SCA) to true event-wise characterization of event topology and comparison with references to search for special event classes having significant dynamical fluctuations in the final-state momentum distribution and 2) analysis of global momentum variables, some with thermodynamic analogs, to search for dynamical fluctuations on an inclusive basis.

The SCA technique has proven to be a highly successful model-independent correlation analysis system. Current work focuses on an upgrade of the SCA analysis package to increase speed and flexibility, on establishing filters to eliminate instrumental effects and multi-collision pileup from candidate anomalous events and on identifying or establishing an upper limit on dynamical fluctuations.

Global variables analysis is presently enjoying intense interest from the theoretical community and rapid technical development. Reexamination of fundamental statistical principles and fluctuation theory accompanies an expanding data analysis program.

STAR Techniques pioneered by the UW group within the NA49 collaboration are now being imported to STAR as we anticipate the first RHIC beam this Summer. This program has required an extensive software development program within the RHIC Computing Facility (RCF) tailored to the needs of STAR EbyE analysis. EbyE software infrastructure provided by UW has been tested in a sequence of two RCF Mock Data Challenges (MDC1,MDC2) in the last six months.

The STAR EbyE program is coordinated within the structure of the EbyE Physics Working Group. Activities in this group, in addition to global variables and SCA analyses which are UW specialties, include flow analysis, low-pt (e.g., DCC) analysis and high-pt (e.g., minijet) analysis. Because of the more complex dynamical picture expected to emerge at RHIC energies we anticipate strong overlap with other Physics Working Groups specializing in strangeness, high-pt and spectra physics as we attempt to unravel the various aspects of full QCD.

EbyE Theory Application of scaling analysis and global-variables analysis to NA49 data has resulted in significant conceptual progress in understanding the basic correlation and statistical measures used. Progress includes a better understanding of finite-system (bounded scale interval) effects, the limitations of classical fluctuation theory and possible extensions, the basis of the Central Limit Theorem and possible extensions and the connection between system symmetries, scale dependence, fluctuations and correlations in a multiparticle final state and what these can tell us about the structure of the QCD phase boundary. Some of these results are quite general and may be broadly applicable to finite-system many-body problems.

5.2 NA49 SCA event-by-event analysis status

L.D. Carr,[*] D.J. Prindle, J.C. Prosser,[†] J.G. Reid, T.A. Trainor, D.D. Weerasundara and the NA49 Collaboration[#]

In 1998, we completed an event-by-event analysis of 300,000 central Pb+Pb collisions using *Scaled Correlation Analysis* (SCA)[1] which proved to be a very powerful method to search for rare processes occurring in Pb+Pb collisions. As a result of this analysis, we identified a class of anomalous events having excess yield of charged particles in the bend plane $\phi = 0°$, $\phi = 180°$ in the main TPC. Analysis and interpretation of anomalous event classes required a thorough search for instrumental effects and conventional hadronic physics as trivial origins of anomalous behavior, and simulation studies with standard and special Monte Carlo (MC) event generators to investigate anomalous behavior that may be nontrivial.

A subsequent detailed analysis[2] of these anomalous events revealed *beam-gas event pile-up* to be the principal source of enhanced secondary particle production in a majority of the anomalous events. In this case event pile-up means that a secondary nucleus or nucleon in the beam interacts with the primary target or a gas nucleus while information from a triggered central Pb+Pb collision is being read out by the detector. By comparing the distribution of charged particles associated with the primary vertex for several collision systems (*e.g.*, pp, pA and AA), as well as from the pile-up vertex (x,y) coordinate distributions, we determined that the pile-up events resulted from a second Pb ion interacting with TPC gas downstream of the primary vertex within 20 μsec of the triggering collision.

Pile-up events contribute a significant background to the search for true rare processes (perhaps due to new physics) for which the SCA was designed. Therefore, we need to develop methods to understand and remove the known backgrounds to extract true physics signals. We have demonstrated in the past[3] that the slopes and intercepts of charged tracks from a common point of origin are correlated. An algorithm which exploits slope-intercept and impact-parameter-slope correlations has been developed to remove the pile-up events and to study in detail the remaining anomalous events. Work is in progress to study the efficiency of this algorithm in identifying pile-up events, especially those occurring in or near the primary Pb target.

NA49 has just completed DST production for 400,000 central Pb+Pb collisions from the 1996 experimental run. A program is underway to analyze these events using SCA.

---

[*] Physics Department, University of Washington, Seattle, WA.
[†] University Computing, University of Washington, Seattle, WA.
[#] CERN, Geneva, Switzerland.
[1] Nuclear Physics Laboratory Annual Report, University of Washington (1998) p. 39.
[2] Nuclear Physics Laboratory Annual Report, University of Washington (1998) p. 40.
[3] Nuclear Physics Laboratory Annual Report, University of Washington (1996) p. 43.

5.3 NA49 pileup detection and EbyE analysis

D.J. Prindle, J.G. Reid, T.A. Trainor and D.D. Weerasundara

We have used a model-independent method to search NA49 data for dynamical fluctuations[1] (see Section 5.2). In this analysis we found a class of anomalous events characterized by excess tracks in the Main TPCs near $\phi = 0^o$ and $\phi = 180^o$. Previous analysis[2] showed that conversions of γ-rays or decays of neutral particles could not account for the characteristics of these anomalous events. We were led to examine beam pileup as the probable cause for these events.

After a beam-particle interaction in the target triggers the start of a readout it takes approximately 50 μs for all the ionization from the tracks passing through the TPCs to drift to the readout chambers. During this time a few beam particles will pass through the detector. A small fraction of these will have minimum bias interactions with the target or gas and create some number of particles, typically 20 or more, originating at a well defined vertex. These pileup interactions occur at random places and times. Some of them will create tracks that are indistinguishable from those tracks due to the primary interaction.

In NA49 the magnetic fields are in the *y* direction, thus there is little curvature of the track in the *y* direction. When plotting *y* versus *dy/dz* at a reference *z* position the locus of tracks originating at a common vertex is a straight line. The slope of this line is related to the *z* position of the vertex. Plotting *y* versus *dy/dz* for all tracks we observe most of them to be along a line corresponding to the target position. Tracks from a pileup interaction are along another line, the slope of this line being determined by the *z* position of the pileup interaction. If the pileup interaction happens later in time, the ionization in the TPCs will reach the readout chambers late (since the clock is started by the trigger interaction) and the inferred *y* position will be lower, displacing the straight line locus. Thus even if the pileup is in the target it may result in a *y* versus *dy/dz* line parallel and distinguishable from the line due to the primary interaction.

To search for pileup interactions we scan the *y* versus *dy/dz* plot after removing tracks along the target locus. We shear this plot parallel to *y* and project on *y*. When we shear by the right amount the pileup tracks all contribute to create a peak in a 1-dimensional histogram which is easy to find algorithmically. The amount of shear required to maximize the height of the peak determines the *z* position of the pileup interaction. Depending on where the pileup interaction occurs we find its tracks in different TPCs. If the pileup occurs in the target then all TPCs should be able to observe it.

We have scanned all the anomalous events and found that the majority of them do have tracks from pileup interactions. Some of them show more than one pileup interaction. The majority of the pileup vertices in the anomalous event sample happened downstream of VT1, but were observable with VT2 and the MTPCs. We compare the *z* position of the pileup vertex as determined by VT2 and the MTPCs and find that they are consistent. Since the drift velocities in VT2 and the MTPCs were different the inferred *y* positions of the pileup interaction are different, but they are linearly related. The observation of this slope confirms that the pileup interactions are happening at random times and thus are not associated with the triggered beam particle.

We still need to quantify the efficiency with which we can find pileup interactions as a function of *z* and also the number of particles coming from the interaction. We need to do this in order to see if pileup can explain the entire anomalous event sample. It is also important for other types of anomalous event searches to know what influence pileup can have.

[1] Nuclear Physics Laboratory Annual Report, University of Washington (1998) p. 39.
[2] Nuclear Physics Laboratory Annual Report, University of Washington (1998) p. 40.

5.4 Event by event global variables analysis

J.G. Reid and T.A. Trainor

Our recent work in event-by-event physics has focused on characterizing each event by a set of global variables (e.g., multiplicity, event-wise mean transverse momentum) and then analyzing the distributions of these event characteristics. We have carried out this analysis both on NA49 central Pb+Pb data and simulated data in the context of NA49 and STAR.

For the purpose of characterizing the events we have focused on two separate analysis methods. First, we have examined the linear correlation coefficient between event multiplicity and eventwise mean transverse momentum. In proton-proton collisions there is an anti-correlation observed between these variables (in part due to simple 4-momentum conservation), so it is natural that we should investigate this correlation in the Pb+Pb data and N+N simulations.

We are also interested in the multi-particle correlations which are present in the eventwise final-state transverse momentum distributions. This is an intractably difficult problem because of the large eventwise multiplicity, so we have limited ourselves to addressing 2-particle correlations, bearing in mind that this can be generalized to an n-particle approach using SCA.

The original motivation for using these two quantities to characterize the data is their relationship to the Φ measure of Gazdzicki and Mrowczynski.[1] Rewriting Φ in a more transparent form it contains a linear correlation coefficient and a 2-particle correlation measure:

$$
\begin{aligned}
\Phi_{p_t} &= \sqrt{\frac{\overline{Z^2}}{\overline{N}}} - \sigma_{p_t} = \sqrt{\frac{\overline{(P-N_e \cdot \overline{p})^2}}{\overline{N}}} - \sigma_{p_t} \\
&\simeq \frac{1}{2\overline{N}\sigma_{p_t}} \left\{ \left[\overline{\sum_{i\neq j} p_i p_j} - \overline{N_e(N_e-1)} \cdot \overline{p}^2 \right] \right. \\
&\qquad \left. - \left[2\overline{p} \cdot \left(\overline{N_e^2 < p >_e} - \overline{N_e^2} \cdot \overline{p} \right) \right] \right\} \\
&= \frac{A^2 + B^2}{2\overline{N}\sigma_{p_t}}
\end{aligned}
$$

After a detailed study of Φ we have found it impossible to interpret the measure Φ unambiguously, so we have turned our focus to the more elementary measures which contribute. Rather than interpret a single number we look at the results of the individual analyses and interpret them separately.

In applying these methods to NA49 central Pb+Pb data we have encountered some interesting results. There is a significant but small (lcc = -0.0307±0.003) anticorrelation between eventwise multiplicity and mean pt which is a factor of three smaller then the value observed for N+N collisions, but still nonzero. Also, looking at the 2-particle correlation space we have found the expected Bose-Einstein correlation peak, the Coulomb correlations, and correlations from resonance decays. But we have also identified significant trends in the data which are absent in the simulations and have yet to be fully understood.

[1] M. Gazdzicki and St. Mrowczynski, Z. Phys. C **26**, 127 (1992).

5.5 Scaled correlation analysis code update

J.G. Reid

After last year's successful effort[1] to convert our main scaled correlation analysis code into an object-oriented framework using C++ the coding tasks this year have been minimal. There were several rounds of bug fixes and modifications to make the code more stable and results from default parameter analyses less opaque. Significant work has been put into better documentation, commenting and adding command-line options which make the code more distributable. A great deal of input from novice users was used in these developments.

The only major change made was a different method for calculating the minimally correlated reference bin occupancies in the 'prior' SCA formalism. Previously we were weighting each bin in the support of the event equally at the scale of the minibinning. As one goes to large scales this can cause problems because a uniform distribution at the scale of the minibinning can be significantly non-uniform at larger scales. This led to uncontrolled behavior of the reference at large scale, and introduced a scale bias into the code.

Dynamically weighting each bin of the minimally correlated reference in the support of the event at each scale point removed this problem. However, this may not be the ideal solution. We do not fully understand the implications of using a dynamically changing reference, although it has not presented any major problems yet. Of course, if the user has a specific reference distribution in mind this change makes no difference. The change will only effect model calculations and SCA theory development.

[1] Nuclear Physics Laboratory Annual Report, University of Washington (1998) p. 43.

5.6 STAR mock data challenge: general DST design and the EbyE analysis chain

L.D. Carr,[*] J.C. Prosser,[†] J.G. Reid, T.A. Trainor, D.D. Weerasundara and the STAR Collaboration[#]

The RHIC Computing Facility (RCF) and four RHIC experiments successfully completed the Mock Data Challenge (MDC), in two phases, during 1998 Fall and 1999 early Spring.[1] The RCF configuration during each phase of the MDC consisted of a Managed Data Server (MDS), a High Performance Storage System, a Central Reconstruction Server farm (CRS), and a Central Analysis Server farm (CAS).

During both phases of the MDC, the RCF and the RHIC experiments exercised key aspects involved in recording and off-line analysis of experimental data. Among the goals achieved during the MDC1, for each of the four experiments, were: recording raw data, reading the raw data into the reconstruction farm and writing the Data Summary Tapes (DSTs) back out.

An aspect common to both the CRS and the CAS operation is the definition of a DST. The DSTs are produced by the CRS operation while analyses running on CAS use DSTs as their input. A DST is defined to be a collection of event information obtained during event reconstruction, for all the events of a given set. The DST event information represents our best knowledge of the individual collision. This information should contain all the necessary information needed for further physics analyses which will lead to the extraction of physics signals. The UW group made a substantial contribution to the development of the DST objects specific to the MCD1 operation. This DST event model included objects that fully define the state of the hardware, state of the software, state of the collision, momentum space of the event, summary of the information content for each event and the summary of the information content for a given set of events. This event object model was successfully employed during the MCD1 to generate DSTs for about 190,000 reconstructed events.

Additional to RCF goals for MDC2, STAR goals for MDC2 were: to exercise off-line software in ROOT environment, fully integrate conditional databases for calibrations and Tag Database for data mining, develop raw & off-line data formats and data models, establish well-defined CAS operations including post-DST analyses & micro-DST generation, and integrate Grand Challenge apparatus for data mining. The STAR collaboration has made significant progress toward achieving its MDC2 goals over the past several months. As part of the MDC2 program STAR generated 0.5 million events run through Geant Detector simulations for several detector configurations and has so far reconstructed about 20% of the total Geant events during the two-week period of MDC2 allocated to STAR.

The UW group have taken a lead role in establishing a post-DST analysis program on the CAS farm. Central to the CAS operation is event-by-event (EbyE) physics analysis, a major emphasis of the UW group within STAR.[2] The EbyE group intend to examine each of 10^7 events per year to extract information content, examine events for anomalous behavior, and sort the event population on the basis of any such behavior. This process involves interfacing with the MDS, the Tag Database, CAS batch job submission mechanism (LSF), etc. We have developed a preliminary analysis chain to be run on the CAS farm to perform an EbyE analysis.

[*] Physics Department, University of Washington, Seattle, WA.
[†] University Computing, University of Washington, Seattle, WA.
[#] Brookhaven National Laboratory, Upton, NY.
[1] Nuclear Physics Laboratory Annual Report, University of Washington (1998) p. 36.
[2] Nuclear Physics Laboratory Annual Report, University of Washington (1998) p. 37.

5.7 Finite-size effects and fluctuations near a phase boundary

T.A. Trainor

General arguments based on universality have recently been put forward in support of a localized structure on the QCD phase boundary: a tricritical point or critical endpoint located at some intermediate position in (T, μ_B). Detection and study of such a structure would be an important contribution to our understanding of full QCD. From an experimental viewpoint the question immediately arises what effect finite system size has on the observability of such a structure?

To explore the consequences of finite system size on critical phenomena the Ising magnet serves as a paradigm. For an infinite lattice (bulk matter) below the critical point the magnetic susceptibility is singular and the magnetization is discontinuous. How does finite system size affect this picture? Finite *scale interval*, bounded by the characteristic size *a* of a spin (or more generally a typical momentum-carrying object) and the characteristic size *L* of a 'causally connected' or 'equilibrated' region, determines the maximum sharpness of structures near critical points.

We can express the total free-energy density in terms of the individual free-energy densities of the two spin populations ϕ_+ and ϕ_-. The overall free-energy density can be written:

$$\Phi(H) \approx -\log\left\{ e^{-\phi_+(H)\cdot(L/a)^d} + e^{-\phi_-(H)\cdot(L/a)^d} \right\}\cdot(a/L)^d$$

If $L/a \to \infty$ and given the nearly linear dependence of $\phi_\pm$ on H near the origin we have $\Phi(H) \approx |H|^1$ for $|H| \approx 0$ at and below the critical temperature, leading to an asymptotic (in scale interval *L/a*) singularity in the magnetic susceptibility. The functional form of *M(H)* depends parametrically on the scale interval $(L/a)^d$ as illustrated in Fig. 5.7-1.

If the QCD phase boundary is 'observed' with a finite collision system dynamical fluctuations may be considerably reduced from bulk-matter expectations because of finite-scale-interval effects. Observability may depend critically on a number of experimental issues such as statistical power of the data sample, measure sensitivity and reduction of systematic effects. Quantitative predictions of fluctuation phenomena should include finite-system effects.

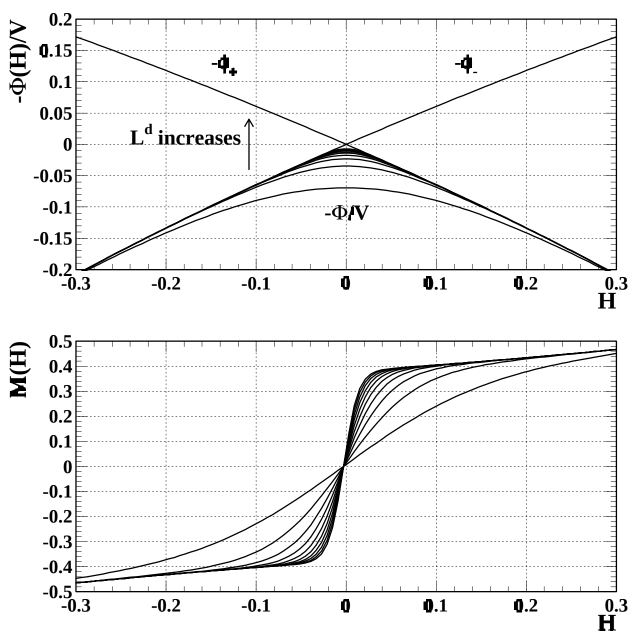

Fig. 5.7-1. Sketch of free-energy Φ and magnetization *M* dependence on external field for the Ising lattice at $T < T_c$ and various system sizes *L*. In the asymptotic limit $L \to \infty$ the magnetization becomes discontinuous and the susceptibility becomes singular. Fluctuations near a phase boundary are expected to be large. For finite systems both quantities vary smoothly, and fluctuations may be greatly reduced and difficult to distinguish from finite-number statistics.

5.8 Linear near response coefficients and fluctuations: beyond the gaussian model

T.A. Trainor

Critical-point phenomena are accompanied by fluctuations with characteristics determined by the dependence of the free energy on relevant state variables. The standard treatment of fluctuations is the Einstein/gaussian theory or linear response theory. This standard treatment cannot predict fluctuation properties in the neighborhood of a critical point.

An equilibrated system can be characterized by a free energy $\phi = (TS, A, G...)$. A local extensive state variable can then be expressed in terms of its conjugate intensive variable and a free energy as $X_\alpha = \partial\Phi / \partial\alpha$. Linear response coefficients $\chi_\alpha(C_V, \kappa_T, ...)$ can be defined by $\chi_\alpha = \partial X_\alpha / \partial\alpha$. The gaussian fluctuation model (free energy assumed quadratic in the neighborhood of its minimum) implies that a fluctuation variance is directly proportional to a corresponding linear response coefficient: $\sigma^2_{X_\alpha} \propto \chi_\alpha$.

These relationships are represented in Fig. 5.8-1. The *E(T)* dependence is piece-wise linear, corresponding to two different DoF (degrees of freedom) density regions separated by a phase boundary. Near the critical temperature fluctuations increase in amplitude but are bounded, whereas the linear response coefficient (slope of *E(T)*) may be arbitrarily large. Paradoxically, gaussian fluctuation theory would predict $\sigma^2_{\chi_\alpha} \to \infty$ when fluctuations are in fact bounded.

The paradox is resolved by noting that linear response coefficients measure the *curvature* of the free energy surface near its minimum. *If* the free energy surface is approximately quadratic in the neighborhood of its minimum then $\sigma^2_{\chi_\alpha} \propto \chi_\alpha$ is a good approximation. However, near a critical point the free energy curvature and the width may have *no well-defined relationship*. The guassian treatment breaks down and linear response coefficients *cannot predict or represent fluctuation amplitudes*. A separate determination must be made of the local variance density and the linear response coefficients. Both linear response coefficients and fluctuation amplitudes are in principle measurable. Instead of being redundant (as in gaussian theory) they actually provide complementary information about the underlying system Hamiltonian.

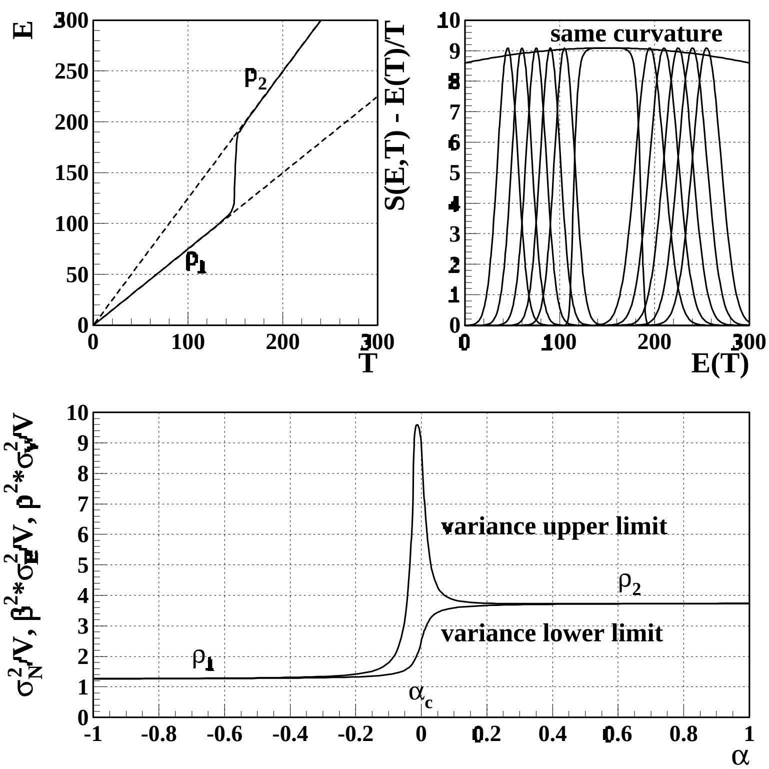

Fig. 5.8-1. Sketch of E(T) dependence near a phase transition (top left), fluctuation distribution for various temperatures (top right) and plot of fluctuation amplitude *vs* temperature estimated by linear response coefficients (upper limit) and DoF density (lower limit) (bottom).

5.9 Symmetry and the Central Limit Theorem

T.A. Trainor

The Central Limit Theorem (CLT) is a fundamental element of statistical analysis. The CLT can be formulated in the following way. If events of N *independent* samples x with event total X are drawn from a *static* parent distribution the distribution of event means $<x> = X/N$ approximates a gaussian distribution with mean approaching the parent mean $\bar{x}$ and variance $\sigma^2_{<x>}$ related to the parent variance σ^2_x by $\sigma^2_{<x>} = \sigma^2_x / N$.

Departures from the CLT are due to 1) correlated samples and 2) variation of the parent during the sample history. Net positive correlation implies that $N_{eff} < N$, that is, the *effective* sample is less than N, leading to an increase in $\sigma^2_{<x>}$ beyond the CLT expectation. The opposite is true for net anticorrelated samples. If the parent distribution varies during the sampling it can be shown that a quantity proportional to $\sigma^2_{\bar{x}}$ contributes to $\sigma^2_{<x>}$, where $\sigma^2_{\bar{x}}$ is a variance measure for the (slowly-varying) parent-distribution centroid.

It is possible to extend the CLT in the following way. The samples x can be seen as the result of a partition of an event. And events in turn can be seen as resulting from the partition of a larger bounded space on which is distributed some additive measure. This picture is consistent with the Grand Canonical Ensemble. The sample number N can be interpreted as the ratio of the event scale to the sample scale e_2 / e_1 (for space dimension 1). The CLT is then a special case of a more general principle: Under certain conditions $\sigma^2(e_2)/e_2 \approx \sigma^2(e_1)/e_1$, or the variance *density* $\sigma^2(e)/e$ is scale invariant over some scale interval $[e_1, e_2]$.

It can be shown that the quantity $\sigma^2(e)/e$ is simply related to the autocorrelation. Thus, the extended CLT is equivalent to saying that the autocorrelation of an additive measure is invariant over some scale interval, which is to say that the measure is *symmetric* over this interval. This situation is represented in Fig. 5.9-1 in which a hierarchy of structures is distributed on some space. Over a particular scale interval in which structures appear point-like and randomly distributed the extended CLT is satisfied and $\sigma^2(e)/e$ is scale invariant. In a scale interval over which new structure is being resolved (correlation onset) the variance density is changing and the CLT is violated. This picture can also be applied to a phase transition in which a change in energy density alters the effective density of degrees of freedom, resulting in increased correlation and departure from the CLT.

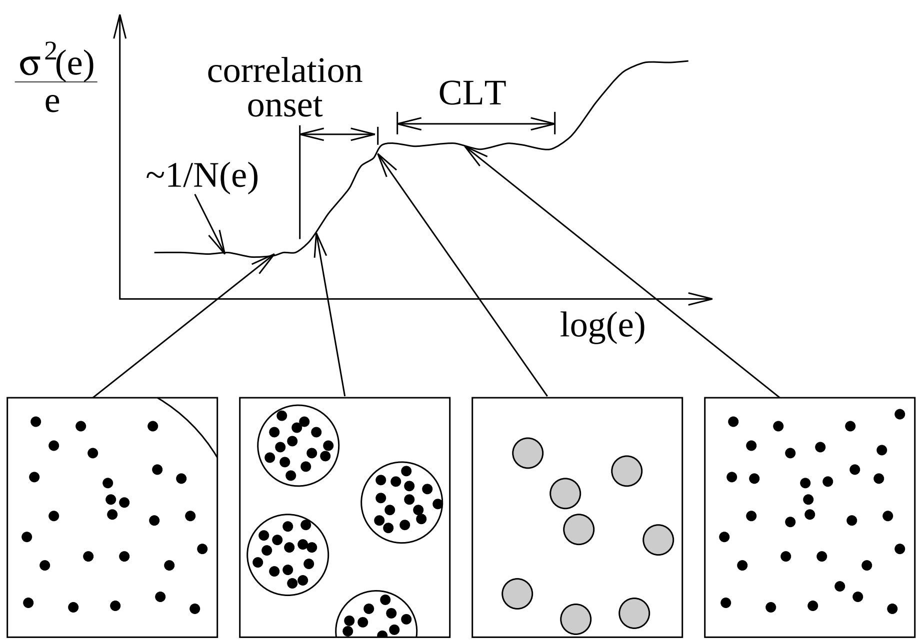

Fig. 5.9-1. Schematic representation of an extended CLT principle applied to a hierarchical system. Over scale intervals containing uncorrelated distributions the extended CLT is satisfied and $\sigma^2(e)/e$ is invariant. For scale intervals in which new structure is being resolved $\sigma^2(e)/e$ varies and the CLT is not valid. Thus, differential measures predicated on the CLT actually probe the symmetry properties of additive measures and are closely related to scaling analysis of correlation structures.

5.10 HBT Physics at STAR

J.G. Cramer and the STAR HBT Physics Working Group.

The STAR HBT Physics working group will use two-particle and multi-particle correlations in momentum space to gain information about the geometry and dynamics of the particle source created in collisions at RHIC. The initial focus of these investigations will be the study of the two-particle correlations of charged pions measured with the STAR detector, both same-sign pairs and opposite-sign pairs. With a data sample of 10^5 to 10^6 events we expect to be able to characterize the longitudinal and transverse size of the source at freeze-out, as well as its time duration of particle emission and its longitudinal and transverse flow characteristics. Similar analyses have already been performed on similar data samples at SPS and AGS energies. We plan to study these source characteristics as a function of centrality with Au+Au collisions and would also like to perform similar studies with a lighter system, e.g., Si+Si. We also plan to apply recently developed transform techniques which may permit reconstruction of an image of the source. Simulations indicate that the lower momentum cutoff of the STAR TPC is lowered to about 50 MeV/c by reducing the field to half its normal value. Since much of the dynamic information from HBT is derived from the momentum dependence of the geometry parameters, some data from central collisions at half field is highly desirable for HBT analysis.

In addition to pion interferometry, we plan to use the same analysis techniques with kaons, protons, and other particles identified with STAR. Further, we plan to investigate the correlations of unlike particles, e.g. pi-K correlations, which can provide independent information on source size. The results of these analyses may provide information on the earlier phases of source evolution and on particle emission order. They will also add extra constraints to comparisons with theoretical models. In the longer term, we will also investigate three and four particle correlations, which can provide information about source asymmetry and source coherence. This effort is likely to require larger event data sets, because of the reduced probability of finding three or four particles in close proximity in momentum space in a given event.

We have requested the following data sets for initial RHIC operation, based on the assumption that the pion multiplicity scales with center of mass energy and that source radii scale as the cube root of multiplicity. Under these assumptions, for a given event sample size the statistical precision of HBT parameters from Au+Au collisions at RHIC will be similar to those for Pb+Pb collisions at the SPS, where experience indicates that a sample of about 10^5 events is sufficient. Since we intend to perform HBT analyses on subsets of data for a particular trigger condition, we estimate that a sample of 10^6 events is needed for HBT analysis at each beam/trigger configuration. Therefore, we have arrived at the following request, in order of priority.

1) 1.0 M events, Au+Au at $(S)^{1/2}$ = 200 GeV, central trigger (5% of σ_{inel}) at full B-field. This is the main data set needed for year-1 physics, and will be used as described above for establishing the geometrical and dynamic characteristics of the source.
2) 1.0 M events, Au+Au at $(S)^{1/2}$ = 200 GeV, minimum bias trigger at full B-field. It is assumed that this data set will be accumulated along with that above by down-scaling a min-bias trigger. It will be used for investigating the dependence of source geometrical and dynamic characteristics as functions of centrality, i.e. participant number.
3) 0.2 M events, Au+Au at $(S)^{1/2}$ = 200 GeV, central trigger (5% of σ_{inel}) at half B-field. As mentioned above, this data set will be used to extend the analysis to the low pT region to obtain a longer "lever arm" for improved extraction of momentum dependence.
4) 0.5 M events, Si+Si at $(S)^{1/2}$ = 200 GeV, central trigger (5% of σ_{inel}) at full B-field. This setting will provide additional information about the dependence of the HBT parameters on participant number over a larger dynamic range and under differenc conditions than (2) above. If some QGP signal e.g., long time duration, is manifest in the analysis if (1), this data set may provide a way of turning off the signal.
5) 0.5 M events, Au+Au at the lowest feasible RHIC energy setting, central trigger (5% of σ_{inel}) at full B-field. This data set, along with that of (1) and SPS data, will be used to construct an "excitation function" of geometrical and dynamic source characteristics.

5.11 Numerical procedures for Coulomb size effects in STAR HBT analysis

J.G. Cramer and L. Ray*

Bose-Einstein interferometry using charged pions must take into account the final-state Coulomb interaction between the identical particles as they emerge from the source. Moreover, the Coulomb interaction is modified by the finite size of the source, with increasing source size leading to decreasing Coulomb repulsion. In simulating or analyzing two-particle pion correlations, this effect must be taken into account.

The best treatment of finite-source Coulomb effects for these purposes is obtained by 6-dimensional integration of numerically calculated Coulomb wave functions over the source distribution. Pratt has written a widely used computer program PIPIBIG for this purpose. It uses 6-dimensional Monte Carlo integration, and it implements the 3-space Coulomb wave function calculation procedure described in Messiah. Unfortunately, for adequate suppression of Monte-Carlo integration noise one must use about 10^6 samples per Coulomb correction output value, leading to a computation time of several hours on a fast computer for a full Coulomb correction function for one source size. For this reason the Pratt code cannot be used directly for simulating or analyzing two-particle pion correlations.

We have addressed this problem by assuming a spherical source and calculating and tabulating the Coulomb correction function for source radii of 6.0 fm to 18.0 fm in steps of 2.0 fm and over a broad range of relative momentum values, for both like-sign and opposite-sign Coulomb interactions between pions. We have used these tables as inputs to an interpolation program that, for a given source size and relative momentum, rapidly returns a value for the finite-size Coulomb correction. In cases where the value of the correction is outside the calculated range, linear interpolation in the Sommerfeld parameter η is used.

Up to now this routine has been used in several simulation programs with success. We plan to incorporate it into the main HBT analysis for STAR, where it will be used in the following way. First, in a particular sub-range of rapidity and average momentum (y, K_T) two particle correlations for opposite-charge pions will be analyzed. These data will be fitted using a version of the Pratt code developed by one of us (JGC) that includes integration over the finite momentum resolution of the detector, and a Coulomb radius for that sub-range will be extracted. This Coulomb radius will then be used as the source size for the Coulomb corrections used to analyze the two particle correlations for same-charge pions, interpolating from the computed tables in both source radius and relative momentum as needed. We feel that this procedure makes optimum use of available computational tools in dealing with Coulomb corrections in HBT analysis.

* University of Texas, Austin, TX.

5.12 An universal pion phase space density

J.G. Cramer, D. Ferenc,[*] [†] U. Heinz,[*] [#] Tomaski[*] and U.A. Weidemann[*] [%]

In ultrarelativistic heavy ion collisions the pion freeze-out phase space density determines the importance of multiparticle pion correlations and of dilepton production from $\pi^+\pi^-$ annihilation. We have extended the procedure of Bertsch[1] for estimating the phase space density to the case where longitudinal flow is present in the system. In this case, the phase space density <f> at a given value of rapidity (y) and transverse momentum (p_T) can be written as:

$$< f > (p_T, y) = \sqrt{\lambda(p_T, y)}\,\frac{\dfrac{dn^-}{dy}\dfrac{1}{2\pi T_{eff}^2}e^{-p_T/T_{eff}(y)}}{\pi^{-3/2}E_p R_S(p_T, y) R_O(p_T, y) R_L(p_T, y)\sqrt{1-(R_{OL}^2(p_T, y)/R_O R_L)^2}}$$

where λ is the "chaoticity parameter", E_p is the total energy of the system, dn^-/dy is the multiplicity of negative pions, T_{eff} is the effective temperature that characterizes the observed transverse momentum spectrum of negative pions, and (R_S, R_O, R_L, R_{OL}^2) is the set of HBT radii which characterize the geometry and longitudinal flow of the source in the Bertsch-Pratt momentum coordinates side (S), out (O), and long (L). The square root term in the numerator is present to include only contributions of pions from direct production or short-lived resonances in the average phase-space density. The square root term in the denominator increases the phase space density due to the effect of "phase-space squeezing" arising from the action of longitudinal flow, which correlates momenta in the out and long directions. Note that at mid-rapidity flow symmetry requires that $R_{OL}^2 = 0$ there, so that this term becomes 1.

We have calculated <f> near mid-rapidity for a range of heavy ion systems and collision energies, measured at the CERN SPS and the Brookhaven AGS. We have compared these densities with thermal estimates of the phase space density for a Bose-Einstein distribution. We find that for most of the data from all of the systems studied, the phase space density points fall on "universal" curves that are in rough agreement with the densities calculated from Bose-Einstein distributions. Near mid-rapidity the characteristic temperature of the Bose-Einstein distribution is about 120 MeV. Note that the latter is not the T_{eff} effective temperature used in the above relation and derived from a particle spectrum that includes radial flow effects, but the lower temperature of the intrinsic local thermal distribution.

In the case of NA49 Pb+Pb data in the rapidity interval $2.9<y<3.4$ and for values of transverse momentum $p_T > 300$ MeV/c we find deviations from the basic Bose-Einstein distribution. We attribute this deviation to the strong radial flow that has been observed in this system.

A letter based on these results has been submitted to Physics Letters B.

---

[*] Institüt für Theoretische Physik, Universität, Regensburg, Germany.
[†] Department of Physics, University of California, Davis, CA.
[#] Theory Division, CERN, Switzerland.
[%] Department of Physics, Columbia University, New York, NY.
[1] G.F. Bertsch, Phys. Rev. Lett. **72**, 2349 (1994); **77**, 789(3) (1996).

5.13 Data set viewer: A powerful data visualizer for relativistic heavy ion collisions

D.J. Prindle, J.G Reid, T.A. Trainor and D.D. Weerasundara

We have previously written an event display program QCDisplay for NA49 in order to provide a visual verification that the tracking code worked.[1,2] QCDisplay worked very well, allowing us to examine the reconstructed space points and tracks in addition to the Monte Carlo generated space points and tracks. We were able to dynamically modify the colors of different classes of points and tracks, show the associations between the points and tracks and display a tabular view of selected point or track structures, all while still allowing rapid rotations and dilations of the data.

Several issues have motivated a QCDisplay upgrade. If one wanted to add a new type of data to the display, for example vertices formed by near intersections of tracks, one had to make modifications to the QCDisplay source code. Also, when the definition of one of the displayed tables was modified, QCDisplay had to be recompiled. We have also realized that it is useful to think of a data table as a multi-dimensional object. The x, y and z values are just three of the axes in the space defined by reconstructed TPC points. Additional interesting axes are the deposited ionization, physical size and eccentricities of the measured ionization, and perhaps a χ^2 fit of a standard shape. These continuous quantities can be represented by a position along an axis of a 1D, 2D or 3D display. There are also discrete axes. For tracks these include the combination of detectors used to define the track, and the identification of the track as a particular type of particle. In 2D and 3D displays these discrete quantities can be distinguished by using different colors. There are also connectivities of the spaces. These include the association of tracks and space points and the association of tracks with each other to form vertices. In QCDisplay we can show these relationships by highlighting related items an item is selected.

We do not believe it is possible to show all interesting attributes of a complex table in one view. Therefore we have written an interface between the STAR data tables and QCDisplay that lets individual physicists map between a table and QCDisplay. This comprehensive new graphical user interface is called Data Set Viewer, or dsv for short. In its simplest mode a physicist can open a data file, select a table from a particular event and then drag and drop columns from the table to QCDisplay. When one wants to combine table columns algebraically, for example forming a radius when the table contains x and y, the physicist can use a simple expression (typed directly into the drop site) or a slightly more complicated procedure written in tcl language. In even more complicated situations, for example calculating points along a particle trajectory, one must write the command in a compiled language such as C or C++, and this can be loaded as a shared library and used like a procedure.

While it is always possible to define the mapping between STAR tables and QCDisplay representation interactively using drag and drop, (useful for exploration) it is tedious and error prone when trying to repeat the mapping a number of times. It is therefore possible to save and restore the current mapping. It is also possible to write a script to define the mapping and load whatever shared libraries are necessary. In this way it is possible to create custom display programs for different purposes, all using the same code.

A future goal of dsv is to incorporate 1D, 2D and tabular displays of table variables, and have these communicate with each other. For example, selecting a range in a 1D graph should highlight the representation of the selected columns in all the other views of the same table.

[1] Nuclear Physics Laboratory Annual report, University of Washington (1995) p. 45.
[2] Nuclear Physics Laboratory Annual report, University of Washington (1996) p. 44.

5.14 Shell corrections in stopping power

H. Bichsel

The expression for the stopping power S derived by Bethe for particles with charge ze and speed $\mathrm{v} = \beta c$ can be written as

$$S = \frac{2\pi e^4 z^2}{mc^2\beta^2} \cdot N \cdot B = 2.55 \cdot 10^{-19} (\mathrm{eVcm}^2) \frac{z^2}{\beta^2} N B, \qquad (1)$$

where m is the rest mass of an electron, N the number of atoms per unit mass (or volume), and B is the "stopping number." A first approximation for B is given by

$$B_a(\mathrm{v}) = 2 \log (2\, m\mathrm{v}^2 / I), \qquad (2)$$

where I is the logarithmic mean excitation energy of the electrons in the atom.

Several corrections must be made to get better approximations. One of them relates to the effect of the binding of the electrons in the atom. It is customarily called a "shell correction" C. One of the methods used to obtain C is to calculate B directly with

$$B(\mathrm{v}) = \int dF \int_{E/\mathrm{v}}^{\infty} f(E,K) dK \;/\; K \quad , \qquad (3)$$

where $f(E,K)$ is the generalized oscillator strength (GOS) for a transition from the ground state of the atom to an excited state of energy E, and a momentum change K of the incident particle. The shell correction then is the difference between B_a and B.

Calculations of C have been made so far with GOS for hydrogenic wavefunctions with a screened potential. Here, calculations are presented which have been made with ground state wave functions and a potential calculated with the Hartree-Fock-Slater approximation. Wave functions for electrons in continuum states are calculated by solving the Schrödinger equation.[1] Preliminary results are shown in Fig. 5.14-1 for 2*p* electrons in Si (solid line) compared to the hydrogenic approximation (dotted line). For convenience the abscissa is given as the energy E of a proton with speed v. At 1 MeV, (B~34.5) the L-shell correction (C_L~3.3) amounts to about 10% of the stopping number and the change from the hydrogenic approximation is about 2.5% in the stopping number.

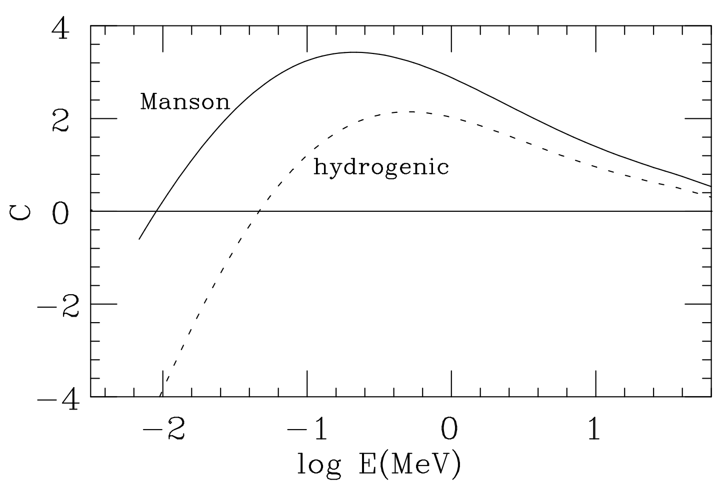

Fig. 5.14-1. Shell correction for 2p electrons in Si.

[1] S. Manson, Phys. Rev. A **6,** 1013 (1972).

6.0 ATOMIC AND MOLECULAR CLUSTERS

6.1 Electron detachment cross sections for carbon atom and cluster anions

C. Cooper,* M.L. Gardel,† B.P. Henry, R. Vandenbosch and D.I. Will

Last year[1] we reported on the destruction cross sections for 10 keV C_8^{1-} and 75 keV C_{60}^{1-} in collisions with H_2. Although the ratio of the C_{60} to C_8 cross sections were similar to the values of Shen et al.[2] at 50 keV total energy for each ion, our absolute cross sections were 2 to 3 times smaller than theirs. In order to try to resolve this discrepancy, we measured some well-known cross sections for simple atomic beams. A smaller yet significant discrepancy was found for these reactions, leading us to find some deficiencies in the design of our gas cell. We have reconfigured the gas cell, shortening the entrance and exit tubes and relocating the gas inlet with respect to the pressure gauge. After these modifications we obtained good agreement with literature values for several well-studied reactions. We have remeasured the cross section for 10 keV C_8^{1-} and measured the cross section at 50 keV, obtaining values that are closer to but still appreciably less than that of Ref. 2. Similarly, the cross section for 50 and 75 keV C_{60}^{1-} are smaller than those reported previously. Our new cross section measurements are summarized in Table 6.1-1. Our cross section for 30 keV C^- on Ar is appreciably larger than a previous measurements.

Table 6.1-1. Electron detachment cross sections
All cross sections are in units of 10^{-16} cm^2.

Reaction	Energy(keV)	This work	Previous work	Reference
$H^- + H_2$	10.0	11.3	12.0	Risley[3]
	22.5	8.6	8.5	Jorgensen *et al*.[4]
	50.0	5.8	5.9	Jorgensen *et al*.
$C^- + H_2$	22.5	10.9		
	50.0	10.7	~10.0	Shen *et al*.[2]
$C_8^- + H_2$	10.0	20.0		
	50.0	23.0	35.0	Shen *et al*.
$C_{60}^- + H_2$	50.0	47.0	90.0	Shen *et al*.
	75.0	50		
$C^- + Ar$	30.0	13.0	6.5	Matic and Cobic[5]
$O^- + H_2$	50.0	6.7	7.2	Jorgensen *et al*.[4]

* Present address: Dartmouth College, Hanover, NH.
† Present address: Brown University, Providence, RI.
[1] Nuclear Physics Laboratory Annual Report, University of Washington (1998) p. 49.
[2] H. Shen, C. Brink, P. Hvelplund and M.O. Larsson, Z. Phys. D **40**, 371 (1997).
[3] J. Risley, Phys. Rev. A **10**, 731 (1974).
[4] T. Jorgensen, Jr. *et al*., Phys. Rev. **140A**, 1484 (1965).
[5] M. Matic and B. Cobic, J. Phys. B:Atom. Molec. Phys. **4**, 111 (1971).

6.2 Search for smallest molecular species predicted to form a stable dianion

R. Vandenbosch and D. I. Will

Single atoms of any element will not form a stable dianion. In order to bind a second electron a molecular species needs to be of sufficient size to minimize electron-electron repulsion. It is also important that the molecular species contain electronegative atoms. Scheller and Cederbaum[1] have considered this problem theoretically and concluded that LiF_3 is the smallest molecular species expected to bind two electrons. F is the most electronegative of the chemical elements. Previously[2] we developed a new method for producing dianions, and demonstrated its efficacy in forming the dianion of the carbon cluster C_9. The method is based on fragmenting a monoanion of a species containing an extra atom of an electropositive element such as an alkali metal. If the alkali metal atom is removed during a collision with a gas target atom it is likely to leave as a positive ion, leaving a dianion behind.

We have attempted to apply this new technique in a search for the dianion of LiF_3. We first tried fragmenting the Li_2F_3 monoanion produced by sputtering ^6LiF with cesium. We used isotopically enriched ^6Li because with this isotope the dianion would have a half-integer m/q value and hence a more unique signature in an electric rigidity spectrum. The fragmentation products are analyzed with a cylindrical electrostatic deflector following the target gas cell. Although we identified Li_2F_3 in a mass spectrum from the sputter source, there was a significant background of other impurity species. We then prepared a target pellet of a mixture of ^6LiF and NaF, and identified the species $LiNaF_3^-$ in the mass spectrum from the sputter source. Attempts to fragment this species have led to an upper limit to the ratio of the yield of the LiF_3 dianion to the yield of the LiF_3 monoanion of about one part in 10^4. On the basis of our previous experience with the C_9 dianion yield it is likely that a smaller ratio might be expected. Thus we will have to increase our sensitivity in order to make a definitive statement about the possible stability of the LiF_3 dianion.

[1] M.K. Scheller and L.S. Cederbaum, J. Phys. B: Atom. Molec. Opt. Phys. **25**, 2257 (1992).
[2] R. Vandenbosch *et al*., Chem. Phys. Lett. **274**, 112 (1997).

7.0 ELECTRONICS, COMPUTING AND DETECTOR INFRASTRUCTURE

7.1 Electronic equipment

G.C. Harper, A.W. Myers and T.D. Van Wechel

Along with the normal maintenance and repair of the Nuclear Physics Laboratory's electronic equipment, projects undertaken by the electronics shop this year included the following:

a. An equipment rack temperature controller was designed and made to regulate the output airflow temperature to within one tenth of a degree C. To be used with experiment described in Section 1.2.

b. Several circuit boards were designed and built for use in experiment described in Section 1.10.

c. Completed a major upgrade to the Analyzing Magnet Power Supply.

d. Finalized design and started board layout of the SNO NCD Multiplexer.

e. Completed one of ten delay line boxes for the SNO NCD Multiplexer boards.

f. Revision b of the emiT / shaper/ADC board is complete. We have two 8-layer prototype boards in house and will populate/test with the next month.

g. Designed and manufactured a 10-channel liquid nitrogen level control system for use in experiment described in Section 4.1.

h. Fiber optic transmitters and receivers have been developed, built and tested to interface between the emiT detector assembly (preamplifiers) and the emiT shaper/ADC board.

i. A controller was designed and built to control the 680-ampere low voltage power supply system, which is used for electropolishing, the SNO neutral current detectors.

j. The emiT preamplifiers have been redesigned for lower power consumption to reduce heat inside of the detector assembly.

k. Assisted in the repair and testing of SNO FEC daughter boards at Queens University.

7.2 VAX-based acquisition systems

M.A. Howe, R.J. Seymour and J.F. Wilkerson

We have retired one of the VAXstation 3200-based data acquisition systems, bringing our active total to three. They consist of Digital Qbus-based VAXStation 3200/GPXs running VMS v4.7a using VWS/UIS as their “windowing” software. Each VAXstation supports a BiRa MBD-11 controlled CAMAC crate. Our primary system is attached to a dozen dedicated 200 MHz Tracor Northern TN-1213 ADCs. Those ADCs and other CAMAC modules are coincidence-gated by a UWNPL-built synchronization interface, which includes monitor (Singles) and routing-Or capabilities. The system also has a bank of 32 10-digit 75 MHz NPL-built scalers.

Our principal VAXStation's dual BA-23 cabinet has an MDB-11 DWQ11 Qbus-to-Unibus converter driving a Unibus expansion bay. The system's Qbus peripherals include a CMD CQD-220/TM SCSI adapter for a Seagate ST41650 1.38 gigabyte disk, an Iomega Jaz 1 gigabyte removable disk and an occasional TTI CTS-8210 8mm tape drive. We also use a DEC IEQ11 IEEE-488 bus controller and a DEC DRV11-J parallel interface to control the scalers. The Unibus bay contains a DR11-C parallel interface for the experiment controller, an LPV11 Printronix lineprinter controller and a Unibus cable continuing on to the MBD-11.

The other acquisition systems each consist of a VAXstation 3200/GPX's BA-23 cabinet and an Able Qniverter providing a Unibus cable direct to stand-alone MBD-11s. Unlike the ‘principal’ system, these do not directly control non-CAMAC-based equipment. One of these systems also has a CMD SCSI adapter for a 4 gigabyte hard drive, a Jaz drive and an 8mm tape system. That system is frequently used for media conversion from the Jaz platters to 8mm archival tapes. All three systems run acquisition software based upon TUNL's XSYS, with major modifications to their DISPLAY program.

7.3 Analysis and support system developments

M.A. Howe, R.J. Seymour, T.A. Trainor and J.F. Wilkerson

The Lab's network is a switched fabric blending over 90 ports of 100baseTX ethernet, some 10baseT ports, and our existing legacy 10base2 net. We use our HP 800T switch's flexibility to partition the 10base cabling into three segments, with the 100baseTX network divided into four segments with stacked Linksys Stackpro hubs. The 800T's eighth port is a full duplex 100baseFX fiber uplink to the campus routers.

Last year's twenty 233MHz Pentium platforms have supplemented with six newer 400- and 450MHz Pentiums for the same price. The new systems are running Windows 98, MS Office97, Novell LanWorksPro for X-server and NFS capability, and a variety of shareware, freeware and campus-site-licensed utilities. Additional “specialty” packages, such as Fortran compilers, are installed as needed. The Electronics Shop's 400 MHz system is running Windows NT to support CADENCE.

Our principal central compute-server base is a pair of dual-CPU Digital AlphaServer 4000/466s running Digital Unix with a gigabyte of ram and a StorageWorks 4 gigabyte system disk. Each has an additional 9 gig dedicated drive and a central RAID disk facility will be added soon. One has an 18 gigabyte "scratch" disk, and a DLT4000 tape system. These machines benefit from Digital's Campus Software License Grant program for their updates, compilers and utilities.

The rest of our offline computing and analysis facility consists of:

- Our VMS cluster, reduced to three VAXstation 3100s, three 3200s and a single Alpha 3000/400. The cluster shares 26 gigabytes of disk space. Hardware failures have claimed 4 of the VAXstations. We have added a standalone AlphaStation 433au running OpenVMS.
- The Ultra-Relativistic Heavy Ion's group of Hewlett Packard Unix systems, consisting of a pair of HP 9000/710s, four 9000/712/60s and a trio of 180 MHz PA-8000 C-180 workstations. The C-180 and 712/60s are running HP-UX v10.20, the 710s run 9.01 and 9.03. The 712/60s travel to CERN and BNL with members of our RHIC contingent. One of the 9000/710s is the lab's World Wide Web server (www.npl.washington.edu).
  The nine HP machines NFS-share 19 disks totaling 62 gigabytes plus two Jaz drives. They have 8mm and two DLT2000XT tape systems.
  For compatibility with RHIC's RCF facility, we've installed Red Hat Linux v5.2 on a 233 MHz Pentium II system.
- The SNO and emiT group has a collection of networked Macintoshes, Power Computing 200 MHz PowerPC Mac “clones” and a growing number of Apple G3 systems. They also have a Sun SparcStation 20 running Solaris 2.5.1 to provide CADENCE circuit layout facilities to our electronics shop, two Sun Ultras and two SparcStation 2s. Many of their systems have migrated to Sudbury, Ontario as SNO nears completion.
- We still share two VMS VAXstation 3200s providing Email and CPU cycles for the Institute for Nuclear Theory and the Physics Nuclear Theory group. We also have a Sun Sparc 5 for developing the Slow Controls software for STAR, a VAXstation 3200 serving as the Linac's control and display system, three PDP-11/23s and six PDP-11/21s built into the Linac for cryogenics, vacuum and resonator control, and four PCs serving as controllers for the rest of the accelerator systems' interlocks, safety and vacuum system.

7.4 A custom VME-based data acquisition system for the emiT and SNO NCD experiments

M.C. Browne, A.W. Myers, T.D. Van Wechel and J.F. Wilkerson

Revision A of the shaper/ADC is a custom 6U VME-based fast shaper/peak detect ADC. This eight channel board contains switchable input coupling and programmable input attenuation. Each channel has a four-stage integration shaping network. Additionally, each channel has an independently-controlled level-crossing discriminator. The peak detection circuit consists of a transistor-buffered, dual-differentiating network. Shaped-pulse conversion is accomplished via a 12-bit ADC and read out through the standard VME bus. The board also contains status monitoring, and two scalers. The board can be run independently, or in parallel with additional boards, and is controlled through an Altera 7192 Field Programmable Gate Array (FPGA).

Revision A of the board was developed for the emiT experiment as the acquisition hardware for the data collected from silicon PIN diode detectors. The board was later modified to collect data for the cool-down phase of the NCD project of SNO. In 1998 revision B was designed to better accommodate both experiments. Prototype modifications were designed to enhance the performance and noise characteristics of the board.

The first revision of the board was prone to damage in the emiT experiment as a result of HV discharge. Revision B was designed with both fiber-optic and copper input capabilities. The emiT experiment will utilize the fiber-optic input to isolate the electronics from the proton detection segments which are operated at ~35 kV. The thresholds of revision A were also determined to be “soft ” during early emiT runs. The peak-detect network was redesigned, prototyped, and tested, resulting in a sharper threshold incorporated into the revision B design. Additionally, the revision A remote-controlled input attenuation network was susceptible to induced noise from the VME data bus. A new design was tested, both increasing the dynamic range of the board, and minimizing noise.

Revision B incorporates a significantly larger FPGA (480 logic cells as opposed to 192 in Rev. A), enabling the inclusion of individual channel scalers in the new design. An additional floating scaler provides channel-by-channel dead-time information by recording the number of both trigger-satisfying events and ADC conversion events. The FPGA was also programmed with new operational logic which should allow the board to run faster. In revision A, a hardware-set lockout dominated the measured dead-time of 87 s. The new revision allows the board to run as quickly as the data is converted and read out.

Finally, several undesirable layout characteristics were identified in revision A. These resulted in induced noise in certain channels of the board. Special attention was paid in revision B to avoid these problems.

Two prototypes of revision B have been received, and are currently beginning the testing process. Full-scale production should begin in April 1999.

7.5 Development of an advanced object oriented real-time data acquisition system

A.A. Hamian, M.A. Howe, F. McGirt,* P.M. Thornewell† and J.F. Wilkerson

Work is underway at NPL to design and implement a new client/server based object oriented data acquisition system. This work builds on our experiences with Object Oriented data acquisition for SNO and from other data acquisition systems developed for experiments at the University of Washington and Los Alamos National Laboratory.

Our present system is Apple (68k and PPC) based primarily because of the MacOS's superior GUI interface (at the time of the original concept in 1987). The appeal of a GUI driven data acquisition is still high, as it's easier for both experts and non-experts to work with and allows real time observation and feedback of the system's parameters and performance. The aim is to develop a mostly platform independent system that will be based on both Intel and PPC hardware architecture. The motivation behind this is to support the widest possible user community.

The new system will take advantage of our experience with GUI driven DAQ (Data AcQuisition) but will separate the core data taking and hardware related code from the graphical interface using a client (GUI) server (hardware/data taking) architecture. We also plan to support data servers for near time monitoring, in a similar fashion as is presently done in SNO. Both the client and server sides will rely heavily on multithreading. This will allow the server to send out information via TCP/IP whilst taking data and the client will be able to process mouse clicks and update windows whilst receiving data.

This multithreading approach scales with processors allowing the full utilization of a multiprocessor machines (which are especially cost effective when using Intel hardware). On the server side, the system is heavily kernel dependent (accessing hardware and ethernet devices are kernel level processes) implying that for true scalability the system must implement threading of the kernel. From examination of current operating systems for the Intel platform, there are at least four viable platforms: Solaris x86, Windows NT, BeOS and LINUX (2.2 kernel and above). However, at present we are concentrating on the LINUX O/S. For the client side, the updating of windows and calculations based on the incoming data are not heavily kernel dependent and therefore do not absolutely require a multithreaded kernel. In addition the anticipated loads on the client are not high and it should not prove necessary to require the use a multiprocessor machine.

The interface between the clients and severs will be provided by CORBA (Common Object Resource Broker Architecture) an industry standard middleware layer. A number of ORB's have been examined, though only those that a multithreaded have been considered, due to the underlying multi-threaded nature of the server. Some possibilities include omniORB (from AT&T) and ORBacus (from Object Oriented Concepts). Both have the advantage that they are free (for non-commercial use) and come supplied with source code. The use of an industry standard communication protocol makes it possible to implement the client and server on various platforms.

* Los Alamos National Laboratory, Los Alamos, NM.
† F5 Networks Inc., Seattle, WA.

8.0 VAN DE GRAAFF, SUPERCONDUCTING BOOSTER AND ION SOURCES

8.1 Van de Graaff accelerator operations and development

G.C. Harper, C.E. Linder, A.W. Myers and T.D. Van Wechel

The Tandem was entered 12 times this year. Eight entrances were for the installation or removal of the Terminal Ion Source (TIS), for TIS development, or to change the TIS ion species. Four unscheduled entrances were made for the repair of a broken part or the fix of another problem. Seven entrances were used opportunistically for additional repairs or engineering changes.

We replaced one chain idler pulley because of a bad bearing. This is a failure rate of one per annual chain time of 1832 hours. This may be compared with:

3 failures per 3468 hours in year 1997-1998, or 1 per 1156 hours

6 " " 3075 " " " 1996-1997, " 1 " 512.5 "

1 " " 3162 " " " 1995-1996, " 1 " 3162 "

Other repairs included:

Fiber optics and computer-end fiber optic feed-throughs were replaced. The right horizontal steering power supply was replaced. The TIS extraction Power Supply was removed and sent back to the manufacturer, Glassman High Voltage, Inc., who repaired and returned it within four days. The TIS extraction and Einzel power supplies were repaired and ruggedized after an unauthorized excursion to a high Tandem terminal voltage caused them spark-related damage.

The (TIS) was re-designed to produce protons and alphas. This is reported in Section 8.3.

The training of tandem operators by professional staff was continued to good effect.

During the year from March 1, 1998 to February 28, 1999 the tandem pellet chains operated 1832 hours. The DEIS operated 344 hours, and the SpIS 582 hours. Additional statistics of accelerator operations are given in Table 8.1-1.

Table 8.1-1.
Tandem Accelerator Operations
March 1, 1998 to February 28, 1999

Activity	Days Scheduled	Percent
Nuclear Physics Research, Deck Ion Sources Alone	36	10
Nuclear Physics Research, ^{1}H, ^{3}He or ^{4}He, from TIS	44	12
Nuclear Physics Research, ^{4}He or below, Tandem only	20	5
Nuclear Physics Research, Heavy ions, Tandem only	3	1
Nuclear Physics Research, ^{4}He or below, Tandem and LINAC	17	5
Nuclear Physics Research, Heavy Ions, Tandem and LINAC	+ 14	+ 4
Subtotal; Nuclear Physics Research	134	37
Scheduled Machine Development or Maintenance	117	32
Unscheduled Maintenance	+ 14	+ 4
Subtotal; Development or Maintenance	131	36
Crew Training	+ 30	+ 8

8.2 Booster operations

J.F. Amsbaugh, G.C. Harper, M.A. Howe, D.W. Storm and D. I. Will

During the period March 1, 1998 to February 28, 1999, the booster was operated for 31 days. This is substantially fewer than the 83 days operated last year or the 55 days the previous year. There was no extensive maintenance on the linac. All resonators are presently operable.

Beams accelerated were ^{1}H, ^{4}He and ^{19}F, which was accelerated up to 197 MeV.

We continue to operate the low beta resonators at an average field of 3.0 MV/m and the high beta ones at average of 2.4 MV/m.

The helium compressors continued to run with no failures this year. Our oldest compressor now has run for 106k hours, and the other two have run for 74k hours in one case and 47k hours in the other case. The compressor with over 100k hours is one of the three originally installed before the booster was completed in 1987.

8.3 Tandem terminal ion source

G.C. Harper, C.E. Linder, A.W. Myers and T.D. Van Wechel

The terminal ion source was used in four experiments during this reporting period, all for the $^{7}Be(p,\gamma)^{8}B$ experiment. Three runs used $^{1}H^{+}$ at terminal voltages from 0.3 MV to 1.5 MV. The other run used $^{4}He^{+}$ at a terminal voltage of 1.37 MV.

The tank was opened four times for unscheduled source repairs. On one occasion the tank was opened to replace the einzel lens power supply which failed. The 10 kV unit was replaced with a 15 kV unit. The second time the tank was opened to repair the extractor supply which had been damaged by a tank spark. On the next occasion the tank was opened to replace a source canal which had sputtered away. Finally, the tank was opened to replace the discharge bottle which had been coated with aluminum sputtered from the exit canal.

Development for this year includes design, fabrication, and testing of a toroidal electrostatic deflector. The toroidal deflector was designed to have optical properties as similar as possible to those of a double focussing magnet. When tested it was found that the deflector had focussing power that was unbalanced in the vertical and horizontal planes or had second order effects that were more significant than expected.

Further developments included design, construction and testing of a new permanent magnet for the deflection of $^{1}H^{+}$ and possibly $^{2}H^{+}$. The new magnet for 13.5 keV $^{1}H^{+}$ has a field of 1.18 kG as opposed to the 1.91 kG magnet used for 11.6 keV $^{3}He^{+}$. Proton output on the high energy cup is 30 μamps from 800 keV to 2.5 MeV and drops fairly rapidly above and below those energies. A 5 μamp beam at 193 keV has been observed on the high energy cup and analyzed with 3 μamps appearing on the image cup.

An additional development was the alteration of the $^{3}He^{+}$ magnet to deflect $^{4}He^{+}$ by replacing the pole pieces with narrower ones. The 1.91 kG magnet used for 11.6 keV $^{3}He^{+}$ has been increased to 2.23 kG for use with 10.2 keV $^{4}He^{+}$. The $^{4}He^{+}$ is a very stable beam at 1.37 MeV with 12 μamps observed on the high energy cup and 11.5 μamps analyzed. So far, it has been used successfully down to 450 keV.

Future plans for terminal ion source use are to develop a gradient which can be successfully used with a high intensity, very low energy (100 keV to 300 keV) ion beam. A new gradient has been designed but not yet tested.

8.4 Cryogenic operating experience

M.A. Howe, D.W. Storm and D.I. Will

The superconducting booster linac is cooled by liquid helium from a Koch Process Systems, Inc.,[1] Model 2830S Helium Refrigerator with three expansion engines, each having two insulated pistons with warm seals. The following table summarizes our maintenance[2] for January 1, 1998 to December 31, 1998:

Item	In Use	Major Services	Times Performed
Helium Refrigerator			
Cold Box	100%	warm/pump/purge	0
Main Dewar	100%	warm/pump/purge	0
Top Expander	~8000 hrs	warm/pump/purge	5
	~130 RPM	belts and valve seals	1
		wrist pin and cam follower bearings	1
		flywheel and crank pin bearings	1
		main piston seals	2
Middle Expander	~8000 hrs	warm/pump/purge	6
	~100 RPM	belts and valve seals	1
		wrist pin and cam follower bearings	1
		flywheel and crank pin bearings	1
		main piston seals	2
Wet Expander	~3000 hrs	warm/pump/purge	3
	~50 RPM	belts and valve seals	0
		wrist pin and cam follower bearings	0
		flywheel and crank pin bearings	0
		main piston seals	0
		replaced DC drive motor/generator	1
Distribution System	94%	warm, pump, purge lines	5

This final table shows screw compressor history here as of March 8, 1998.

Item	Total	1997	Status	Maintenance
RS-1	106,041 hours	8759 hours	running	None
RS-2	57,547 hours	0 hours	phases shorted	Core removed 1993
RS-2a	46,976 hours	8704 hours	running since 1993	None
RS-3	22,752 hours	0 hours	shorted to ground	Core removed 1990
RS-3a	74,347 hours	8704 hours	running since 1990	None

Mean RS compressor pump core lifetimes are as follows: All five cores listed above, 61,533 hours; those four cores operated to minimize starts (RS-1, RS-2, RS-2a and RS-3a), 71,228 hours.

[1] Koch is now Process Systems International Inc., Westborough, MA.
[2] Nuclear Physics Laboratory Annual Report, University of Washington (1998) p. 60.

9.0 OUTSIDE USERS

9.1 10 MeV proton induced cascade solar cell degradation

D.L. Oberg* and D.A. Russell*

The University of Washington Nuclear Physics Laboratory tandem Van de Graaff was used to produce an uniform proton beam over a 4-inch diameter for the purpose of irradiating solar cells and look for the degradation induced. The 60 inch scattering chamber was used with a 3 mil titanium scattering foil mounted at the beam entrance. The cascade cells were mounted 51 inches from the foil. A Faraday cup was used to map the beam area and was mounted on one of the rotating arms of the chamber. A unique alignment rod was connected between the Faraday cup and the scattering foil such that the cup face was always pointed directly at the foil as the cell area was mapped. The beam uniformity map (shown below) matched the predicted very well.

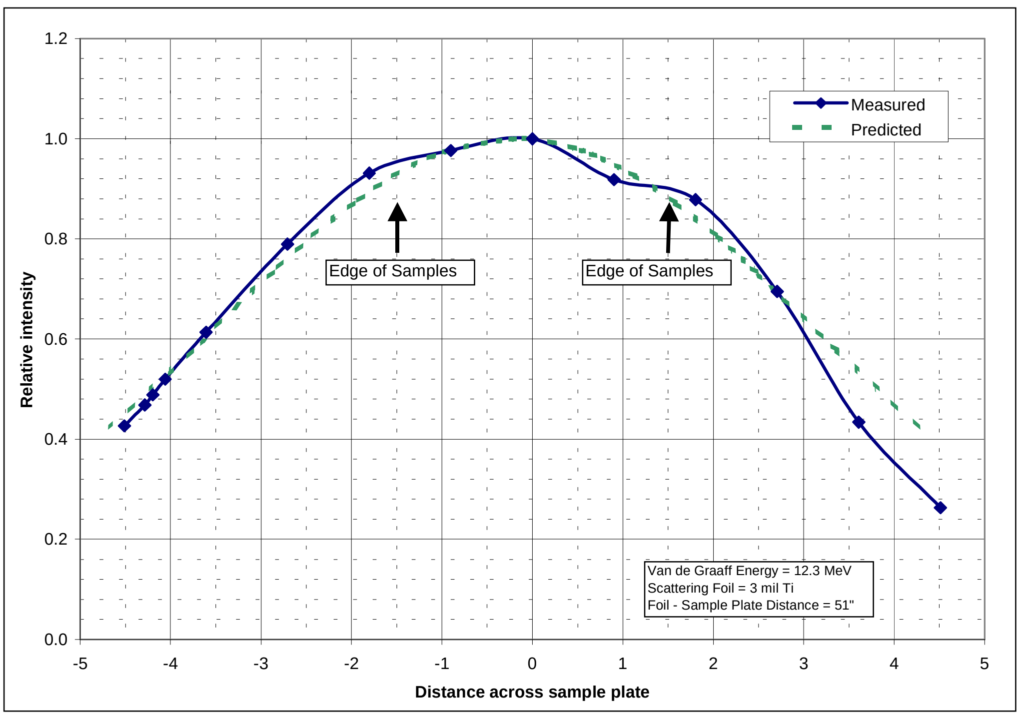

* Boeing Company, Seattle, WA.

9.2 Scientific Imaging Technologies (SITe) CCDs in the space radiation environment

J. Janesick,* M. Klinglesmith* G. Soli* and M. Blouke*

Solar flare protons are of primary concern to CCDs operating in GEO or interplanetary space. Protons, in addition to producing total dose damage in the oxide, also create displacement damage in the bulk silicon. The rate of displacement production is a fundamental property of the interaction between high energy protons and silicon, and is therefore not very sensitive to technological variations, as demonstrated by displacement damage effects, measured in Cassini 12 micron,[1] SITe 27 micron, and SITe 12 micron CCDs. The SITe 12 micron CCDs were irradiated at the NPL during the previous year. This note models these effects and ties the SITe 12 micron technology to radiation damage physics as understood in previous experiments. This allows CCD performance in the space radiation environment to be accurately predicted from minimal ground test data.

The silicon-bulk displacement-damage generated by high-energy protons causes a linear increase in parallel Charge Transfer Inefficiency (CTI). This CTI as a function of displacement damage is shown in Fig. 9.2-1 for three different technologies. These technologies are the SITe 27 micron TK512 CCD, the SITe 12 micron 018 CCD and the Loral Cassini 12 micron CCD. The Cassini and 018 CCDs both have 12 micron pixeles, and the TK512s have 27 micron pixels. The TK512 CTI was measured with Fe-55 x-rays at –30° C with an 11 ms row-shift time. The Cassini and 018 CCD CTI was measured with Fe-55 x-rays at – 50° C with a 20 ms row-shift time. The linear relationship between displacements per pixel and CTI varies as a function of row-shift time and test temperature. The CTI performance recovers at temperatures below – 90° C for row-shift times less than 20 ms, identifying the displacement-damage generated traps as PV centers in the bulk silicon. The traps "freeze out" because the PV-center emission –time constant becomes longer than the row-shift time.

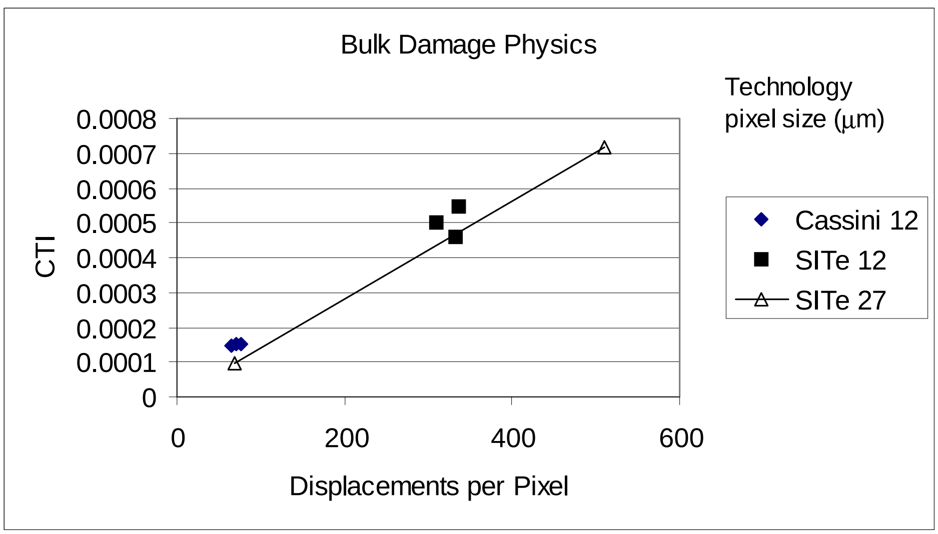

Fig. 9.2-1. Measured CTI as a function of computer displacements per pixel showing data for SITe 27 and 12 micron technologies and the Cassini (Loral) 12 micron technology.

Lower energy protons produce more bulk damage, as shown in Fig. 9.2-2, and this energy dependence is used to predict Charge Transfer Efficiency (CTE = 1 – CTI) performance degradation in the space proton environment.

This experiment ties the SITe 12 micron technology to radiation damage physics as understood in previous experiments. This allows CCD performance in the space radiation environment to be accurately predicted from minimal ground test data.

* Scientific Imaging Technologies, Inc., Beaverton, OR.

[1] J. Janesick, G. Soli, T. Elliott and S. Collins, "The effects of proton damage on charged coupled devices," *in Charged Coupled Devices and Solid State Optical Sensors II*, Proc. SPIE 1447.87 (1991).

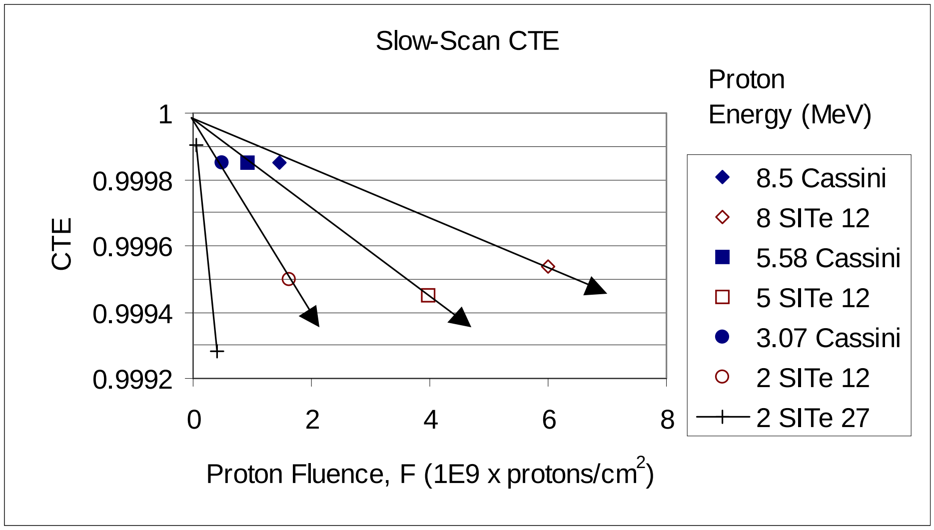

Fig. 9.2-2. CTE as a function of proton fluence showing increased damage for lower energy protons and for larger pixel areas. The CTE performance degradation is linear with increasing protone fluence for a given protons energy, as indicated by the arrows.

The Tandem Van de Graaff particle accelerator at the University of Washington's Nuclear Physics Laboratory was used to accelerate protons into SITe 12 micron technology CCDs. In order to expose the CCDs to a uniform fluence of protons, gold scattering foils were used to spread the proton beam out over the CCDs. The scattering foils were placed in the beam pipe 130" up-stream from the CCDs.

The proton detector was exposed through a (1/493) cm^2 collimator in order to maintain a PIN detector count rate less than 1E4 protons per second (to avoid pulse pileup) and a 4 krad exposure time of about 10 minutes. The proton count was accumulated in a present scalar that turned off the proton beam at a preset total count where counts times 493 equals the total fluence.

10.0 NUCLEAR PHYSICS LABORATORY PERSONNEL

Faculty
Eric G. Adelberger, Professor
Hans Bichsel, Affiliate Professor
John G. Cramer, Professor
Peter J. Doe, Research Professor
Steven R. Elliott, Research Assistant Professor
George W. Farwell, Professor Emeritus
Jens H. Gundlach, Research Assistant Professor
Isaac Halpern, Professor Emeritus
Blayne R. Heckel, Professor
R.G. Hamish Robertson, Professor, Scientific Director, Nuclear Physics Laboratory
Hardy Siefert, Visiting Scientist[1]
Kurt A. Snover, Research Professor
Thomas Steiger, Research Assistant Professor
Derek W. Storm, Research Professor; Executive Director, Nuclear Physics Laboratory
Thomas A. Trainor, Research Associate Professor
Robert Vandenbosch, Professor
William G. Weitkamp, Research Professor Emeritus
John F. Wilkerson, Professor

Research Staff
Arnd Junghans, Research Associate
Stefan Baessler, Research Associate
Marcus Beck, Research Associate[2]
Anne L. Caraley, Research Associate
Jean-Marc Casandjian, Research Associate[3]
Alice Araz Hamian, Research Associate
Stephen M. Merkowitz, Research Associate
Ulrich Schmidt, Research Associate
Gregory Smith, Research Associate
Josephus P. van Schagen, Research Associate
Dhammika Weerasundara, Research Associate[4]

Predoctoral Research Associates
Qazi Rushdy Ahmad
Michael Browne
Theresa Bullard
Gopal Brugalette[6]
Lincoln D. Carr[7]
Charles Duba
Robert M. Fardon
Phil Geissbuhler[7]
Karsten Heeger
Bruce Henry
Charles D. Hoyle
Michael Kelly[5]
Erik Leder[7]
Hans Pieter Mumm
John Orrell
Alan W.P. Poon[8]
Jeffrey Reid
Miles Smith
Eric Zager

[1] Sudbury Neutrino Observatory, Creighton Mines, Sudbury Ontario, Canada.
[2] Katholieke Universiteit, Leuven, Belgium.
[3] GANIL, Caen, FRANCE.
[4] BSQUARE Corp., Bellevue, WA.
[5] 3231 Fox #2B, Woodridge, IL.
[6] IBM, Seattle, WA.
[7] Physics Department, University of Washington, Seattle, WA.
[8] Lawrence Berkeley Laboratory, Berkeley, CA.

Professional Staff
John F. Amsbaugh, Research Engineer
Thomas Burritt, Research Engineer
James Franklin, Research Engineer
Gregory C. Harper, Research Engineer
Mark A. Howe, Research Engineer
Carl E. Linder, Research Engineer
Duncan Prindle, Research Scientist
Richard J. Seymour, Computer Systems Manager
H. Erik Swanson, Research Physicist
Pete Thornewell, Research Engineer[9]
Timothy D. Van Wechel, Electronics Engineer
Douglas I. Will, Research Engineer

Technical Staff
James Elms, Instrument Maker
Allan Myers, Electronics Technician
Hendrik Simons, Instrument Maker, Shop Supervisor
Steve Zsitvay, Instrument Maker

Administrative Staff
Barbara J. Fulton, Administrator
Karin M. Hendrickson, Fiscal Specialist

Part Time Staff
Katie Ayers[10]
Kevin Ayers
Joseph Bainer[10]
Misty Bentz
Phoug Dong Bach[10]
Nathan Collins
Sean Conner[10]
Clara Eberhardy[10]
Adam Elias
Jonathan Jerke[10]
Laura Grout
Derrick Johnson[10]
Inho Kim[10]
Ellen Kuperstein
Hwang Kyu[10]
Joshua Leingang
Jennifer Loveless[10]
Angus MacNab
Tami McGonagle
Keven McKenney[10]
Christy McKinley
Lisa Murray[10]
Anika Peter
Justin Prosser[10]
Antonio Ramos
Margaret Reitz[10]
Kevin Saur[10]
Gwynn Robbins[10]
Andrew Sharp[10]
Craig Standley[10]
Kyle Sundqvist
Lincoln Webbeking
Willie White
Matthew Wilson

[9] F5 Networks Inc., Seattle, WA.
[10] No longer associated with the Nuclear Physics Laboratory.

11.0 DEGREES GRANTED, ACADEMIC YEAR, 1998-1999

"The giant dipole resonance in highly excited nuclei: does the width saturate?" Michael P. Kelly, University of Washington (1999).

"Energy calibration of the Sudbury Neutrino Observatory using monoenergetic gamma-ray sources," Alan Wing Pok Poon, University of Washington (1998).

12.0 LIST OF PUBLICATIONS FROM 1998-1999

Published papers:

"Spectator nucleons in Pb+Pb collisions at 158 A-GeV," H. Appelshauser and the NA49 collaborators (including J.G. Cramer, D.J. Prindle, J.G. Reid, T.A. Trainor and D.D. Weerasundara), Eur. Phys. J. A **2**, 383 (1998).

"Charged particle production in proton, deuteron, oxygen and sulfur nucleus collisions at 200 GeV per nucleon," T. Alber and the NA35 collaborators, (including J.G. Cramer, D.J. Prindle, J.G. Reid, T.A. Trainor and D.D. Weerasundara), Eur. Phys. J. C **2**, 643 (1998).

"Hadronic expansion dynamics in central Pb+Pb collisions at 158 GeV per nucleon," J.G. Cramer, Eur. Phys. J C **2**, 661 (1998).

"Recent results on central Pb+Pb collisions from experiment NA49," H. Appelshauser and the NA49 collaborators (including J.G. Cramer, D.J. Prindle, J.G. Reid, T.A. Trainor and D.D. Weerasundara), Nucl. Phys. A **638**, 91 (1998).

"Phi emission in central Pb+Pb collisions at 158-Gev/U," H. Appelshauser and the NA49 collaborators (including J.G. Cramer, D.J. Prindle, J.G. Reid, T.A. Trainor and D.D. Weerasundara), Nucl. Phys. A **638**, 431 (1998).

"Directed and elliptic flow in 158-Gev/nucleon Pb+Pb collisions," H. Appelshauser and the NA49 collaborators (including J.G. Cramer, D.J. Prindle, J.G. Reid, T.A. Trainor and D.D. Weerasundara), Nucl. Phys. A **638**, 463 (1998).

"Recent developments on the STAR detector system at RHIC," H. Wieman and the STAR collaborators (including J.G. Cramer, D.J. Prindle, J.G. Reid, T.A. Trainor and D.D. Weerasundara), Nucl. Phys. A. **638**, 559 (1998).

"Xi and anti-Xi production in 158-GeV/nucleon Pb+Pb collisions," H. Appelshauser and the NA49 collaborators (including J.G. Cramer, D.J. Prindle, J.G. Reid, T.A. Trainor and D.D. Weerasundara), Phys. Lett. B **444**, 523 (1998).

"Scaling properties of the giant dipole resonance width in hot rotating nuclei," D. Kusnezov, Y. Alhassid and K.A. Snover, Phys. Rev. Lett. **81**, 542 (1998).

"Fragmentation partners from collisional dissociation of C_{60}," R. Vandenbosch, Phys. Rev. Lett. **81**, 1821 (1998).

"Comment on 'Anomalous peaklike structure in the fission fragment anisotropies at sub-barrier energies in ^{11}B, ^{12}C, ^{16}O, ^{19}F + ^{232}Th Reactions,'" J.P. Lestone, A.A. Sonzogni, M.P. Kelly and R. Vandenbosch, Phys. Rev. Lett. **81**, 4776 (1998).

"Baryon stopping and charged particle distributions in central Pb + Pb, collisions at 158-GeV per nucleon," H. Appelshauser and the NA49 collaborators (including J.G. Cramer, D.J. Prindle, J.G. Reid, T.A. Trainor and D.D. Weerasundara), Phys. Rev. Lett. **82**, 2471 (1999).

"Hadronic expansion dynamics in ultra-relativistic Pb+Pb collisions at 158 GeV/nucleon," T. Alber and the NA49 collaborators (including J.G. Cramer, D.J. Prindle, J.G. Reid, T.A. Trainor and D.D. Weerasundara), Phys. Rev. Lett. **2**, 661 (1998).

"Solar fusion cross sections," 28 authors (including E.G. Adelberger, L. de Braeckeleer, C.A. Duba, S.R. Elliott, W.C. Haxton, K.M. Heeger, E. Henley, R.G.H. Robertson, K.A. Snover, E. Swanson and J.F. Wilkerson), Rev. Mod. Phys. **70**, 1265 (1998).

"Is quasifision responsible for anomalous fission fragment anisotropies?" A.A. Sonzongni, R. Vandenbosch, A.L. Caraley and J.P. Lestone, Phys. Rev. C **58**, R1873 (1998).

"Neutrino absorption efficiency of an ^{40}Ar detector from the β decay of ^{40}Ti," 15 authors (including E.G. Adelberger and H.E. Swanson), Phys. Rev. C **58**, 3677 (1998).

"Solar neutrino interactions with ^{18}O in the SuperKamiokande Water Cerenkov Detector," W.C. Haxton and R.G.H. Robertson, Phys. Rev. C **59**, 515 (1999).

"Calculating fission rates at high spin: incorporation of rotational degrees of freedom in thermodynamically fluctuating axially symmetric systems," J.L. Lestone, Phys. Rev. C **59**, 1540 (1999).

Papers submitted or to be published:

"Electron detachment and fragmentation in collisions between 1.25 keV/carbon C_8^- and C_{60}^- clusters and H_2," M.L. Gardel, R. Vandenbosch, B.P. Henry, C. Copper and D.I. Will, Eur. Phys. J D, in press.

"Positron-neutrino correlations in ^{32}Ar and ^{33}Ar decays: probes of scalar weak currents and nuclear isospin mixing," A. Garcia, E.G. Adelberger, C. Ortiz, H.E. Swanson, M. Beck, O. Tengblad, M.J. G. Borge, I. Martel, H. Bichsel and the ISOLDE collaborators, submitted to Hyperfine Interactions.

"Universal pion freeze-out phase-space, density," D. Ferenc, U. Heinz, B. Tomasik, U.A. Wiedemann and J.G. Cramer, accepted for publication, Phys. Lett. B.

"Event-by-event fluctuations of average transverse momentum in central Pb+Pb collisions at 158 GeV per nucleon," H. Appelshauser and the NA49 collaborators (including J.G. Cramer, D.J. Prindle, J.G. Reid, T.A. Trainor and D.D. Weerasundara), submitted to Phys. Lett. B.

"Statistical model for fragmentation of C_{60}," R. Vandenbosch, Phys. Rev. A, in press.

"Measurement of the response of the Russian-American Gallium experiment to neutrinos from a ^{51}Cr source," J.N. Abdurashitov and the SAGE collaborators (including S.R. Elliott and J.F. Wilkerson), Phys. Rev. C, in press.

"Short-range tests of the Equivalence Principle," G.L. Smith, C.D. Hoyle, J.H. Gundlach, E.G. Adelberger, B.R. Heckel and H.E. Swanson, to be submitted to Phys. Rev. D.

"The giant dipole resonance width at high excitation energy: does it saturate?" M.P. Kelly, K.A. Snover, J.P.S. van Schagen, M. Kicinska-Habior and Z. Trznadel, Phys. Rev. Lett., in press.

"Positron-neutrino correlation in the $0^+ \rightarrow 0^+$ decay of ^{32}Ar," E.G. Adelberger, C. Ortiz, A. Garcia, H.E. Swanson, M. Beck, O. Tengblad, M.J.G. Borge, I. Martel, H. Bichsel and the ISOLDE collaborators, submitted to Phys. Rev. Lett.

"An improved test of the Equivalence Principle for gravitational self-energy," S. Baessler, B.R. Heckel, E.G. Adelberger, J.H. Gundlach, U. Schmidt and H.E. Swanson, to be submitted to Phys. Rev. Lett.

"Low-background ^3He proportional counters for use in the Sudbury Neutrino Observatory," M.C. Browne, T.J. Bowles, S.J. Brice, P.J. Doe, C.A. Duba, S.R. Elliott, E.I. Esch, M.M. Fowler, J.V. Germani, A. Goldschmidt, K.M. Heeger, A. Hime, K.T. Lesko, G.G. Miller, R.W. Ollerhead, A.W.P. Poon, R.G.H. Robertson, M.W.E. Smith, T.D. Steiger, R.G. Stokstad, P.M. Thornewell, J.B. Wilhelmy, J.F. Wilkerson and J.M. Wouters, IEEE Trans. Nucl. Sci., in press.

Invited talks, abstracts and other conference presentations :

"Bose-Einstein Interferometry in CERN experiment NA49," J.G. Cramer, invited paper, American Physical Society, Columbus, OH, Bull. Am. Phys. Soc 43, 1051 (1998).

"The giant-dipole resonance in hot Sn nuclei," M.P. Kelly, K.A. Snover, J.P.S. van Schagen, M. Kicinska-Habior and Z. Trznadel, *Proceedings of the Topical Conference on Giant Resonances*, May, 1998, Varenna, Italy, Nucl. Phys. A, in press.

"GDR decay and bremsstrahlung emission in ^{12}C + $^{58,62}Ni$ reactions," M. Kicinska-Habior, Z. Trznadel, M.P. Kelly, K.A. Snover and J.P.S. van Schagen, *Proceedings of the Topical Conference on Giant Resonances*, May, 1998, Varenna, Italy, Nucl. Phys. A, in press.

"Scaling properties of the GDR in hot rotating nuclei," D. Kusnezov, Y. Alhassid and K.A. Snover, *Proceedings of the Topical Conference on Giant Resonances*, May, 1998, Varenna, Italy, Nucl. Phys. A, in press.

"Observation of $2p_{1/2}$-$2p_{1/2}$ M1 and E2 transitions in U^{81+} through U^{88+}," B. Beiersdorfer, A. Osterheld, and S.R. Elliott, American Physical Society, Santa Fe, NM, Bull. Am. Phys. Soc. **43**, 1319 (1998).

"Light-charged particles from fusion-evaporation in the $^{19}F+^{181}Ta \rightarrow {}^{200}Pb$ system: status report," A.L. Caraley and J.P. Lestone, *Gordon Conference*, June, 1998, Colby-Sawyer College, New London, NH.

"^{3}He neutral current detectors at SNO," S.R. Elliott, M.C. Browne, P.J. Doe, C.A. Duba, J. V. Germani, K.M. Heeger, A.W.P. Poon, R.G.H. Robertson, M.W.E. Smith, T.D. Steiger, P.M. Thornewell, J.F. Wilkerson and the SNO collaborators, *Solar Neutrinos Symposium,* to be published in *Proceedings New Era in Neutrino Physics*, June, 1998, Tokyo, Japan.

"The emiT experiment: a study of time reversal in neutron beta decay," T. Steiger, *Fifth International WEIN Symposium*, June, 1998, Santa Fe, NM.

"Precision measurement of the $^{4}He(\alpha,\gamma)^{8}Be$ radiative capture reaction and CVC/SSC in the mass-8 isomultiplet," poster presentation, J.P.S. van Schagen, K.A. Snover, D.W. Storm, M.P. Kelly, J.F. Amsbaugh, J.H. Gundlach and D.C. Wright, *Fifth International WEIN Symposium*, June, 1998, Santa Fe, NM.

"Searches for new long-range forces: Equivalence Principle violation and planckscale physics," E.G. Adelberger, S. Baessler, J.H. Gundlach, B.R. Heckel, C.D. Hoyle, S.M. Merkowitz, G.L. Smith and H.E. Swanson, *Fifth International WEIN Symposium*, June, 1998, Santa Fe, NM.

"Event-by-event analysis and the QCD phase transition," T.A. Trainor, invited talk, *Summer Workshop on Particle Distributions in Hadronic and Nuclear Collisions,* June, 1998, University of Illinois at Chicago, Chicago, IL.

"Results on the strong Equivalence Principle, dark matter, and new forces," B.R. Heckel, E. Adelberger, S. Baessler, J. Gundlach, M. Harris, C. Hoyle, A. Sharp, G. Smith and E. Swanson, *Advances in Space Research*, *Proceedings of the 32nd COSPAR Scient. Assembly,* July 1998, Nagoya, Japan.

"Scaling properties and the behavior of the nuclear giant dipole resonance under extreme conditions," D. Kusnezov, Y. Alhassid and K.A. Snover, *Proceedings of the International Workshop on many Fermion Systems,* Serra Negra, Brazil, Sept. 1998, World Scientific, to be published.

"Symmetry, scale and dimension in high-energy collisions," T.A. Trainor, invited talk, *International Workshop on Event-by-Event Physics*, Sept. 1998, ECT* Trento, Italy.

Neutral-current detection via $^{3}He(n,p)^{3}H$ in the Sudbury Neutrino Observatory," R.G.H. Robertson, *International School of Nuclear Physics*, 19th Course, Sept. 1998, Erice, Italy; Prog. Part. Nucl. Phys. 40, 113 (1998).

"A model-independent analysis of the solar neutrino anomaly," K. Heeger and R.G.H. Robertson, *International School of Nuclear Physics*, 19th Course, Sept. 1998, Erice, Italy; Prog. Part. Nucl. Phys. 40, 135 (1998).

"Methods for neutral-current neutrino detection in the Sudbury Neutrino Observatory," R.G.H. Robertson, *Proceedings 5th International Workshop on Topics in Astroparticle and Underground Physics* (TAUP97), Laboratori Nazionale del Gran Sasso, Italy, Sept. 1997, Nucl. Phys. B (Proc. Suppl.) **70**, 332 (1999).

"The solar neutrino problem," R.G.H. Robertson, invited talk, *International Conference Baryons '98*, Sept. 1998, Bonn, Germany.

"Time reversal in polarized neutron decay: improving the emiT detector," H.P. Mumm, M.C. Browne, R.G.H. Robertson, T.D. Steiger, J.F. Wilkerson and the emiT collaborators, American Physical Society, Santa Fe, NM, Bull. Am. Phys. Soc. **43**, 1532 (1998).

"The role of *hep* neutrinos in the search for solar neutrino oscillations," M.W.E. Smith, S.R. Elliott and R.G.H. Robertson, American Physical Society, Santa Fe, NM, Bull. Am. Phys. Soc. **43**, 1548 (1998).

"The neutral current detector project of the Sudbury Neutrino Observatory," S.R. Elliott, M.C. Browne, P.J. Doe, C. Duba, J.V. Germani, K.M. Heeger, A.W.P. Poon, R.G.H. Robertson, M. Smith, T.D. Steiger, J.F. Wilkerson and the SNO collaborators, American Physical Society, Santa Fe, NM, Bull. Am. Phys. Soc. **43**, 1549 (1998).

“Background results from the cooldown phase of the SNO NCD project,” M.C. Browne, C. Duba, K.M. Heeger, R.G.H. Robertson, T.D. Steiger, J.F. Wilkerson, P.M. Thornewell and the SNO collaborators, American Physical Society, Santa Fe, NM, Bull. Am. Phys. Soc. **43**, 1549 (1998).

“In situ determination of backgrounds from neutral current detectors in the Sudbury Neutrino Observatory,” K.M. Heeger, C. Duba, S.R. Elliott, A.W.P. Poon and R.G.H. Robertson, American Physical Society, Santa Fe, NM, Bull. Am. Phys. Soc. **43**, 1549 (1998).

“Charged-current energy spectrum at the Sudbury Neutrino Observatory in the presence of the neutral current detector array,” A.W.P. Poon, S.R. Elliott and R.G.H. Robertson, American Physical Society, Santa Fe, NM, Bull. Am. Phys. Soc. **43**, 1549 (1998).

“Possible supernova detection with neutron detectors near the SNO laboratory,” C.A. Duba, M.C. Browne and R.G.H. Robertson, American Physical Society, Santa Fe, NM, Bull. Am. Phys. Soc. **43**, 1550 (1998).

“The mass of ^{36}Ca and the isobaric mass multiplet equation,” A Komives, A. Garcia, D. Peterson, D. Bazin J. Caggiano, B. Sherrill,, N. Alahari, A. Bacher, W. Lozowski, J. Greene and E.G. Adelberger, American Physical Society, Santa Fe, NM, Bull. Am. Phys. Soc. **43**, 1561 (1998).

“Light-charged particles from fusion-evaporation in the ^{19}F+^{181}Ta $\rightarrow$ ^{200}Pb system,” A.L. Caraley, B.P. Henry, J.P. Lestone and R. Vandenbosch, American Physical Society, Santa Fe, NM, Bull. Am. Phys. Soc. **43**, 1573 (1998).

“Future solar neutrino experiments,” J.F. Wilkerson, invited talk, American Physical Society, Santa Fe, NM, Bull. Am. Phys. Soc. **43**, 1584 (1998).

“Event-by-event physics capabilities of the STAR experiment at RHIC,” D.D. Weerasundara and other STAR collaborators, American Physical Society, Santa Fe, NM, Bull. Am. Phys. Soc. **43**, 1589 (1998).

“Multiparticle correlation analysis based on dimension transport,” T.A. Trainor, J.G. Reid, D.D. Weerasundara and the STAR collaborators, contributed talk, American Physical Society, Santa Fe, NM, Bull. Am. Phys. Soc. **43**, 1589 (1998).

“The physics of HBT interferometry with STAR at RHIC,” J.G. Cramer and the STAR collaborators, American Physical Society, Santa Fe, NM, Bull. Am. Phys. Soc. **43**, 1590 (1998).

“Event-by-event physics in heavy ion collisions,” T.A. Trainor, invited talk, *CERN Heavy Ion Forum*, Dec. 1998, CERN, Geneva, Switzerland.

“Probing the QCD phase boundary with scale-local measures,” T.A. Trainor, contributed talk, *15th Winter Workshop on Nuclear Dynamics*, Jan. 1999, Park City, UT.

“Status of SNO,” P.J. Doe, *WINN’99*, Jan. 1999, Cape Town, South Africa.

“Pion phase-space density from HBT interferometry on Pb+Pb collisions at 158 GeV/nucleon,” J.G. Cramer and the NA49 collaborators, American Physical Society, Atlanta, GA, Bull. Am. Phys. Soc. **44**, 405 (1999), to appear in *Proceedings to the HBT Mini-Symposium*.

“The GDR width in hot nuclei: Does it saturate?” M.P. Kelly, K.A. Snover, J.P.S. Van Schagen, M. Kicinska-Habior and Z. Trznadel, American Physical Society, Atlanta, GA, Bull. Am. Phys. Soc. **44**, 492 (1999).

“Current mode neutron beam flux measurement with a ^{3}He ion chamber,” C.S. Blessinger, G.L. Hansen, W.M. Snow, H. Nann, S.D. Penn, B.R. Heckel, E.G. Adelberger, D.M. Markoff and H.E. Swanson, American Physical Society, Atlanta, GA, Bull. Am. Phys. Soc. **44**, 988 (1999).

The ^{4}He(α,γ)^{8}Be radiative capture reaction: a precision measurement of CVC/SCC in the mass-8 isomultipleet,” J.P.S. Van Schagen, K.A. Snover, D.W. Storm, M.P. Kelly, J.F. Amsbaugh, J.H. Gundlach and D.C. Wright, American Physical Society, Atlanta, GA, Bull. Am. Phys. Soc. **44**, 988 (1999).

“An overview of the solar neutrino problem,” S.R. Elliott, American Physical Society, Atlanta, GA, Bull. Am. Phys. Soc. **44**, 1306 (1999).

“Model-independent constraints on neutrino mixing from solar neutrinos,” K.M. Heeger and R.G.H. Robertson, American Physical Society, Atlanta, GA, Bull. Am. Phys. Soc. **44**, 1307 (1999).

"The neutral current detector array in the Sudbury Neutrino Observatory," M.W. E. Smith and the SNO collaborators (including M.C. Browne, P.J. Doe, C. Duba, S.R. Elliott, K.M. Heeger, A.W.P. Poon, R.G.H. Robertson, T.D. Steiger and J.F. Wilkerson), American Physical Society, Atlanta, GA, Bull. Am. Phys. Soc. **44**, 1307 (1999).

"The Sudbury Neutrino Observatory," R.G.H. Robertson, American Physical Society, Atlanta, GA, Bull. Am. Phys. Soc. **44**, 1406 (1999).

"A new $^7Be(p,\gamma)^8B$ experiment," J.M. Casandjian, K.A. Snover, T.D. Steiger, E.G. Adelberger, H.E. Swanson, A.Y. Zyuzin, N.P. Bateman, L.R. Buchmann, J.S. Vincent and K.R. Buckley, American Physical Society, Atlanta, GA, Bull. Am. Phys. Soc. **44**, 1529 (1999).

"The SNO data acquisition system," A.A. Hamian, R. Ahmad, P. Harvey, M. Howe, R. Meijer Drees, P. Thornewell, J.F. Wilkerson and the SNO collaborators, American Physical Society, Atlanta, GA, Bull. Am. Phys. Soc. **44**, 1530 (1999).

"Background signal discrimination at the Sudbury Neutrino Observatory," Q.R. Ahmad, A.A. Hamian and J.F. Wilkerson, American Physical Society, Atlanta, GA, Bull. Am. Phys. Soc. **44**, 1531 (1999).

"Conserved vector current test and second class current search in the A=8 isotriplet," K.A. Snover, invited paper, *International Symposium on Nuclear Electro-Weak Spectroscopy* (NEWS 99), March, 1999, Osaka, Japan.

"The GDR at high excitation energy; does the width saturate?" K.A. Snover, invited paper, *Riken Symposium on Selected Topics in Nuclear Collective Excitations* (Nucolex99), March, 1999, Tokyo Japan.

Conference presentations by collaborators of NPL personnel:

"Time reversal in polarized neutron decay—data analysis issues for the emiT experiment," S.R. Hwang and the emiT collaboration (including M.C. Browne, H.P. Mumm, R.G.H. Robertson, T.D. Steiger, and J.F. Wilkerson), American Physical Society, Columbus, OH, Bull. Am. Phys. Soc. **43**, 1109 (1998).

"HBT correlations in 158-A GeV Pb+Pb collsions," R. Ganz and the NA49 collaboration (including J.G. Cramer, D.J. Prindle, J.G. Reid, T.A. Trainor and D.D. Weerasundara*), Proceedings of the 2nd Catania Relativistic Ion Studies: Measuring the Size of Things in the Universe: HBT Interferometry and Heavy Ion Physics (CRIS 98)*, June 1998, Acicastello, Italy.

"NA49 results on single particle and correlation measurements in central Pb+Pb collisions," F. Wang and the NA49 collaborators (including J.G. Cramer, D.J. Prindle, J.G. Reid, T.A. Trainor and D.D. Weerasundara), invited talk, *28th International Symposium on Multiparticle Dynamics*," June 1998, Delphi, Greece.

"Time reversal in polarized neutron decay: results from the first run of the emiT experiment," L.J. Lising, H.P. Mumm, R.G.H. Robertson, T.D. Steiger, J.F. Wilkerson and the emiT collaborators, American Physical Society, Santa Fe, NM, Bull. Am. Phys. Soc. **43**, 1532 (1998).

"A metallic beryllium-7 target of small diameter," A.Y. Zyuzin and beryllium-7 collaborators, (including K.A. Snover, J.-M. Casandjian, T. Steiger, H.E. Swanson and E.G. Adelberger), *Proceedings of the 19th World Conference on Nuclear Targets*, to be published, Oct. 1998, Oak Ridge, TN.

"Time reversal in polarized neutron decay – the emiT experiment," G.L. Jones and the emiT collaborators, (including H.P. Mumm, R.G.H. Robertson, T.D. Steiger and J.F. Wilkerson*), International Workshop on Particle Physics with Slow Neutrons*, Oct. 1998, Institut Laue-Langevin, Grenoble, France, Nucl. Instrum. Methods A, in press.

"The TRIUMF parity violation experiment," S.A. Page and the TRIUMF collaborators (including A.A. Hamian), American Physical Society, Atlanta, GA, Bull. Am. Phys. Soc. **44**, 987 (1999).

"Results from SAGE III," J.S. Nico and the SAGE collaborators (including S.R. Elliott and J.F. Wilkerson), American Physical Society, Atlanta, GA, Bull. Am. Phys. Soc. **44**, 1306 (1999).

"Correction for first moments of transverse polarization in the TRIUMF 220 MeV *pp* parity violation experiment," W.D. Ramsay and the TRIUMF collaborators (including A.A. Hamian), American Physical Society, Atlanta, GA, Bull. Am. Phys. Soc. **44**, 1520 (1999).